STRUCTURE AND ENVIRONMENT

KIELCE UNIVERSITY OF TECHNOLOGY

Quarterly
Vol. 16, No. 2, 2024

ISSN 2081-1500
e-ISSN 2657-6902

• Architecture and urban planning • Civil engineering and transport • Environmental engineering, mining and energy

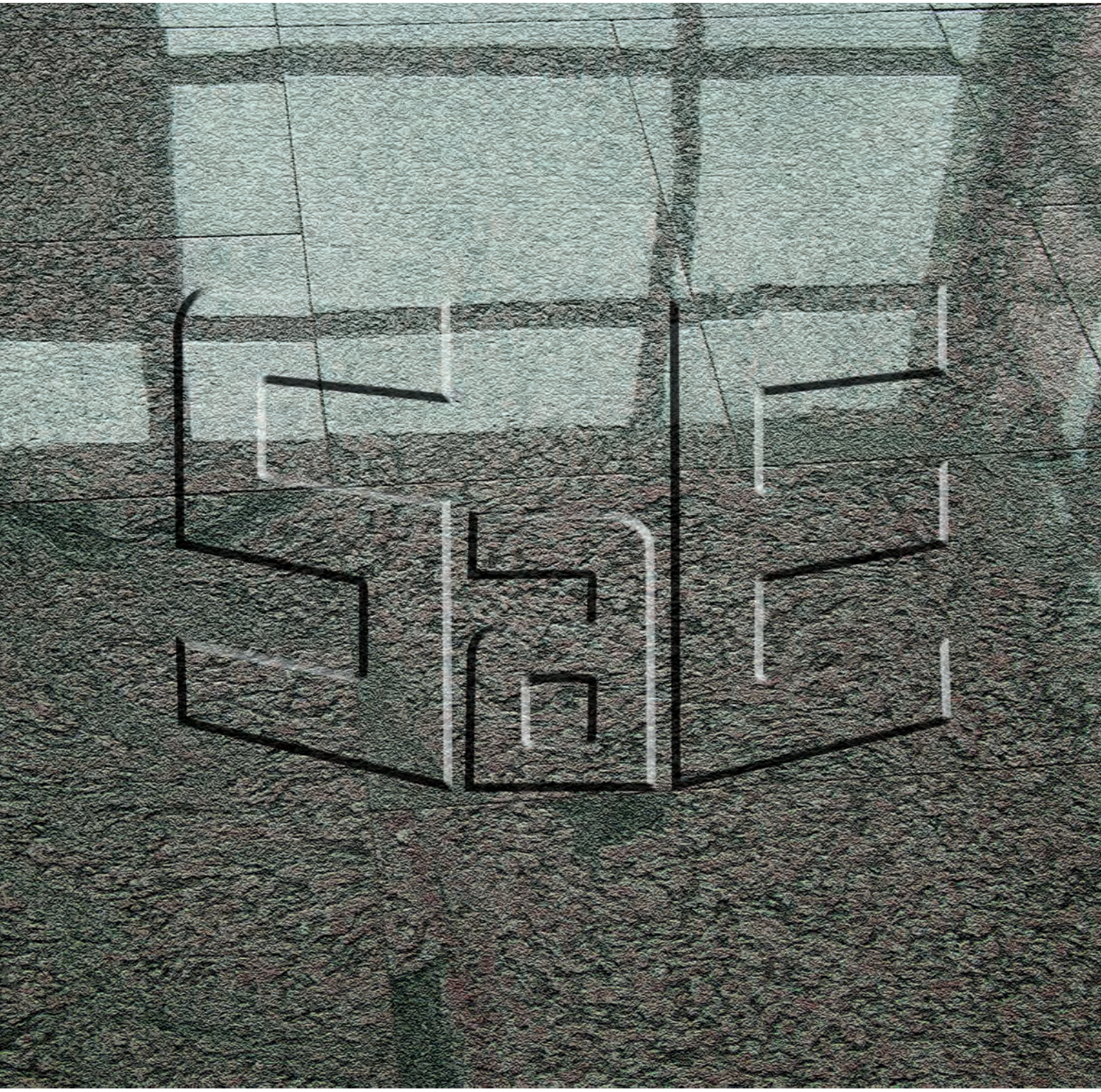

Available online at: https://sae.tu.kielce.pl

Contents

structure

environment

General data:

Format of the journal – electronic form

Frequency of publication – quarterly

The quarterly issues of Structure and Environment are their original versions

e-ISSN 2657-6902

ISSN 2081-1500

DOI: 10.30540/sae/0000

The journal published by:

Kielce University of Technology, Tysiąclecia Państwa Polskiego 7 Str. 25-314 Kielce, Poland
T.: +48 41 342 45 41

De Gruyter Poland:
Bogumiła Zuga 32A Str. 01-811 Warsaw, Poland
T.: +48 22 701 50 15

Journal Metrics:

Index Copernicus Value (IVC) 2021 = 100

The Polish Ministry of Education and Science 2024 = 40 points

Kielce University of Technology
2024

INDEX COPERNICUS
INTERNATIONAL

structure

Apolonia Kuc
Structure and Environment 2024, vol. 16, (2), pp. 67-75, Article number: el 006
https://doi.org/10.30540/sae-2024-006

Structure and Environment
ISSN 2081-1500
e-ISSN 2657-6902
https://content.sciendo.com/sae
https://sae.tu.kielce.pl

sciendo

Kielce University of Technology

DOI: 10.30540/sae-2024-006

IMPORTANCE OF HISTORICAL BACKGROUND OF THE PLACE AND CULTURAL AWARENESS IN DESIGNING COMPETITION PROJECTS DURING STUDENTS' WORKSHOPS

ZNACZENIE TŁA HISTORYCZNEGO DANEGO MIEJSCA I ŚWIADOMOŚCI KULTUROWEJ W TWORZENIU PROJEKTÓW KONKURSOWYCH PODCZAS WARSZTATÓW STUDENCKICH

Apolonia Kuc*
Jagiellonian University, Poland

Abstract

This article's primary objective is to illustrate how an understanding of the historical and cultural context of a location can significantly enhance students' academic workshops, fostering interdisciplinary knowledge acquisition and aiding them in designing projects for international architectural competitions. Frequently, such projects tend to conform to global trends, often imitating fashionable patterns without regard for the local context, traditions, or cultural nuances.
The first section of this article describes the methodology employed in international student workshops. The second section delves into the application of the problem-based learning method (PBL) when conceiving projects for architectural competitions, emphasizing the importance of factoring in historical and cultural heritage when selecting design concepts. The third section provides a comprehensive analysis of the workshop outcomes and initiates a discussion on the pivotal role of historical context and the significance of cultural awareness in this educational context.

Keywords: international architectural competition; architectural project; students' academic workshops; historical background of the place; cultural awareness

Streszczenie

Ten artykuł ma na celu pokazanie, w jaki sposób zrozumienie historycznego i kulturowego kontekstu danego miejsca może znacząco wzbogacić warsztaty akademickie dla studentów, sprzyjając interdyscyplinarnej akwizycji wiedzy i pomagając im w projektowaniu prac na międzynarodowe konkursy architektoniczne. Często takie projekty mają tendencję do podążania za globalnymi trendami, często naśladując modne wzorce bez uwzględnienia lokalnego kontekstu, tradycji czy kulturowych niuansów.
Pierwsza część tego artykułu opisuje metodykę stosowaną w międzynarodowych warsztatach studenckich. Druga część zagłębia się w zastosowanie metody nauki przez realizację projektów (PBL) poprzez tworzenie projektów na konkursy architektoniczne, podkreślając znaczenie uwzględniania dziedzictwa historycznego i kulturowego przy wyborze koncepcji projektowych. Trzecia część artykułu przedstawia szczegółową analizę wyników warsztatów i rozpoczyna dyskusję na temat kluczowej roli kontekstu historycznego oraz znaczenia świadomości kulturowej w tym kontekście edukacyjnym.

Słowa kluczowe: Międzynarodowy konkurs architektoniczny, projekt architektoniczny, studenckie warsztaty akademickie, historyczne tło miejsca, świadomość kulturowa

*Jagiellonian University, Poland, e-mail: apolonia.kuc@doctoral.uj.edu.pl

1. INTRODUCTION

In education of architects-engineers around the world the integration of interdisciplinary methodologies [1-3] and the strategic deployment of workshops [4, 5], particularly those with a competitive edge, are increasingly gaining traction globally. This pedagogical evolution is indicative of a broader, more collaborative approach to learning, where the confluence of diverse scientific and humanistic disciplines fosters a rich, multifaceted educational environment. This arenas with the rich interdisciplinary converge, attract a diverse assembly of students and experts from universities and academic institutions across the globe [6]. Such workshops, often hosted by prestigious universities and academic institutions both domestic and international, serve as crucibles for innovation and intellectual exchange.

The architecture workshops are one of the education elements of architects-engineers. These workshops, whether embedded within the academic curriculum or offered as supplementary activities, vary greatly in focus, ranging from specialised topics to broader themes including preparation projects for architectural competitions [6, 5].

The format and venue of these workshops are equally diverse, from traditional classroom at the campus to the internet communication and conference platforms such as MS Teams, Zoom, and Skype, and even global broadcasts, thereby transcending geographical boundaries to create a virtual platform for learning. The methodologies of the workshops differ depending on the adopted educational patterns and therefore, can have various approaches to the education process [8, 9]. The pedagogical strategies employed within these workshops are as varied as their formats, reflecting a spectrum of educational philosophies and approaches. This diversity underscores the dynamic nature of architectural education, highlighting the field's adaptability and its continuous evolution in response to the changing landscapes of technology, society, and culture.

This article shows the role and importance of historical and cultural background of the place as a part of an education process during architectural workshops, because human *race without the knowledge of its history is like a tree without roots* [7].

It is crucial to highlight how students gain a deeper understanding of transdisciplinary professional knowledge, skills, and competences through student led project-based learning [10, 11], which implements learning by doing, and blended learning approaches in the realms of architecture, design and construction [12]. Architecture, as a discipline, is intricately woven into the tapestry of history and culture [13]. It's important to note that architectural design is significantly influenced by historical context, which includes the physical, cultural, religious elements [14], and the evolving social dimensions of a place over time [15].

The significance of historical context cannot be overstated in architectural design; it serves as a wellspring of inspiration for creating buildings that honour their surroundings. Research consistently demonstrates that integrating historical context into architectural education enhances students' comprehension of their role as architects in preserving cultural heritage [16-18]. This involves conducting comprehensive analyses of the location and delving into historical studies, encompassing both the natural and cultural facets of the source [19].

Awareness of the imperative nature of preservation and historical context within architectural design education is crucial for future architects. The integration of heritage and historical context into architectural curricula fosters an appreciation for the importance of preservation and cultural heritage in the practice of architectural design [20-22] and creates possibilities for creating designs that are culturally appropriate and significant. By instilling this awareness, architecture students are better equipped to design structures that honour and safeguard the cultural heritage and historical context of a site, ultimately contributing to a sustainable and liveable built environment [13].

The primary objective of this article is to present how students acquired insights regarding the importance of understanding the historical and cultural background of a place during the 3rd International Student Workshop "2019 Kaira Looro Architecture Competition Peace Pavilion".

2. HISTORY OF INTERNATIONAL STUDENT WORKSHOPS

The 3rd International Student Workshops: "2019 Kaira Looro Architecture Competition Peace Pavilion", that took place from the 18th until the 26th of March 2019 in Krakow, Poland, are the result of long-lasting continuations cooperation between the Institute of Building Design, Faculty of Architecture Cracow University of Technology (CUT) in Krakow, Poland and the College of Environmental Design, Faculty of Architecture University of California Berkeley (UC Berkeley) in San Francisco, USA.

Fig. 1. Students and atutors: a) 1st workshops at the CUT in Krakow, Poland; b) 2nd workshops: at the UC Berkley in San Francisco, USA

Since the beginning of the cooperation in 2016, prof. Mark Anderson (UC Berkeley), prof. Peter Anderson (California College of the Arts, San Francisco) and prof. Sabina Kuc (CUT) organised three series of International Student Workshops. The 1st workshops in this collaboration were organised at the CUT in Krakow, Poland between the 18th and the 22nd of June 2018 an were entitled: "International Student Workshops: Drawing on City: King Kazimierz and The Secret Kiss" (Fig. 1). The 2nd workshops took place at the UC Berkeley in San Francisco, USA entitled: "International Student Workshops: Walls and Others: King Kazimierz and the Secret Kiss; Building toward Africa", 22 February-March 3, 2019 were part of Architectural Design IV classes supervised by prof. M. Anderson at Berkeley [23] (Fig. 2). In years 2018-2019 after prof. Mark Anderson and prof. Peter Anderson were beneficiaries of Fulbright Specialist Program, it became continuous trilateral scientific and didactic cooperation. The same group of students from the CUT and the UC Berkley participated in the workshops. The consultants partly changed due to the specificity of the topics of the workshops. The specialists of the 3rd workshops at the CUT included: prof. Carol Batker (University of San Francisco), prof. Wacław Celadyn (CUT), prof. Mateusz Gyurkovich (CUT), dr Paweł Mika (CUT) and mgr Apolonia Kuc (PhD student Jagiellonian University).

3. THE ROLE OF INTERNATIONAL STUDENT WORKSHOPS

The series of International Student Workshops were constructed based on the methodology used during prof. Mark Anderson "Architectural Design IV" design studio classes at UC Berkeley [23] and the philosophy of the educational process implemented during all three levels of university education (bachelor, master and PhD) at Faculty of Architecture at the CUT [24]. This approached was broaden by the introduction of international specialist in various fields (2nd and 3rd workshops) and the cross-continental cooperation between students from CUT and UC Berkeley with the use of conference video conversations (3rd workshops). Moreover, the experience of the use of internet communication and conference platforms during the 3rd workshops is especially useful during the COVID-19 pandemic for all participating universities to organise and conduct online classes with students at all education levels. During the workshops students worked with the interdisciplinary specialists from various fields of science and humanities, who "*can help, lead, keep track and determine the right direction"* of the competition projects [8]. This philosophy is widely used in the engineering and architectural education at the CUT: *"Interdisciplinary is the way of contemporary world"* [24]. This phrase shows the current trend in, not only, technical higher education, but the educational direction in general. It discloses the necessity of inclusion of the interdisciplinary approach to studies of architecture. Above-mentioned methodology is depicted on the graph (Fig. 2).

During the workshops, various ways of working, teaching and learning were implemented. These were design studio type of workshops [23]. The same group of students participated during three consecutive workshops and benefited from various forms of work: lecture, discussion, hand and computer drawings of the project [6]. The student's participation in specialists lecture, discussions and collation of their vision of the project combined with the expertise and knowledge of the specialists led to the deepening understanding of the project's issues and challenges that needs to be addressed and resolved. During the workshops, students worked with other students and

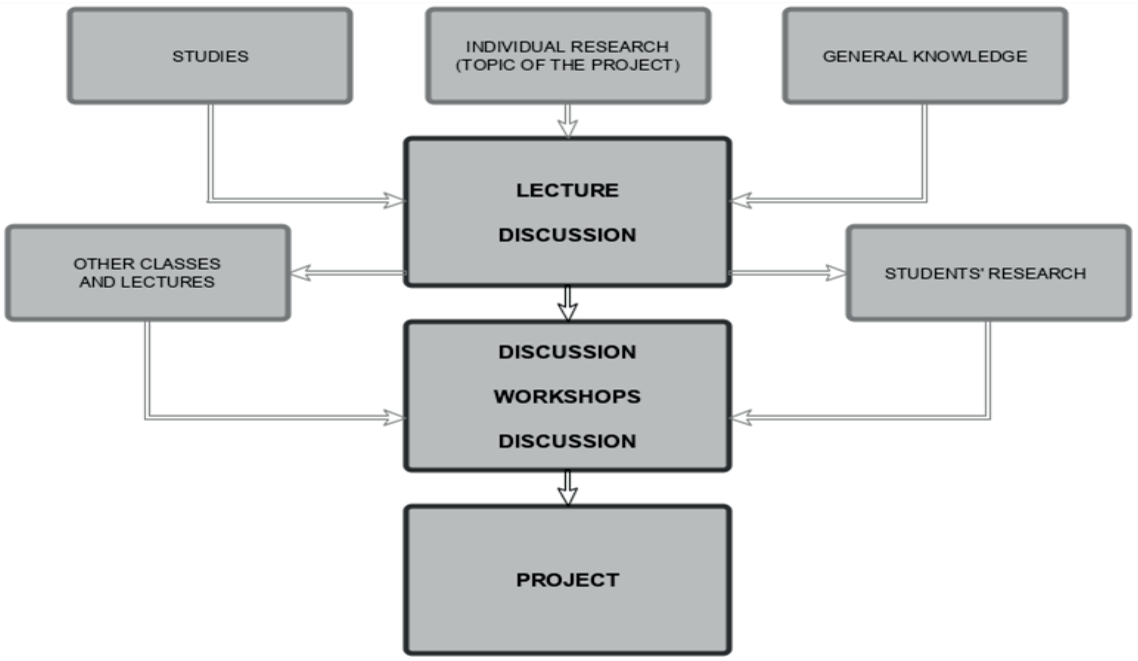

Fig. 2. The methodology of the workshops. The form of work (graph by A. Kuc)

specialists in the workshops' teams and therefore, they were introduced to the like-architectural office type of cooperation and worked as the team of professional architects. *Practicing architecture is asking one-self questions, finding one's own answers with the help of the teacher, whittling down, finding solutions. Over and over again. The strength of a good design lies in ourselves and in our ability to perceive the world with emotion and reason* [25]. The knowledge gain by students in this way helps them to make projects that are internationally competitive, interesting and can win international competitions.

This process fostered the growth of creativity [9] and other complex skills vital for their forthcoming professional endeavours. Given the ubiquitous nature of creativity, spanning from artistic and design fields to technology, science, and contemporary business practices, its development is particularly beneficial. The synergy between students and specialists (Fig. 2) not only enhances the students' general technical and architectural knowledge but also broadens their artistic perspectives. The varied background and general knowledge of each participant mixed with their specialised expertise and higher education plays a crucial role in knowledge exchange. This diversity fosters an environment where students can integrate multifaceted knowledge into their projects and further work. It also raises their historical sensitivity and awareness.

The objective of teaching design skills is to equip students, who are aspiring architects, with the capability to make autonomous design choices. These choices are crucial in shaping both architectural structures and the open spaces connected to them, aiming to fulfil the requirements of both individuals and communities. Making independent design decisions must be supported by foundation of knowledge, not only technical, but also holistic, interdisciplinary approach that includes historical perspectives. These workshops serve to enhance the participants' interdisciplinary understanding while simultaneously strengthening the collaborative ties between peers and colleagues from a range of universities and institutions, both in Poland and abroad.

4. THE CONCEPT OF PEACE PAVILION AS THE AIM OF THE 3RD INTERNATIONAL STUDENTS' WORKSHOPS

Peace is a dream, it can become a reality… but to build it we must be capable of dreaming.

Nelson Mandela [26]

The series of workshops was designed to familiarise students with potential challenges encountered during the architectural design phase. Spanning three sequential sessions, the workshops introduced diverse methodologies to engage students in exploring their cognitive and creative capacities. The culmination of this creative journey was the conceptualization of an architectural masterpiece – the Peace Pavilion. Inspired by Nelson Mandela's

vision of a harmonious Africa, *of an Africa which is in peace with itself* [26], the final project of the Pavilion ought to be the symbol and embody the dream of African continent, a beacon symbolizing the continent's aspirations for peace. Mandela's poignant words shaped the competition's ethos and informed the guidelines for the pavilion's design, becoming the main motto of the competition and the basis for the creation of the competition rules.

The essence of the Peace Pavilion lies in its dedication to fostering global universal peace, serving as a sanctuary for reflection, contemplation, and remembrance of those who have suffered or unjustly lost their lives in African conflicts.

The pavilion aims to establish a versatile space conducive to hosting both permanent and temporary exhibitions from artists championing peace and historical awareness. It is intended to be a repository of African history, offering insights through photographs and documents [26].

This location would have a rich historical heritage and is poised to function as the perfect backdrop for experimentation with diverse strategies that showcase the impact of historical context on design processes [15]. It aspires to transcend its role as a mere historical site; the pavilion project aims to create an innovative platform for exploring design strategies that vividly demonstrate the profound influence of historical narratives on architectural creativity.

In order to fulfil the competition guidelines including: the ideas of the competition, the symbolic message and ideological legibility, the following steps were implemented during the workshops: a) cultural and historical study, b) searching for inspiration, c) designing the project (Fig. 3). To achieve this, students got help and guidance from knowledgeable and experienced consultants – specialists in various fields, among many: architecture, history, building construction, and building construction in landscape architecture. One of them was a specialist in history and culture specialising in migration history and cultural heritage of ethnical minorities.

All the stages gave the students time for working with the specialist of history and culture. Figure 4 shows the methodology designing projects for architecture competition and choosing the right concept with the accordance with the historical, cultural and ethnical heritage. The first step was to research the historical and cultural background of the place/city/ region/ country. The second was the research of accessible materials in this region of Africa, and popular and culturally desirable colours and shapes. The third was the design stage of creating a conceptual design of the architectural project. Next, there was the verification of the design according to the history and culture of the place and implantation of knowledge and corrections into the architectural project. Lastly, the verification of the final elements of the architectural project. By using this methodology all the projects made during the workshops fulfilled the guidelines of Competition Agenda [26] and created good context-aware architecture.

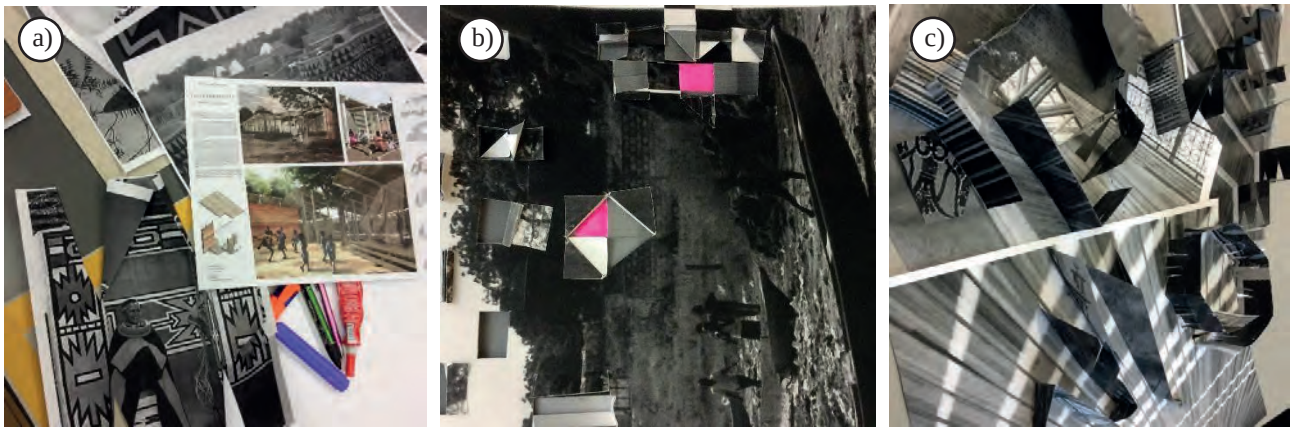

Fig. 3. The stages of the design process: a) cultural and historical study; b) searching for inspiration; c) designing the project (photographs by A. Kuc)

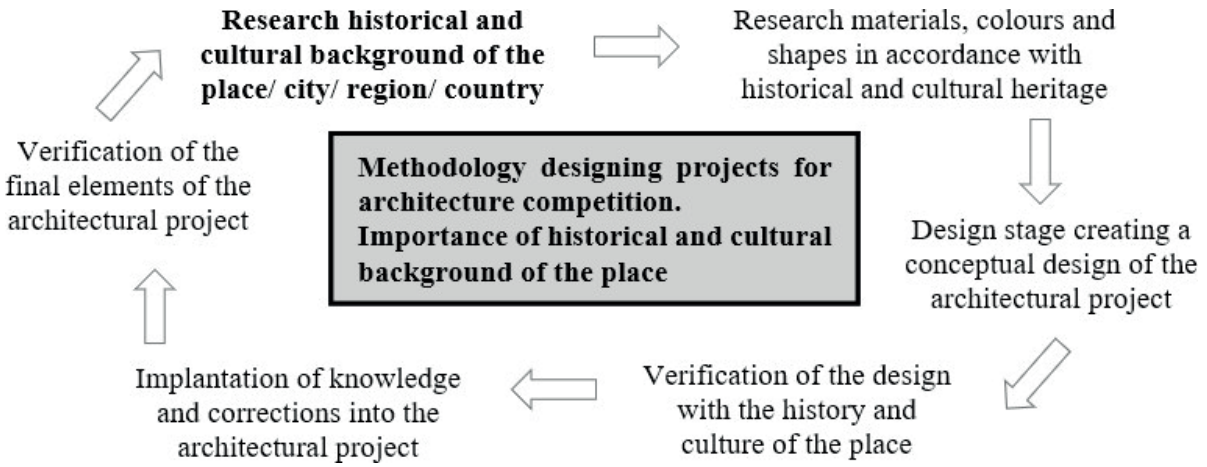

Fig. 4. Methodology designing projects for architecture competition and choosing the right concept with the accordance to the historical, cultural and ethnical heritage (author: A. Kuc)

5. IMPORTANCE OF HISTORICAL BACKGROUND – HISTORICAL AND CULTURAL AWARENESS

The evaluation of one's own social circumstance is part of the analysis of facts and events, and this kind of evaluation is, I feel, as good a starting point of the inquiry into the relations between philosophy and society as any other. Philosophy, in understanding human society, call for an analysis of facts and events, and an attempt to see how they fit into human life, and so how they make up human experience. In this way, philosophy, like history, can come to enrich, indeed to define, the experience of man.

Kwame Nkrumah [27]

In the 20th century, the African continent is an area that has experienced violence and mass migration. These conflicts resulted in millions of deaths and innumerable refugees. Families were forced to flee to other countries or cities in search of safety. The main reason for lack of stability in Africa's regions is internal conflicts on an ethnic, economic and political level. Cultural or religious differences or an effort to grab Africa's resources directly impacted the reason for the escalation of military conflicts in the region. Those issues directly and negatively contributed to the outbreak of the following conflicts mentioned in the competition agenda: War in the Democratic Republic of the Congo (1998-2003), Civil War in Sudan (1984-2005), Civil War in Angola (1975-2002), Genocide in Rwanda (April 1994-July 1994), Civil War in Mozambique (1977-1992), The Casamance Conflict (1982-now). War or any other conflict directly causes a stain on the community's memory. Exploring this difficult part of African history before creating a competition project is of high importance, especially when creating an architectural project in a foreign country or heritage side. Unfortunately, there is a lack of knowledge about those conflicts in the international community and occasionally among African communities themselves. Therefore, possessing basic knowledge of historical background is key to the creation of good context-aware architecture [26].

Before and while designing the project, students answered several questions regarding history and culture of the place such as: What is a general history of the place, the country, the region and the city? What topics/issues might be still present and sensitive (such as war, internal conflicts,corruption) in this area? Extremely important is, to begin with asking the questions with a broad scope that will help to understand general historical/cultural/ethnical background and "feel the atmosphere" of the area. Then, essential is to narrow it down to understand the history of the place-land, piece of ground and/or plot, on which there is a plan to design the project.

The awareness regarding the history and the culture of the place is extremely important. Firstly, it allows students to gain methodological tools that will enrich their design planning and future structure of the project. Secondly, it allows students to gain additional knowledge as a part of their degrees. Not only in history and the culture but especially brothering their horizons and being aware or sensitive issues that may accrue regarding design and realisation of their projects. Thirdly, architect- students, in this case, will have to answer certain historical and cultural questions. Choosing the wrong project for a certain place may lead to offence against religious feelings and historical inaccuracy. Understanding the complexity of historical and cultural background of the place and therefore, choosing right building material, shape

and placement of the element or construction in the project for a certain place is a key in a successful project. This will raise student's awareness sensitivity and regarding historical and ethical issues.

Understanding African culture, ethnical and religious diversity play a key role in the process of designing the competition project, for example, being aware of certain cultural differences between European, American and African regarding shapes and colours. That for some would not have any profound meaning, and for others would have complex positive and/or negative connotations. The historical, cultural, mythical, religious and ethnical background change the meaning of certain symbols. Many questions and issues needed to be addressed during the creation of the project for the 2019 Kaira Looro Architecture Competition, among many: What factors influence architecture? How does war or peace affect it? What is the symbolism of colours in this culture? What are the cultural conditions related to religion, tribalism and other intra-social relations? What research needs to be conducted in order to create relevant and influential architecture? What people who live there would like, appreciate and value in the design? The most important is to be fully aware of the implications of certain symbols and structures, history and culture of the place and to research what are the aesthetics and conceptual preferences of the design. In the case of 2019 Kaira Looro Architecture Competition Peace Pavilion workshops, students had a chance to discuss the above aspects with the specialist of history and culture and learned about culture, art, ethnographic aspects and history of geopolitical situations which directly became an inspiration in their design and influenced the final product- the architecture (Fig. 4).

Fig. 5. Materials created by one of the students during the workshops, showing ethnic African motifs and popular colours (author: Magda Samek)

Using certain colours and shapes has its consequences and implications. This issues were researched during the consultation with the specialist of history and culture, and some of the materials created by the students are showed in the Figure 5. Many motifs and popular colours were examined. For example, red- the colour of extremes. Some meanings are universal, red can mean blood, conflict, aggression, but in European and American culture has also positive implications. It means love, positive relationships and various happy celebration (Christmas, Valentine's Day etc.). In the case of the 2019 Kaira Looro Architecture Competition, using Scarlet Red should be extremely well-considered and using red shades that have more yellow or blue tones, would be much more apposite. By African culture, red is also seen as ambivalent colour. Some African tribes rub their bodies in red clay during various celebrations (for example Ndembu in Central Africa) [28]. They believe red is a symbol of life and good health. In other parts, it is seen as a representation of death and the colour of mourning [29]. The same issue is with using shapes, as for most students the shape of the African vessel would not have any religious and cultural implications, but for many visitors of the Peace Pavilion, it will. Therefore, not every shape we like can be applied in the design and before the use shapes need to be properly researched. Consequently, using certain colour and shapes in the wrong place within a certain culture may cause irreversible damage to the community, controversy or misinterpretations. Therefore, the specialist in history and culture helped to reduce those issue by advising students and teaching them about various aspects of the historical background of the place during the workshops. In order to understand history, human society, and culture, one should analyse facts and events and attempt to check how they fit into human life, and thus how they make up human experience. In this way, history of the place can enrich and even define human experience of architecture.

The cultural, ethical, and at times, religious heritage of a locale inhabitants can profoundly influence architectural project development. This is particularly evident in many countries in Africa, where cultural regions and group identities often transcend conventional geographical and administrative boundaries. Selecting a design concept that aligns with the unique essence of the surrounding environment, the historical context of the location, and the collective spirit of the community is essential for seamless integration of the Peace Pavilion. It ensures harmony

with the natural and built environment, and more importantly, with the historical essence and communal ethos of the users. The challenge lies in capturing and representing the nuanced, transboundary nature of cultural identity within the architectural design [30], a task that demands a deep understanding of the interplay between culture, history, and space. This careful consideration guarantees its relevance and utility in the years to come.

The winning entry of the 2019 Kaira Looro Architecture Competition exemplifies this with the following description: *The narrow and long gap between the two exhibition halls allows you to see the outside world. But as you pass by, the scenery outside the building will fade slowly and eventually fade away as the angle changes. It encourages visitors to reflect on and remember the relentlessness of the turmoil and its depression, as well as the fresh life that has fallen from the war, but most importantly, to look forward to a peaceful and beautiful world and the future. Light shines through the gap between the eaves and the rammed earth wall, hits the wall, increases the quietness of space, and the space in this area materializes the meaning of peace* [31]. The project intricates previously mentioned relationships between the project and its context by creating a space that gradually transitions visitors from the external world to a contemplative environment. This spatial design, with its narrow, elongating gap between exhibition halls, symbolizes the gradual fading of external chaos, encouraging reflection on turbulent and difficult past with a hopeful outlook towards a peaceful future. The interplay of light and structure in this design materializes the essence of peace, demonstrating the profound impact of thoughtful, context-sensitive architecture.

The jury of international architectural competitions pay attention to many aspects of project including construction, function, town planning, aesthetics, reference to cultural, historical context, tradition and the of the study. International architectural competition jury scrutinize various aspects of a project, including the general graphics design, its construction, functionality, urban planning, aesthetics, and the dialogue with cultural and historical narratives. Historical references often carry significant weight in these evaluations. The decision-making panels, comprising government representatives, architects, specialists, and journalists, frequently highlights the approach towards cultural and historical context as a decisive factor in award recognition [32]. Achieving a design that offers a timeless, universal commemoration while honouring the delicate, sometime even fragile, authentic remnants of history is crucial. The design should seamlessly blend with the existing landscape, introducing bold geometric forms and the strategic use of light to create spaces that are both timeless and functional [33]. Powerful forms with a clear geometry of squares, cubes, pillars, combined with a sense of universality and the articulate expression of the building's form, plays a pivotal role in the design's historical accuracy, ultimately influencing the project's perceived value and significance.

6. CONCLUSIONS

The current emphasis on an interdisciplinary approach in guiding young architects through independent project design is crucial. The synergy of cooperation between specialists and students not only facilitates the organization and execution of workshops but also fosters the interdisciplinary essence inherent in the development of competition projects. The examination of international student workshops emphasises the vital importance of historical and cultural inquiries in the project design, establishing it as a key component of the architectural competition design process.

These workshops engage students with the historical narrative and the ethnic and cultural components of the place chosen as a competition site. Such engagements significantly expand the students' perspectives, enhancing their understanding of profound societal concepts and issues like peace, memory, war, and the remembrance of victims. This enriched awareness is then skilfully woven into architectural projects, which are distinguished by their context-sensitive design and functionality.

REFERENCES

[1] Robinson K., *Out of our Minds*; Capstone (2011), In: *More about Interdisciplinarity*, 5 October 2018, https://www.ucl.ac.uk/basc/prospective/faq/interdisciplinarity (dostęp: 2023.12.02).
[2] Jacobs J.A., Frickel S., *Interdisciplinarity: a critical assessment*, Annual Review of Sociology, 35, 43-65 (2009).
[3] Condee W., *The interdisciplinary turn in the arts and humanities*, Issues in Interdiscipl. Studies, 34, 12-29 (2016).
[4] Białkiewicz A., *Architectural competitions support student creativity*. World Trans. on Engng. and Technol. Educ., 18, 2, 157-162 (2020).

[5] Haupt P., Wijas M., Mochacka S. and Chyb A., *Teaching architectural design through competition, motivation and challenge*. World Trans. on Engng. and Technol. Educ., 17, 3, 338-342 (2019).
[6] Białkiewicz A., *Aspects of teaching architecture in the context of educators' professional experience*. World Trans. *on Engng. and Technol. Educ.*, 17, 3, 244-249 (2019).
[7] Seifert Ch.C., *The Negro's or Ethiopian's Contribution to Art*. Baltimore: Black Classics Press, 5 (1983).
[8] Legény J., Špaček R. and Morgenstein P., *Binding architectural practice with education*. Global J. of Engng. Educ, 20, 1, 6-14 (2018).
[9] Sadykova S., Semenyuk O., Khvan E., Kuc S., *Development of students' creative skills through architectural workshops*, Global J. of Engng. Educ., 18, 3, 223-231 (2016).
[10] *How can you use project-based learning to teach history and social studies effectively?*, https://www.linkedin.com/advice/1/how-can-you-use-project-based-learning-teach-history- social (dostęp: 2023.12.02).
[11] Burlbaw L.M., Ortwein M.J. and Williams J.K., *2. The Project Method In Historical Context*, [in:] R.M. Capraro, M.M. Capraro and J. Morgan (eds.), *STEM Project-Based Learning: An Integrated Science, Technology, Engineering, and Mathematics (STEM) Approach*, p. 7-14, 2013.
[12] *"Back2Future" Project Learning Environment*, https://www.back2fut.eu/moodle/course/index.php (dostęp: 2023.12.02).
[13] Ceylan S., *The influence of historical context on architectural design: a retrospective analysis of student work*, World Transactions on Engineering and Technology Education, 21, 3, 205-210 (2023).
[14] Gil-Mastalerczyk J., *The importance of the relationship between religion and architecture through the lens of architectural education*, World Transactions on Engineering and Technology Education, 20, 1 (2022).
[15] Salama A.M., *A theory for integrating knowledge in architectural design education*. ArchNet- IJAR: Inter. J. of Architectural Research, 2, 1, 100-128 (2008).
[16] Embaby M.E., *Heritage conservation and architectural education: An educational methodology for design studios*. HBRC J., 10, 3, 339-350 (2014).
[17] Boarin P., Martinez-Molina A. and Juan-Ferruses I., *Understanding students' perception of sustainability in architecture education: a comparison among universities in three different continents*. J. of Cleaner Produc., 248, 119237 (2020).
[18] Banachowska E., *Second life of the 19th and 20th century buildings on the example of the revitalization of architecture buildings art galleries culture centres*, Structure and Environment, 11, 1/2019, s. 35-53.
[19] Gil-Mastalerczyk J., *Green architecture and natural-cultural teams – in the teaching process*, Structure and Environment, 8, 4/2016, s. 243-250.
[20] Pasha Y.N., Adnan S. and Naz N., *Status of culture in architectural education: a case study of Architectural School in Mehran University*, Jamshoro. Technical J., 25, 02, 15-32 (2020).
[21] Uzunoglu S.S. and Özden Ö., *Is cultural heritage still considered important in architectural education?* Inter. J. of Educational Sciences, 19 2-3, 120-126 (2017).
[22] Pasha Y.N., Adnan S. and Ahmed N., *Positioning historical evidences in architectural education: review of methods and contents*. Open House Inter., 45, 4, 481-507 (2020).
[23] Anderson M., *Architectural Design IV,* Berkeley Academic Guide 2019-20.
[24] Kuc S., Tadewicz A., *Interdisciplinary studies for PhD students in the Faculty of Architecture at Cracow University of Technology: part 1 - first year study*. Global J. of Engng. Educ, 20, 3, 224-229 (2018).
[25] Zumthor P., *Thinking Architecture*. Basel: Birkhäuser – Publishers for Architecture, 57 (1999).
[26] Kaira Looro Architecture Competition, Competition agenda (2019), 13 March 2019 www.kairalooro.com (dostęp: 2023.12.02).
[27] Nkrumah K., *Consciencism*. New York: New York University Press (1970).
[28] Red: Symbolic And Cultural Associations*, Object Retrieval*, project by artist Joshua Sofaer and is curated by Simon Gould in association with UCL (University College London) Museums & Collections, 15-21 October 2009, https://www.ucl.ac.uk/museums- static/objectretrieval/node/277 (dostęp: 2023.12.02).
[29] Pritchett J.A., *The Lunda-Ndembu: Style, Change and Social Transformation in South Central Africa*. Madison, Wis. (2001).
[30] Jordan P., *The Concept of the Cultural Region and the Importance of Coincidence between Administrative and Cultural Regions*. Romanian Review of Regional Studies. I. (2005).
[31] Kaira Looro Architecture Competition, List of Winners (2019), 16 March 2019 www.kairalooro.com (dostęp: 2023.12.02).
[32] Leading Architecture Design *Adjaye Associates Unveil New Landmark Project In Abu Dhabi For Higher Committee Of Human Fraternity* 10 January 2022, www.architectmagazine.com (dostęp: 2023.12.02).
[33] Announcement of the results of the competition for the development of the urban and architectural concept of the Polish Military Cemetery in Westerplatte 6 January 2022, www.muzeum1939.pl (dostęp: 2023.12.02).

Andrzej Szymon Borkowski, Marta Maroń, Patrycja Olszewska, Krzysztof Wójcik
Structure and Environment 2024, vol. 16, (2), pp. 76-83, Article number: el 007
https://doi.org/10.30540/sae-2024-007

Structure and Environment
ISSN 2081-1500
e-ISSN 2657-6902
https://content.sciendo.com/sae
https://sae.tu.kielce.pl

sciendo

Kielce University of Technology

DOI: 10.30540/sae-2024-007

PROBLEMS OF CALCULATING THE CARBON FOOTPRINT IN SCOPE 3 USING BIM

PROBLEMATYKA OBLICZANIA ŚLADU WĘGLOWEGO W ZAKRESIE 3 Z WYKORZYSTANIEM BIM

Andrzej Szymon Borkowski*, Marta Maroń, Patrycja Olszewska, Krzysztof Wójcik
Warsaw University of Technology, Poland

Abstract

The article presents the requirements of the EU EPBD (Energy Performance of Buildings Directive) for counting the carbon footprint (especially in Scope 3) and including it in construction projects from 2030. The obligation to count the carbon footprint will burden mainly designers, who are increasingly using BIM (Building Information Modelling) in the design process. Performing analysis and calculation of the carbon footprint in BIM models is hampered by the lack of non-graphical information on the subject in library components. The paper explains the concept of CO_2 in 3 scope, also discusses currently available tools for counting the carbon footprint, and examines how many components available on the Internet already contain non-graphical information on emissions, as well as ideas for implementing this directive. The advantages and disadvantages of these approaches were presented from the perspective of various stakeholders in the planning and investment and construction processes. The aim of the paper was to present possible solutions, ensuring compliance with the EU directive by proposing specific techniques, enabling the calculation of the Scope 3 carbon footprint, using BIM. In addition to a review of existing ideas, an authorial proposal for a national repository of carbon footprint information taking into account all stakeholders was presented.

Keywords: carbon footprint, CO_2, scope 3, EPBD, building information modeling, BIM

Streszczenie

W artykule przedstawiono wymagania unijnej dyrektywy EPBD (ang. Energy Performance of Buildings Directive) dotyczące liczenia śladu węglowego (zwłaszcza w zakresie 3) i uwzględniania go w projektach budowlanych od 2030 roku. Obowiązek liczenia śladu węglowego obciąży głównie projektantów, którzy coraz częściej wykorzystują BIM (ang. Building Information Modelling) w procesie projektowania. Przeprowadzanie analiz i obliczeń śladu węglowego w modelach BIM jest utrudnione ze względu na brak niegraficznych informacji na ten temat w komponentach bibliotecznych. W artykule wyjaśniono koncepcję liczenia CO_2 w tzw. zakresie 3, omówiono również obecnie dostępne narzędzia do liczenia śladu węglowego oraz zbadano, ile komponentów dostępnych w internecie zawiera już niegraficzne informacje na temat emisji, a także przedstawiono pomysły na wdrożenie tej dyrektywy. Zalety i wady tych podejść zostały zaprezentowane z perspektywy różnych interesariuszy procesów planistycznych i inwestycyjno-budowlanych. Celem artykułu było przedstawienie możliwych rozwiązań, zapewniających zgodność z dyrektywą UE poprzez zaproponowanie konkretnych technik umożliwiających obliczenie śladu węglowego z zakresu 3, z wykorzystaniem BIM. Oprócz przeglądu istniejących pomysłów przedstawiono autorską propozycję krajowego repozytorium informacji o śladzie węglowym z uwzględnieniem wszystkich interesariuszy.

Słowa kluczowe: CO_2, zakres 3, EPBD, modelowanie informacji o budynku, modelowanie informacji o obiekcie budowlanym, BIM

*Warsaw University of Technology, Poland, e-mail: andrzej.borkowski@pw.edu.pl

1. INTRODUCTION

Currently, the construction sector is the largest producer of CO_2 in the world. It accounts for almost 40% of all emissions of this greenhouse gas (Fig. 1) (Huang et al., 2018). The fundamental problem is that the construction industry, together with the transportation industry, directly contributes to climate change (Gallego-Schmid et al., 2020). For this reason, there is an emerging need to regulate the carbon footprint created at each stage of a construction project (Webber et al., 2009).

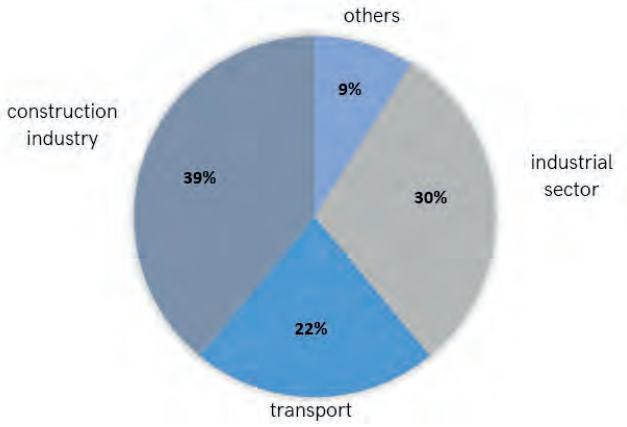

Fig. 1. Global CO_2 emissions by sector in 2018
Source: own elaboration based on (Sweco, 2023)

The European Union has set itself the goal of reducing CO_2 emissions and achieving climate neutrality by 2050 (Gilewski et al., 2023). Part of this plan set by the EPBD recast of March 14, 2023, is to give EU member states deadlines for providing details of the action plan – January 1, 2027. These concern the introduction of limits on the total cumulative global warming potential over the life cycle of all new buildings and the setting of targets for new buildings from 2030. The directive requires calculating the GWP (*Global Warming Potential*) and disclosing it on building energy performance certificates. CO_2 emissions are divided into operational (*OCF – Operational Carbon Footprint*) and embodied (*ECF – Embodied Carbon Footprint*) (Zima and Przesmycka, 2021). Currently, Polish law requires the calculation of only operational emissions, i.e. direct energy and water consumption. The directive's assumptions will also require the calculation and reporting of embedded emissions, which will translate into much more work (Wcisło-Karczewska, 2023) (Wcisło-Karczewska, 2023). Emissions CO_2 are divided, calculated and tracked by three scopes according to ISO 14067:2013. Scope 1 (Fig. 2) refers to direct emissions from sources owned or supervised by the organization. Indirect energy emissions refer to emissions in the generation of electricity, heat or steam consumed by organizations that occur in scope 2. Scope 3 emissions are those that arise from the organization's operations, but at locations under the control of other entities, e.g., the production of building materials (Kulczycka and Wernicka, 2015).

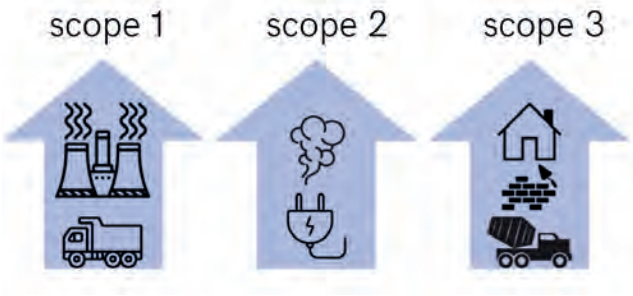

Fig. 2. Ranges of CO_2
Source: own elaboration

Scope 3 are indirect emissions that occur in an organization's value chain. This can include greenhouse gas emissions that are not controlled by organizations, but can affect them (Ruszkowski, 2022) (Ruszkowski, 2022). The problem of counting emissions in Scope 3 is complex, as they are divided into (*upstream*) higher-level and (*downstream)* lower-level emissions. Upstream emissions are those generated by organizations and institutions of which the organization counting the carbon footprint is a customer, and downstream emissions are those generated by the organization's customers. The biggest problem that occurs when counting Scope 3 emissions is that it counts the largest scope, which is also difficult to assess (Anquetin et al., 2022). It is important to determine how such emissions are counted because for many companies they account for more than 70% of the carbon footprint, e.g., a large portion of a building materials company's carbon footprint is Scope 3 emissions from mining, material handling and raw materials (Deloitte, 2023). The obligation to count the carbon footprint will fall mainly on design companies, and thus on designers, library object modelers, or analysts, who increasingly use modern digital technologies in their work.

BIM (Building Information Modeling) is defined as a collaborative process of people, systems, software, and in an even broader sense can include tangible, intangible or knowledge resources (Borkowski,

2023). From the designer's perspective, however, it is a relational database of the building object, which should be semantically rich, meaning that it contains all the necessary geometric and non-graphical information needed throughout the building life cycle (design, project implementation, management of the building object). There are also only six years to implement the objectives of the directive. Moreover, it is unrealistic to achieve it in Poland, due to the fact that the country does not have an official mandatory BIM standard (there is only an optional BIM Standard PL), nor a developed procedure for implementing it in the design process. According to experts, counting the carbon footprint is complicated, especially in the third scope, which includes the entire supply chain, yet it needs to be done (Pandey, Agrawal, Pandey, 2011). Thus, the purpose of this work was to present possible solutions to ensure compliance with the EU directive by proposing techniques to calculate the carbon footprint in scope 3. The paper conducted a deep literature review of methodologies and IT tools for tracking the carbon footprint. This poses a challenge because there is currently no established method for obtaining this information and adding it to a construction project. The biggest problem seems to be BIM library objects that do not include CO_2 information. Solutions to such a problem continue to evolve and are realizing the first steps to achieve targets for future years. This goal is very difficult or, according to some, even impossible to achieve, as it implies a very large amount of work.

2. LITERATURE REVIEW

Building products and related materials and processes require targeted requirements with more linkages between sectors and changes in production practices of commonly used materials associated with high greenhouse gas emissions (Maduta et al., 2022). At a minimum, the goal appears to be to calculate and track both embedded and operational carbon footprints. There are a number of different methods for calculating the carbon footprint of, among other things, Scope 3. They make it possible to obtain the full dimension of CO_2 for the entire life cycle of a given investment. The choice of a particular method depends on needs and data availability. A common way is to use plug-ins and services that augment any BIM-type software. One of them is Green Building Studio, which is a cloud service that allows for extensive analysis in the energy sector. It allows calculating a building's energy consumption based on building type and location (Borkowski et al., 2022). Carbo Life Calculator, on the other hand, is a tool for calculating the carbon footprint that is emitted throughout the life cycle of a building. It retrieves information on the value of materials at the scale of a model in Autodesk Revit, for example. The add-on significantly improves carbon footprint analyses and allows you to know the full scale of emissions. Carbo Life Calculator uses databases from EPD, among others, to obtain reports. Another plug-in for studying the carbon footprint is Design Builder. It is a tool for performing complex energy consumption analysis and checking the compliance of projects with energy certifications like EPCs in the UK. The software also allows you to manage lighting or other building systems like air conditioning. This makes it possible to make changes to a project to improve the conditions of the building's occupants and reduce CO_2 (Pawar and Kanade, 2018). Counting the carbon footprint is now also possible through websites or online services (Dreijerink, Paradies, 2020). These focus on electricity consumption, home heating or vehicle driving, among other things. One such program is the Carbon Footprint Calculator. It counts the approximate and total amount of CO_2 that is emitted by a household (Łasut and Kulczycka, 2014). Another group of websites are those that count direct emissions and are related to one's activities, as well as indirect emissions that are not directly influenced. A site that does such calculations includes "Carbon Footprint Ltd." It uses external databases where data on current environmental impacts are available (Łasut and Kulczycka, 2014). One Click LCA is an automated building life cycle assessment software. Among other things, it is used to quantify the operational and embedded carbon footprint of a building. It will also estimate CO_2 emissions based on the size and type of the facility in question, and compare, optimize and visualize the carbon efficiency of alternative designs (LCA, 2023).

Currently, there is no universal program for calculating the carbon footprint, nor is there a method for this program to use. This is a big problem because it makes it difficult to track the total carbon footprint for investments and makes it difficult to count the amount of CO_2 for smaller companies. Thus, the discussion on this topic is ongoing, and there are at least several proposals.

Table 1. Selected software for calculating the carbon footprint of buildings and construction projects. Source: own elaboration

Tool	Type	Destination	Properties	Cost
Green Building Studio	plug-in/web service	Energy analysis in the design phase (Borkowski et al., 2022)	Allows calculation of building energy consumption based on building type and location	Commercial (30-day free trial period)
Carbo Life Calculator	plug	Calculating the carbon footprint that is emitted throughout the life cycle of a facility	Uses databases including EPD to obtain reports; Retrieves carbon footprint information at model scale in Revit	Free
Design Builder	plug	Analyzing energy consumption and verifying projects' compliance with energy certifications like EPCs in the UK (Pawar and Kanade, 2018)	Ability to manage building systems and make changes to improve the comfort of its occupants	Commercial (30-day free trial period)
One Click	software	Counting a building's carbon footprint and its emissions (LCA, 2023)	Automated building life cycle assessment, database of information on carbon footprint of individual elements	Commercial
Carbon Footprint Calculator	website	Counting the approximate and total amount of CO_2 that is emitted by a household (Łasut and Kulczycka, 2014)	Focuses on electricity consumption and heating	Free
Carbon Footprint Ltd.	website	Counting the building's indirect and direct emissions (Łasut and Kulczycka, 2014)	Uses external databases where data on current environmental impacts are available	Free

3. COMPONENT RESOURCES WITH AN INDICATED CARBON FOOTPRINT

Working in BIM requires that the building is equipped with library components available in digital form, oriented to a certain degree of geometric information (LoD, Level of Detail), enriched with non-graphical information (LoI, Level of Information). As a rule, such objects (components) can be easily downloaded and used in currently used software. However, there is a growing demand for each object to have not only physical information, but also non-geometric data such as product information, instructions, operating costs or just the carbon footprint of the manufactured product. The website bimobject.com is one popular site that has a huge resource of building product components. For Revit software alone, it has tens of thousands of so-called families. However, there are only 1,481 components that have CO_2 included. Currently, 32 brands produce such components, and one such manufacturer is the Hansgrohe brand. It produces about 590 models that include parameters about emissions. Of all the families that offer information on CO_2, not a single one is manufactured in Poland. A significant number of components are manufactured in Germany, as many as 1152. The main reason for this result is the high level of BIM implementation in the construction sector in Germany (Schumacher et al., 2022). Thus, the awareness of building material manufacturers on this topic is growing.

Using the bimobject browser (bimobject, 2018) one product was checked: a kitchen faucet from hansgrohe (Fig. 3). It has all the necessary information along with those for producing a carbon footprint at each stage of production (Fig. 4). This can be a benchmark for other companies that intend to include CO_2 parameters for each model in the future.

Fig. 3. Kitchen faucet by hansgrohe Source: (bimobject, 2018)

EPD Data (Simplified) A1-A3
Energy Consumption (A1-A3) 123.7 MJ
EPD Declaration Unit 1 piece of an average kitchen faucet incl. packaging
EPD Document Link
https://epd-online.com/PublishedEpd/Download/14889
EPD Expiration Date 2028-02-23
EPD Issue Date 2023-02-24
EPD Registration Number EPD-HAN-20230024-ICC1-EN
Global Warming (A1-A3) 5.977 kgCO2
Non Renewable Resources Consumption (A1-A3) 97.8 MJ
Waste Production (A1-A3) 1.15375 kg
Water Consumption (A1-A3) 0.215 m³

EPD Data (Simplified) A4-A5
Energy Consumption (A4-A5) 3.1435 MJ
Global Warming (A4-A5) 0.91033 kgCO2
Non Renewable Resources Consumption (A4-A5) 2.933 MJ
Waste Production (A4-A5) 0.43152 kg
Water Consumption (A4-A5) 0.00043 m³

EPD Data (Simplified) B1-B7
Energy Consumption (B1-B7) 5893.1 MJ
Global Warming (B1-B7) 341.0379 kgCO2
Non Renewable Resources Consumption (B1-B7) 5754 MJ
Waste Production (B1-B7) 25.60579 kg
Water Consumption (B1-B7) 0.2653 m³

EPD Data (Simplified) C1-C4
Energy Consumption (C1-C4) 1.46044 MJ
Global Warming (C1-C4) 0.82579 kgCO2
Non Renewable Resources Consumption (C1-C4) 1.1345 MJ
Waste Production (C1-C4) 1.60261 kg
Water Consumption (C1-C4) 0.00197 m³

EPD Data (Simplified) D
Energy Consumption (D) -63.2 MJ
Global Warming (D) -4.55112 kgCO2
Non Renewable Resources Consumption (D) -48.2 MJ
Waste Production (D) -0.85953 kg
Water Consumption (D) -0.167 m³

Fig. 4. List of CO_2 information found in the hansgrohe kitchen faucet family. Source: (bimobject, 2018)

Adhering to the EPBD, there is no established framework or solution for how to calculate and insert carbon footprint information in architectural and building designs. However, there are currently several proposals for systems for calculating and inserting this information. They are extremely different, each of which contains peculiar problems for particular stakeholder groups. The stakeholder groups that will be most affected by the new obligation are: (i) manufacturers, (ii) suppliers, (iii) contractors, (iv) investors, and (v) intermediaries.

4. CARBON FOOTPRINT INVOICING

One widely discussed proposal is carbon footprint invoicing. The proposal calls for each stakeholder group to independently calculate and then invoice information about the CO_2 it emitted in the course of manufacturing or performing another activity. Such information is then to be entered manually, as non-graphical information, into the BIM model that forms the basis of project development. This would most likely be the responsibility of contractors, as this is the lowest stakeholder group in the supply chain. Such a system would most likely require the hiring of additional people to enter this data, or a significant expansion of the responsibilities of BIM modelers and BIM coordinators. This is a transfer of almost all responsibility for complying with the EPBD to contractors, suppliers and manufacturers, without any help from the legislature. Moreover, the solution does not involve the introduction of a predetermined method or tool for counting the carbon footprint. Finding one then becomes the responsibility of stakeholders, which can be a problem, especially for micro and small companies. The advantage is that this information can be entered into the model using Dynamo scripts, but this requires a great deal of familiarity with programs working in BIM, which again favors large companies that use such solutions to a greater extent. In addition, all intermediaries would be required to know the process and follow it. Otherwise, there could be a disruption in the invoicing process.

5. CREATE BIM COMPONENTS SUPPLEMENTED WITH CARBON FOOTPRINT INFORMATION

The ability to create library components supplemented with the necessary carbon footprint data would allow the investment model to be enriched. The unit responsible for creating such components could use the aforementioned plug-ins or BIM-compatible tools. The process of creating them would begin at the production stage. By design, this is an innovative proposal, but unfortunately it is quite problematic in reality. In Poland, the construction industry is largely not using BIM (Apollo and Grzyl, 2023). The early stage of advancement, or lack thereof, does not only affect smaller companies. A materials manufacturer is unlikely to have access to the software and the appropriate qualifications to produce a library component enhanced with the required non-graphical carbon footprint information. Such an opportunity will be possible for larger companies with specialists in this field. Therefore, the exchange of library components between stakeholders and supplementing them with the necessary data could occur in a small number of cases. A certain solution to offset the problem would be to hire a qualified person in this area. In this case, the BIM Modeler would be responsible for enriching with information all components concerning the

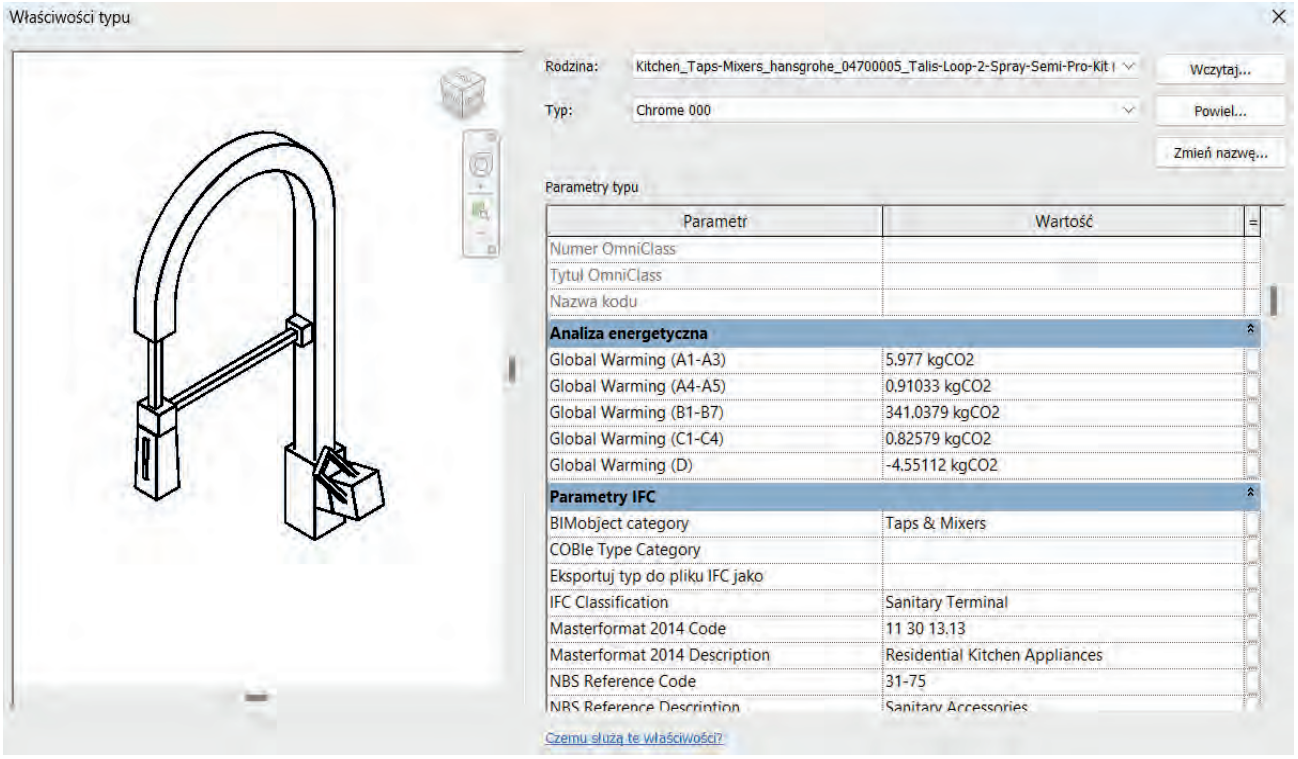

Fig. 5. Table of family parameters with included carbon footprint information
Source: own compilation based on bimobject, 2018

entire investment process. However, the person most likely to be hired on the developer's side might not have such detailed information on CO_2 in the material creation process. Theoretically, carbon footprint data can be entered by the designer using catalog information from manufacturers (Meinrenken et al., 2022). This will involve more work, but it is possible. Entering such data as entity, type or shared parameters can improve the performance of subsequent analyses (Al-Obaidy, Courard, Attia, 2022).

One example that deals with supplementing in carbon footprint information is the aforementioned kitchen faucet from hansgrohe (Fig. 5). Revit software was used to carry out the work on the family. The process began with loading the model into the project and verifying the existing parameters in it, which were provided by the manufacturer. The information was then implemented into the parameters of the family model. The result of the work was a family rich in non-graphical data on the extent of the carbon footprint, which meets the guidelines of the EU EPBD. If each library component was developed with non-graphical data, it would be a great convenience for stakeholders. Potentially, a library object modeler or designer could supplement the information manually with the properties and environmental footprint of the product from the following stages, among others: extraction and processing of raw materials, production and packaging, distribution and storage, use or disposal. Unfortunately, the level of BIM in Poland is not developed enough to make this possible and feasible (Apollo and Grzyl, 2023). The results of other research studies show that the diffusion of sustainable products can be hindered due to problems with the mechanisms for creating and exchanging BIM objects, the quality of BIM objects, the usability of BIM library platforms and participation on sharing platforms (Bahrami, Atkin, Landin, 2019).

6. PROPOSAL FOR CHANGE

A proposal to meet the objectives of the EU directive is for the legislature to create a nationwide repository of carbon footprint information. To this end, there could be a database containing information on the carbon footprint of individual facilities, along with specific codes for each product and category. The repository could use CCI (*Construction Classification International*) codes. These codes, based on the Danish CCS classification system, are a common international classification. It is hierarchical and based on the properties of the individual elements being described. The main tenets of CCI are

a language understandable to humans and machines, a logical structure and standardized nomenclature, online usability and uninterrupted flow of information (Idzkowski et al., 2021). An example code for a wall of wallboard is B10.AD30.ULM(ESE.21), and the basic code for a tap is: HB01, but can be supplemented with additional information including Stage of Design, requirements for additional fixtures, costs, etc. (Liias et al., 2021). The repository could also include a tool for calculating the carbon footprint in a one-size-fits-all manner. A website would allow users to post information about their products or services, among other carbon footprints, and the system, based on the product and category, would assign it a unique CCI code used later to track changes at each stage of the investment. The repository could also allow components with CO_2 information, but this would not be mandatory. This would make it possible for larger companies with resources and BIM specialists to post their product components, while smaller companies could post non-graphical information. An additional advantage of this solution is the possibility of creating plug-ins for BIM-enabled programs, which would greatly streamline the process of adding carbon footprint information or even the components themselves to a project. The disadvantage of such a repository, however, is the large amount of work on the part of the legislator who would have to create and operate such a system, which would entail a large financial outlay. The information system of such a repository should allow plurality of BIM platforms and give the possibility to place components from different design software vendors. It may also be a problem e m to implement all stakeholders in the new process. Each of the involved stakeholder groups of the investment and construction processes (designers, general contractors, building material manufacturers, clients or administrators) would have to be given detailed instructions on how to post reliable footprint information in the repository. For the purpose of calculating the carbon footprint for an investment, new software could be developed based on data from the repository, or even an integrated tool that could be built into the IT platform. At the same time, this is a direction for further research that the authors want to undertake in the future.

7. CONCLUSION

Counting the carbon footprint, especially in Scope 3, for each investment component, as required by the EPBD, is challenging. Moreover, there is currently no legally established way to calculate CO_2 or a system for including this information in projects. The situation is further exacerbated by the fact that Poland currently has no officially established BIM standard. The systems currently proposed are unrealistic because they assume that every subcontractor and supplier would be able to calculate the carbon footprint on their own, or create a BIM component with non-graphical information. This would require training or hiring many people solely for this purpose. The repository idea, on the other hand, would make the task easier for stakeholders and make the CCI code base more widespread in Poland, but it would require significant funding and the creation and requirement of a system by the legislature. The time to introduce efficient enabling solutions is only 6 years. Therefore, it requires coordinated action by experts and the legislature to establish a standardized plan for implementing the requirements of the EPBD as smoothly as possible.

REFERENCES

[1] Anquetin T., Coqueret G., Tavin B., Welgryn L. (2022). *Scopes of carbon emissions and their impact on green portfolios*. Economic Modelling, 115, 105951.
[2] Al-Obaidy M., Courard L., Attia S. (2022). *A parametric approach to optimizing building construction systems and carbon footprint: A case study inspired by circularity principles*. Sustainability, 14(6), 3370.
[3] Apollo M., Grzyl B. (2023). *Aktualny stan wdrożenia BIM w polskich firmach budowlanych*. Materiały Budowlane, 606 (2), 28-31 (in Polish).
[4] Bahrami S., Atkin B., Landin A. (2019). *Enabling the diffusion of sustainable product innovations in BIM library platforms*. Journal of Innovation Management, 7(4), 106-130.
[5] bimobject, 2018. www.bimobject.com. [Online] URL: https://www.bimobject.com/pl/hansgrohe/product/04700005 [accessed on december 2023].
[6] Borkowski A.S., Osińska N., Szymańska N. (2022). *Analizy energetyczne w modelach BIM 6D*. Materiały Budowlane, 8, 55 (in Polish).
[7] Borkowski A.S. (2023). *A Literature Review of BIM Definitions: Narrow and Broad Views.* Technologies, 11(6), 176.
[8] Deloitte 2023. www2.deloitte.com. [Online] URL: https://www2.deloitte.com/uk/en/focus/climate-change/zero-in-on-scope-1-2-and-3-emissions.html [accessed on November 2023].

[9] Dreijerink L.J.M., Paradies G.L. (2020). *How to reduce individual environmental impact? A literature review into the effects and behavioral change potential of carbon footprint calculators.* https://publications.tno.nl/publication/34637488/DtNct6/TNO-2020-P11148.pdf [accessed on Janurary 2024].
[10] Gallego-Schmid A., Chen H.M., Sharmina M., Mendoza J.M.F. (2020). *Links between circular economy and climate change mitigation in the built environment*. Journal of Cleaner Production, 260, 121115.
[11] Gilewski P., Pierzchalski M., Węglarz A. (2023). *Wymagania prawne wybranych krajów europejskich dotyczące obliczania śladu węglowego budynków*. Budownictwo i Prawo, 26(2), 3-7.
[12] Huang L., Krigsvoll G., Johansen F., Liu Y., Zhang X. (2018). *Carbon emission of global construction sector*. Renewable and Sustainable Energy Reviews, 81, 1906-1916.
[13] Idźkowski F. i in. (2021). *W poszukiwaniu wspólnego systemu klasyfikacyjnego dla procesów budowlanych*. Przewodnik Projektanta, 4/2021, s. 44. (in Polish).
[14] Kulczycka J., Wernicka M. (2015). *Metody i wyniki obliczania śladu węglowego działalności wybranych podmiotów branży energetycznej i wydobywczej*. Zeszyty Naukowe Instytutu Gospodarki Surowcami Mineralnymi i Energią PAN, (89), 133-142 (in Polish).
[15] LCA, O.C. (2023). One Click LCA. [Online] URL: https://www.oneclicklca.com/ [accesed on November 2023].
[16] Liias R. i in. (2021). *CCI-EE CLASSIFICATION SYSTEM: ESSENCE AND USE*, Tallinn: Tallinn University of Technology.
[17] Łasut P., Kulczycka J. (2014). *Metody i programy obliczające ślad węglowy*. Zeszyty Naukowe Instytutu Gospodarki Surowcami Mineralnymi i Energią PAN, (87), 137-147 (in Polish).
[18] Maduta C., Melica G., D'Agostino D., Bertoldi P. (2022). *Towards a decarbonised building stock by 2050: The meaning and the role of zero emission buildings (ZEBs) in Europe*. Energy Strategy Reviews, 44, 101009.
[19] Meinrenken C.J., Chen D., Esparza R.A., Iyer V., Paridis S.P., Prasad A., Whillas E. (2022). *The Carbon Catalogue, carbon footprints of 866 commercial products from 8 industry sectors and 5 continents*. Scientific Data, 9(1), 87.
[20] Pawar B.S., Kanade G.N. (2018). *Energy optimization of building using design builder software*. International Journal of New Technology and Research, 4(1), 263152.
[21] Pandey D., Agrawal M., Pandey J.S. (2011). *Carbon footprint: current methods of estimation*. Environmental monitoring and assessment, 178, 135-160.
[22] Ruszkowski P. (2022). *Ślad węglowy w świadomości społecznej.* Energetyka – Społeczeństwo – Polityka. 10/2022, s. 43 (in Polish).
[23] Schumacher R., Theißen S., Höper J., Drzymalla J., Lambertz M., Hollberg A., ... Meins-Becker A. (2022). *Analysis of current practice and future potentials of LCA in a BIM-based design process in Germany*. In E3S Web of Conferences (Vol. 349, p. 10004). EDP Sciences.
[24] Sweco A. (2023). Sweco. [Online] URL: https://www.sweco.pl/aktualnosci/blog/jak-potezny-jest-slad-weglowy-budownictwa/ (accessed on December 2023).
[25] Wcisło-Karczewska K. (2023). *Obowiązki w zakresie śladu węglowego*. RP Nieruchomości (accessed on November 2023) (in Polish).
[26] Webber C.L., Matthews H.S. i Huang Y.A. (2009). *Calculating the carbon footprint of scope three using BIM*. Environmental Science i Technology, 43(22), 8471-8702.
[27] Zima K., Przesmycka A. (2021). *Koncepcja zintegrowanej analizy kosztów i generowanego śladu węglowego w cyklu życia budynku*. Przegląd Budowlany, 92(10), 42-48 (in Polish).

Łukasz Kapusta, Szymon Sobura
Structure and Environment 2024, vol. 16, (2), pp. 84-96, Article number: el 008
https://doi.org/10.30540/sae-2024-008

Structure and Environment
ISSN 2081-1500
e-ISSN 2657-6902
https://content.sciendo.com/sae
https://sae.tu.kielce.pl

sciendo

Kielce University of Technology

DOI: 10.30540/sae-2024-008

ASSESING THE POTENTIAL OF DIGITAL TERRAIN MODELS FOR MONITORING ADDITIONAL SUBSIDENCE OF COMMUNICATION EMBANKMENTS IN MINING AREAS – A CASE STUDY

OCENA MOŻLIWOŚCI NUMERYCZNYCH MODELI TERENU DO MONITOROWANIA DODATKOWYCH OBNIŻEŃ NASYPÓW KOMUNIKACYJNYCH NA TERENACH GÓRNICZYCH – STUDIUM PRZYPADKU

Łukasz Kapusta, Szymon Sobura*
Kielce University of Technology, Poland

Abstract

Today's technologies make it possible to capture certain phenomena that were very difficult or impossible to observe in terms of classical measurements. One of them is the so-called sinking of embankments. It is common in mining areas. It consists in the additional subsidence of the embankments into the ground, above the value of the lowering of the adjacent area. It takes place primarily in the zone of horizontal tensile deformations. The paper presents the results of comparative DTM (Digital Terrain Model) analyzes from 2001, 2014, 2018 and 2021. Their aim was to assess the usefulness of DTM data for monitoring the additional sinking of the communication embankment on the example of the northern bypass of Bytom. The authors analyzed digital terrain models generated in the process of rasterization of data from ALS (Airborn Laser Scanning).

Keywords: mining subsidence, digital terrain model, communication embankments, post-mining areas

Streszczenie

Dzisiejsze technologie pozwalają wychwycić pewne zjawiska, które w ujęciu pomiarów klasycznych były bardzo trudne lub też niemożliwe do zaobserwowania. Jednym z nich jest zjawisko tzw. tonięcia nasypów. Występuje ono powszechnie na terenach górniczych. Polega na dodatkowym zagłębianiu się budowli w podłoże, ponad wartość obniżenia terenu przyległego. Ma ono miejsce przede wszystkim w strefie poziomych odkształceń rozciągających. W pracy przedstawiono wyniki analiz porównawczych NMT z lat 2001, 2014, 2018 i 2021. Ich celem była ocena przydatności danych z NMT do monitorowania dodatkowego zagłębiania nasypu komunikacyjnego na przykładzie północnej obwodnicy Bytomia. Autorzy poddali analizom numeryczne modele terenu wygenerowane w procesie rasteryzacji danych pochodzących głównie z lotniczego skanowania laserowego ALS.

Słowa kluczowe: osiadania górnicze, numeryczny model terenu, nasypy komunikacyjne, tereny poeksploatacyjne

1. INTRODUCTION

Mining activities can lead to negative environmental impacts in the area of road infrastructure and safety of engineering structures [1-5]. For this reason, monitoring activities are being undertaken [6]. Geographic information systems (GIS) is a digital

*Kielce University of Technology, Poland, e-mail: e-mail: ssobura@tu.kielce.pl

technology that enables the collection, management, analysis and presentation of spatial data for a wide range of applications, including mining [7]. GIS provides effective support for classical surveying in the process of monitoring hazards caused by mining operations [8]. The digital terrain models (DTMs) included in the GIS database, which are the result of laser scanning, can be used to observe phenomena within the road infrastructure, till now difficult to monitor. One of them is the so-called sinking of embankments. It commonly occurs in mining areas. It consists in additional sinking of embankment structures into the ground, above the value of lowering the adjacent land [9, 10].

This paper presents the results of comparative analyses of DTMs from 2012, 2018 and 2021, with the aim of assessing the suitability of DTM data for monitoring the additional sinking of the traffic embankment of Bytom's northern ring road. The numerical terrain models subjected to analysis were generated by rasterization of airborne laser scanning (ALS) data.

2. THEORETICAL BACKGROUND

The phenomenon of so-called embankment sinking, consisting of additional lowering of structures into the subsoil, above the value of the adjacent ground depression, occurs primarily in the zone of horizontal tensile strain of the subsoil in the boundary zone of the depression basin. It arises when the ultimate bearing capacity of the subsoil is exceeded due to the redistribution of the horizontal components of the state of stress [9-10]. The theoretical basis of the phenomenon of additional embankment subsidence has been known since the 1970s. The first publications in this area in the Polish literature are the works of: Szumierz [11], Litvinowicz [12] or Rosikon [13]. The description of changes in the state of stress in the subsoil loaded with a traffic embankment is presented, among others, in the work of Klosek [14].

In the subsoil loaded with an embankment, there is a state of stress caused by the dead weight of the soil medium and the weight of the embankment. The stress relation in soil takes the form [14]:

$$\sigma_{ik} = \gamma_0 \cdot h \cdot \begin{vmatrix} 1 & 0 & 0 \\ 0 & (m-1) & 0 \\ 0 & 0 & (m-1) \end{vmatrix}$$

where:
γ_0 – average volumetric soil mass;
h – the depth of the point under examination;
m – the transverse deformation coefficient of the soil.

$$m = \frac{1}{\vartheta}$$

ϑ – Poisson coefficient.

Horizontal tensile strains induce changes in the stress components of the stress state. The increments of the stress state components for the principal directions can be written in the form of a tensor:

$$\Delta\sigma_{ik} = \begin{vmatrix} 0 & 0 & 0 \\ 0 & \frac{2G(m+\rho)}{m-1}\varepsilon_{22} & 0 \\ 0 & 0 & \frac{2G(1+m\rho)}{m-1}\varepsilon_{22} \end{vmatrix}$$

where:
ρ – ratio of horizontal deformations in the principal directions:

$$\rho = \frac{\varepsilon_{33}}{\varepsilon_{22}}$$

G – transverse modulus of elasticity of the soil:

$$G = \frac{E_\varepsilon \cdot m}{2m+1}$$

E_ε – modulus of elasticity of soil under conditions of ground strain.

Assuming that the vertical stress does not change significantly during horizontal strain, it is primarily the horizontal stress that is redistributed according to the relationship:

$$\sigma_{ik} = \sigma_{22} - \Delta\sigma_{ik} \geq \sigma_{gr}^{22} = \sigma_{min}^{22}$$

where:
σ_{gr}^{22} – minimum value of the horizontal stress ($\sigma_{\min}^{22}$) in the total active Rankine state [15].

The theory presented above dates back to the 1980s. The introduction of widespread computerization at the beginning of the 21st century gave the opportunity to use FEM models to model the phenomenon of cooperation of structures with the mining ground. Recognition of the phenomenon of cooperation of structures with the ground in terms of soil mechanics is still the subject of research by many authors. Guidelines for the construction of FEM models are presented in the works of Fedorowicz: [16-18]. Selected results of numerical analyses describing the phenomenon of cooperation of traffic embankments with the subsoil are presented in [19-21], among others.

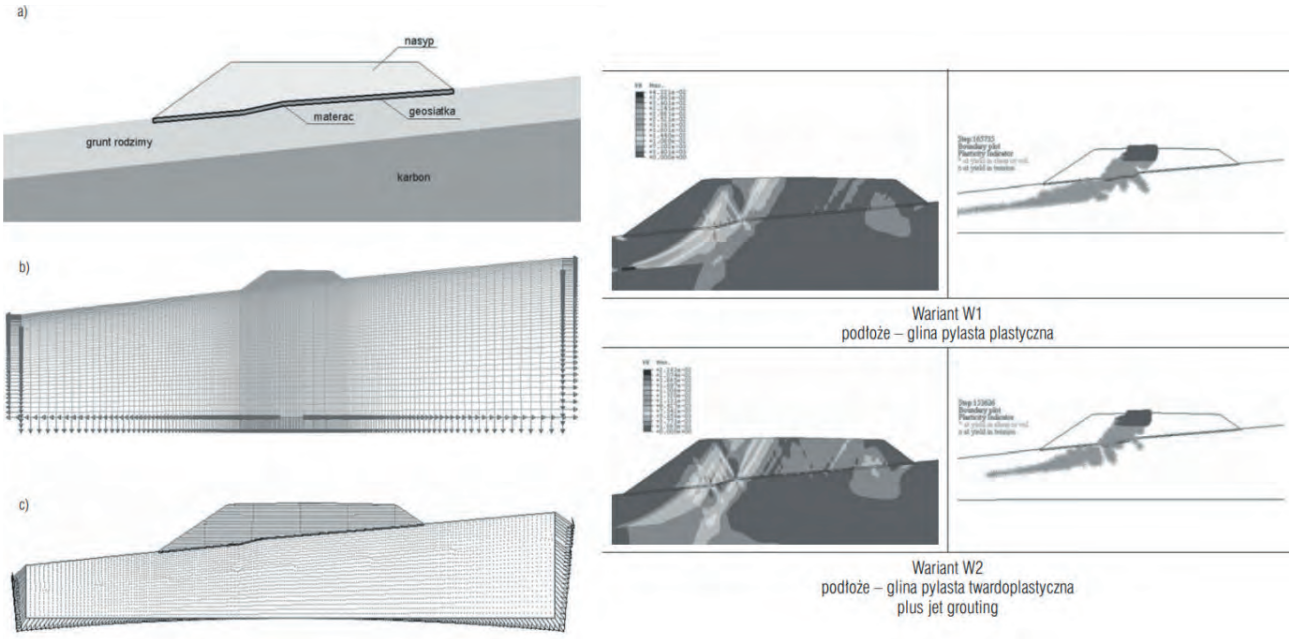

Fig. 1. Examples of published FEM numerical analyses for embankment construction on mining ground [20, 21]

3. GEODETIC MONITORING OF THE PHENOMENON OF EMBANKMENT DEFORMATION IN MINING AREAS

Classical geodetic measurements are a very valuable source of information about the behavior of the surface of a mining area with development [22, 23]. Thanks to the results collected in nature, it is possible to recognize the mechanics of the occurrence of a given phenomenon in greater depth and thus calibrate FEM computational models representing the problem under study [24].

For years, surveying work has been carried out for linear objects in mining areas. In the National literature one can find many studies of the results of classical geodetic surveys conducted for the purpose of inventorying changes in the geometry of transportation routes in mining areas. The results of geodetic measurements are a fundamental argument in assessing the impact of land surface deformation on buildings, including infrastructure facilities. Therefore, they are widespread. In terms of classical geodesy, measurements of deformation of a mining area are mostly carried out on field lines [25], possibly on so-called rosettes [26]. The results obtained in the form of deformation indices are characterized by high accuracy. Their disadvantage is that indicator values are obtained only for one direction – on the direction of the measuring line. In the case of deformation of transportation routes in mining areas, running on embankments, only the magnitude of deformation of the pavement is known. However, the changes in the geometry of the embankment itself are not known. This is because the measurement lines run in the crown of the embankment, parallel to the axis of the route. The results of the measurements are strongly concentrated on the pavement itself. As an example, Figure 2 shows the shape of one of the field lines monitored for changes in the geometry of the route in the mining area – the Bytom bypass.

Fig. 2. Survey line (blue color) stabilized to monitor changes in the geometry of the City's ring road [45]

However, in the context of the study of additional embankment subsidence in mining areas, measurements must be carried out more extensively, including outside the crown of the embankment. Measurement works focused on the problem of additional embankment subsidence are already much fewer. However, as early as the 1980s, the first publications appeared showing the scale in the effect of sinking embankments in nature (Fig. 3) [27].

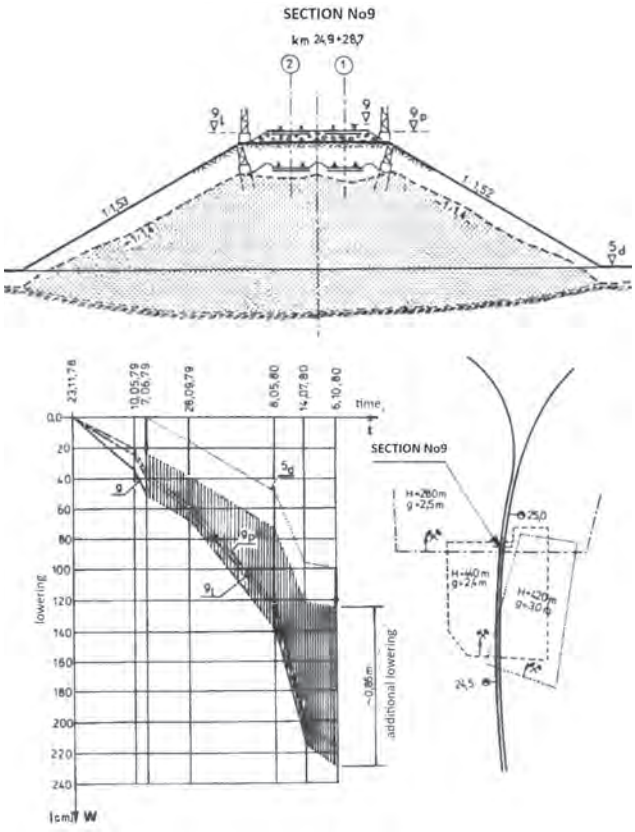

Fig. 3. Results of geodetic observations for the railroad embankment in the crawl space [27]

For the analyzed example, the results indicate the occurrence of additional subsidence of more than 90 cm for a railroad embankment with a height of 10 m located in a zone where horizontal tensile strains of 3-4 mm/m were recorded [27].

It is difficult to carry out such observations using classical measurement techniques. First of all, because observations are made at specific points representing cross sections, defined even before the deformation is revealed – mainly on the basis of forecasts, which, as is well known, are not error-free. Global navigation satellite system (GNSS) surveying techniques introduced in recent decades have become an alternative to measuring deformation of objects in mining areas. Already at the beginning of the 21st century, the first textbooks were written describing the usefulness of satellite techniques for deformation measurements [28]. Today, satellite techniques are displacing classical measurements in most surveying work. They are also one of the basic tools for measuring deformation of mining areas. Publications in this field constitute a very large group of works. The cited examples represent only a part of them [29-34]. GNSS techniques are also widely used to monitor changes in the shape of transportation routes in mining areas, including major strategic facilities, such as the A4 highway in Poland [35].

Rapidly developing laser scanning is also of great importance in observing changes in the shape of the surface of a mining area [36]. Aerial scanning is mainly used in the inventory of changes in the shape of the mining area surface. The paper [38] analyzed data from ALS laser scanning and precision leveling for the city of Bytom to assess the compatibility of the two measurement methods in the context of analysis of land subsidence caused by mining activity. When comparing the two measurement time periods, the deviations at the reference points were within the absolute accuracy of ALS measurements. The suitability of ALS technology for monitoring the subsidence of extensive areas with relatively large increments was rightly pointed out. Similar observations were made in [39], which emphasized the usefulness of ALS technology for comprehensive measures of the impact of mining activities. Besides, remote methods of monitoring land deformation such as interferometric synthetic aperture radar (InSAR) are also intensively developing [37]. For several years, one can notice a widening interest in multi-criteria GIS analyses, which, according to [40, 42], effectively help to assess land subsidence risks or identify subsidence of post-mining basins by analyzing factors related to the geometry and characteristics of the analyzed area (slopes, drift depth, groundwater level, ground permeability and others). Current and archival thematic maps and their derivative products, stored as successive spatial information layers in GIS, provide a rich source of data that can be effectively used in protecting the surface of a mining area [41].

4. STUDY AREA

4.1. Characteristics of the studied traffic embankment

Within Poland, it is in areas affected by mining that the road network is one of the most dense. This is

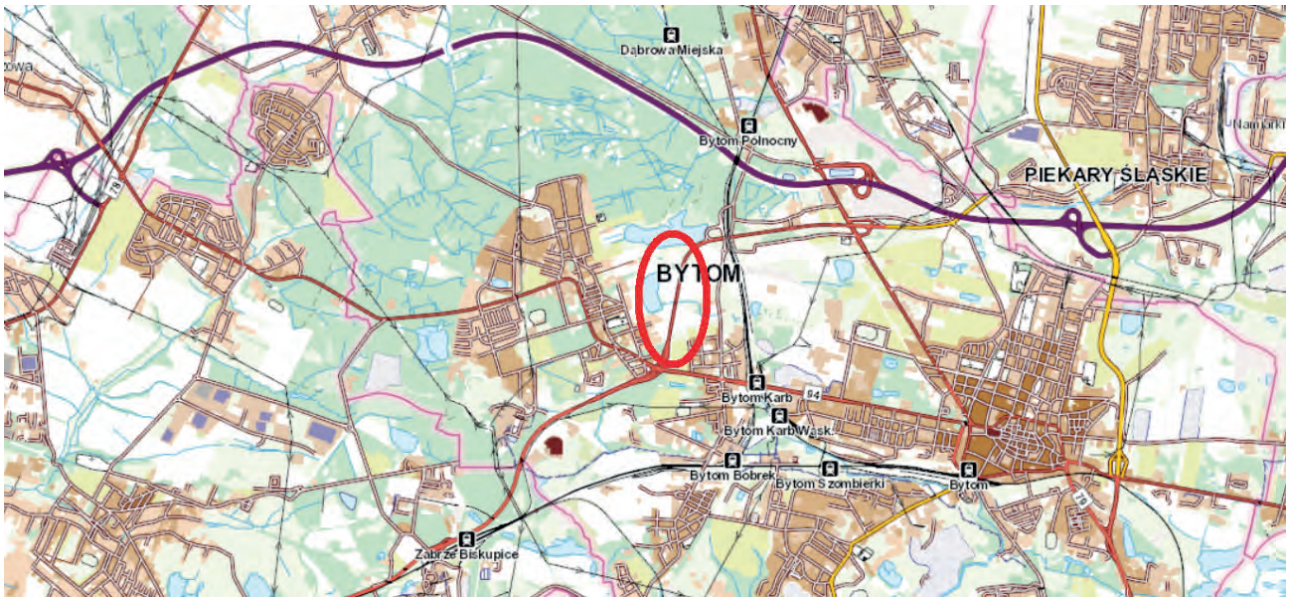

Fig. 4. Location of the study object

due to the fact that the area of Upper Silesia, which is a large mining ground, is also densely populated [43]. One of the most interesting locations in terms of studying the impact of deforming mining ground on infrastructure is the city of Bytom. Many years of coalseam mining there have caused depressions that have already reached more than 30 meters over the past sixty years [44]. The Northern Bypass of the Upper Silesian Agglomeration constructed in 2012, which is a connection between the DK88 and the A1 highway, is located in this difficult terrain (Fig. 4).

In the north-south direction, the route of the bypass follows an embankment with an average height of about 6.0 m (Fig. 5). This is the main object of interest in this work.

The embankment construction was completed in 2012. Figure 6 illustrates the progress of embankment erection between 2009 and 2012.

Fig. 5. Northern bypass of the Upper Silesia Agglomeration in Bytom, a section of the route that runs on an embankment visible in the distance, October 2018

Fig. 6. Orthophotos from the years: 2009, 2011 and 2012 – completion of embankment construction source: http://geoportal.gov.pl

4.2. Performance data

The facility was subjected to the impacts of two longwall operations immediately after construction. The first of these took place in 2014-16 (Fig. 7a). Mining was carried out with two walls: a longwall of about 400 m (east) and a longwall of about 550 m (west), located directly under the analyzed bypass and the discussed road embankment. The depth of mining was about 710 m, the average thickness of the seam was 1.8 m, and there is mining with caving carried out. The second caving exploration mining started in September 2018 was carried out with a longwall of 280 m. Total run-out – 1630 m. Average thickness of the mined layer – 3.0 m, average depth of mining (650-700 m). In May 2019, a runout of about 830 m (1/2 of the total runout length) was reached here. Exploitation runs from north to south, approximately parallel to the axis of the bypass (Fig. 7b).

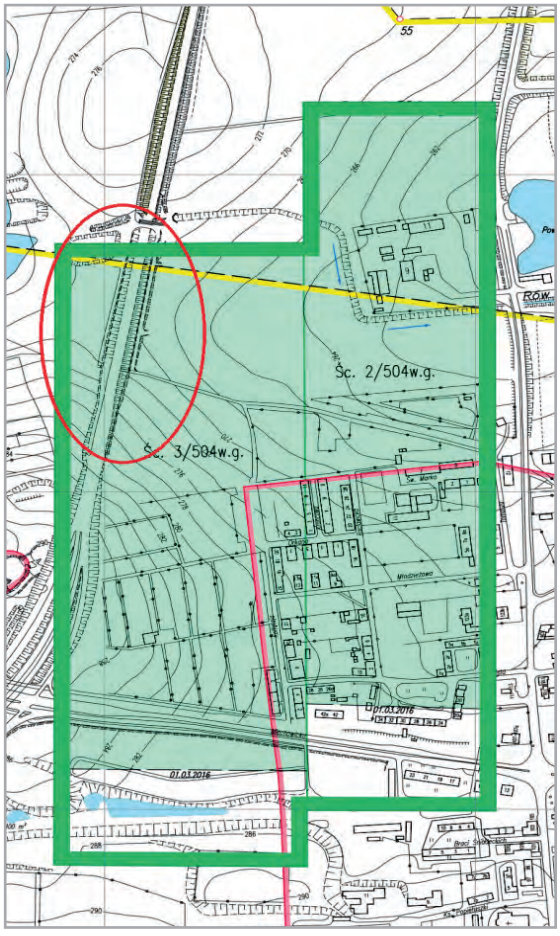

Fig. 7a. Location of the facility in relation to the parcel of land exploited in 2014-16 (green indicates the location of the exploitation front on 1.03.2016) [45]

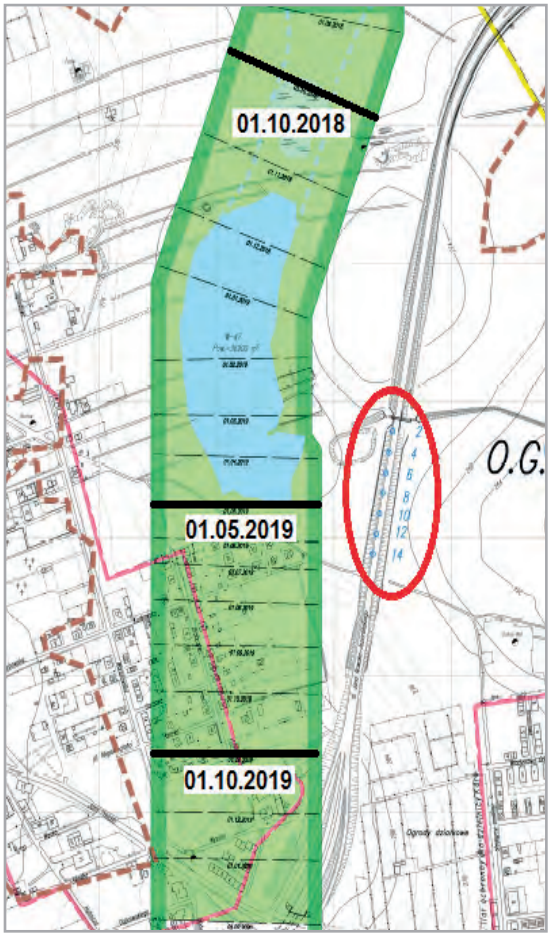

Fig. 7b. Location of the bypass in relation to the long wall in operation in the period 2018-20 [45]

5. PREPARATION OF THE DTMS

Comparison of DTMs from different time periods makes it possible to catch the appearance of depressions in the terrain, and consequently prevent potential hazards. In the present study, numerical terrain models for the city of Bytom subjected to subsequent analysis were generated by rasterization of airborne laser scanning (ALS) data (excluding the 2001 digital terrain model, which were created after processing aerial photos). The data were sampled at a density of no less than 6 pts/m^2, and the average elevation error for the ALS data and the surveyed durations was no greater than 0.15 m. Based on the processed point clouds from LiDAR, numerical terrain and land cover models were developed in ASCII GRID format with an average error of m_h = 0.25 m. Processed results from airborne laser scanning were made available for research by the Department of Geodesy of the City Hall in Bytom. Due to the large time span of the acquired DTM data, the raster models figured in different elevation systems. Harmonization of the data to the current PL-EVRF2007-NH elevation system in effect in Poland and all analyses based on raster algebra were carried out in the open source software Qgis.

Figures 8-10 summarize the results of the analyses in the form of DTM comparisons from 2001-21, 2012-21 and 2018-21.

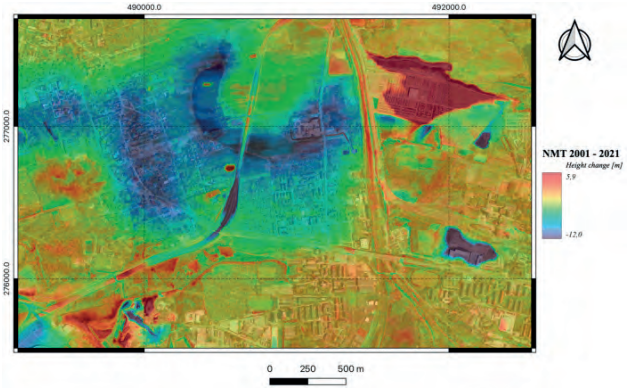

Fig. 8. DTM comparison results for the years: 2001-2021

The comparison shown in Figure 8 was generated to show the shape of the Bytom Basin over 20 years. All uplifts are the result of anthropogenic activity. The areas highlighted in red mostly have sharp edges and their shapes are strongly constrained. These zones should be interpreted as embankments. The blue zones visible in the interior, with their blurred contours, are the result of mining activities. This is an image of a subsidence basin formed over a period of 20 years.

The colour palette in the following figures should be interpreted similarly: 9 and 10. In particular, in Figure 9 it is clear that the traffic embankment of the Bytom Ring Road analysed in the paper is located in a zone of additional subsidence caused by mining activities. The light blue zone located at the site of the analysed embankment roughly coincides with the shape of the parcel of land mined at this site in 2015-16 (Fig. 7a). The dark blue zone located to the west of the analysed embankment is also the image of a basin, caused by the exploitation of another wall. In this case, the thickness of the mined layer was 3.0 m, which caused subsidence greater than in the embankment case, where the thickness of the seam was 1.8 m.

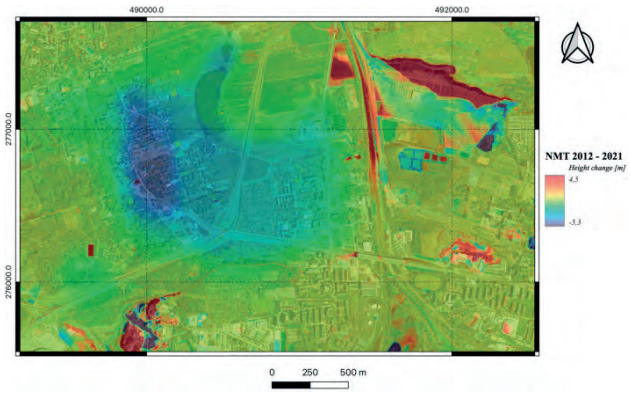

Fig. 9. DTM comparison results for the years: 2012-2021

In Figure 9 to the west of the analyzed road embankment, the effect of the beginning of the formation of a subsidence basin from the mining of wall 4 is visible – Figure 7b. Its exploitation took place in 2018-19. In this case, the final shape of the subsidence basin has not yet fully revealed itself on the ground surface. The 2021 DTM was generated on the basis of scans carried out in May. By this period, the final subsidence had not yet been observed on the ground surface.

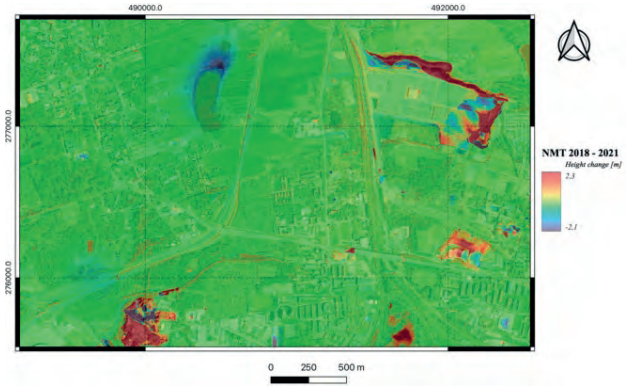

Fig 10. DTM comparison results for the years: 2018-2021

6. DTM VERIFICATION

In order to verify the DTMs analyzed in this paper, the results of classical surveying measurements conducted by an independent team [45] were used. The results of cyclic precision leveling measurements made on the field line stabilized in the crown of the embankment along which the bypass of the city of Bytom runs (Fig. 2) showed the appearance of subsidence. In this article, attention is focused on a section of the line between measurement points: 2-16, representing the surveyed road embankment (Figs. 5, 6). The graph (Fig. 11) shows the progress of the lowering of the individual line reperes in the period: 06.2018 - 08.2020.

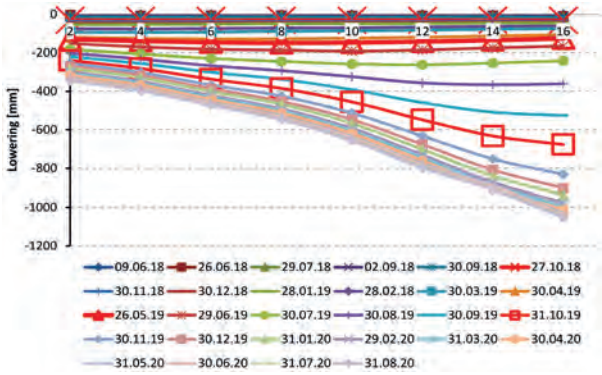

Fig. 11. Decreases of the survey benchmarks on the road embankment (source: own elaboration based on survey results [45])

In order to verify the correctness of the DTM 2018 prepared by the authors, a longitudinal cross-section through the crown of the embankment was generated (black curve – Fig. 12). Then the obtained shape of the longitudinal section was compared with the results of independent surveying measurements. Figure 12 shows a summary of the results.

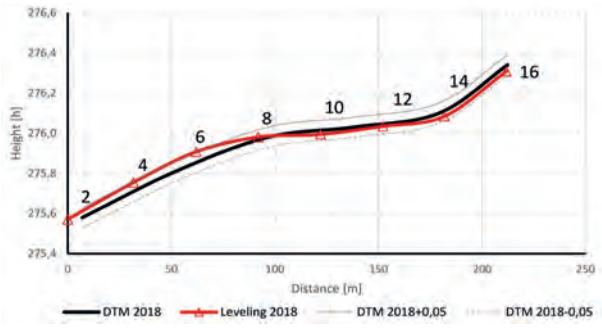

Fig. 12. Comparison of longitudinal sections through the crown of the analyzed embankment obtained from geometric leveling [46] and from the author's DTM

The shape of the two cross sections is very similar. Differences in elevation ordinates differ by a maximum of 5 cm (the gray curves in Figure 12 represent differences of +/-5 cm). A similar comparison of the shapes of the longitudinal cross-section through the crown of the embankment was made on the basis of the 2021 DTM (Fig. 13).

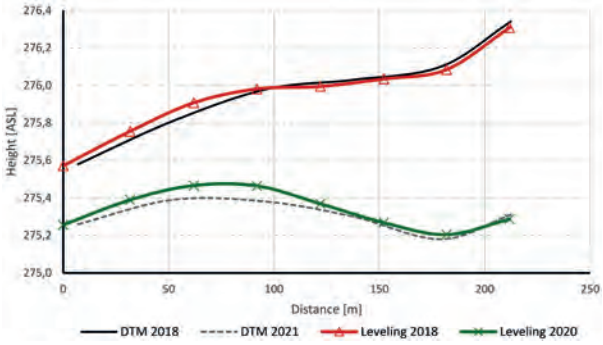

Fig. 13. Comparison of ground elevations for the DTMs analyzed in the paper with independent geodetic results

The following two curves, placed in the graph (Fig. 13) above, also follow a similar course. These are the results of leveling at points 2-16 taken on 30/08/2020 and the cross-section through the DTM taken from the May 12, 2021 images. Such a comparison, despite the shift in time, is shown because the results from Figure 11 show that the effects of mining activities on the analyzed embankment practically ceased in August 2020.

The next verification step is to compare the results of lowering the crown of the embankment over time. Figure 14 shows the result of embankment lowering obtained from two independent measurements, as a result of leveling measurements [45] and as a result of comparing changes in ground ordinates from the Author's DTM (2018-2021 – Fig. 10).

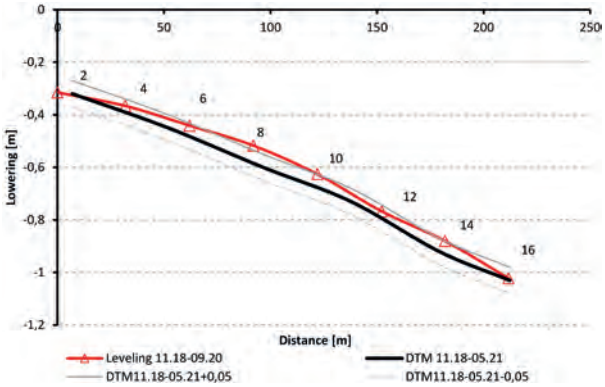

Fig. 14. Lowering of the crown of the embankment in the longitudinal section obtained from precision leveling and from the DTM

It can be seen from the graph (Fig. 14) that the reductions in the crown of the embankment obtained

from comparing the two DTMs from the years: 2018-21 give a very similar picture to that obtained from independent leveling measurements. The values of the depressions obtained from the DTMs (black curve – Fig. 14) are only slightly larger than those derived from leveling. In part, this can be explained by the fact that the red curve representing the lowering of the embankment from leveling measurements shows lowering values over a slightly shorter time interval. In general, however, it should be noted that the differences in the subsidence obtained from the DTM are at most only a few centimeters greater than those from independent leveling measurements.

The author's verification of the DTM performed in a longitudinal section through the crown of the embankment showed that the image of the shape of the route running along the embankment obtained from the DTM is very close to the reality represented here by the much more accurate leveling measurements.

7. REPRESENTATION OF ADDITIONAL LOWERING OF THE EMBANKMENT CREST ON THE DTM

After positively verifying the prepared DTMs in the next step, the results were used to illustrate additional reductions in the crown of the embankment. This is clearly an advantage of classical leveling measurements, conducted on a line running along the pavement. Using DTMs, which are in fact a model of the terrain surface in the form of a 1×1 m mesh, it is possible to generate and thus observe any cross sections. One of the interesting places along the route of the bypass is cross-section A-A (Fig. 15).

Fig. 15. Location of cross-section A-A (the place where the greatest damage is revealed)

This is the zone where the greatest damage to the asphalt surface has occurred. The corpus of the embankment has also suffered damage that reveals itself in the form of cracks (Figs. 16, 17).

Fig. 16. Longitudinal crack in the crown of the embankment along with the deformed road barrier

Fig. 17. Vertical slots in the embankment corpus

Based on the cross sections generated from the 2012, 18 and 2021 DTMs, vertical and horizontal movements can be observed at any arbitrary location, including the interesting cross section A-A (Fig. 15). The results of land subsidence for cross-section A-A obtained from the DTM comparisons are shown in Figure 18.

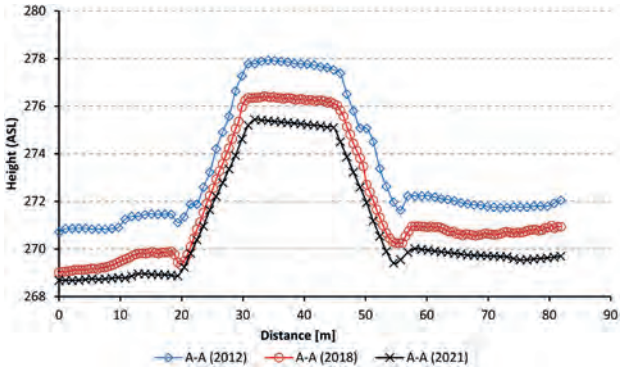

Fig. 18. Cross-section through the embankment (A-A) generated from DTM from 2014, 2018 and 2021

Based on the known ordinates of the points: representing the surface of the adjacent terrain and the points lying in the crown of the embankment for the studied section, the average ordinates of the terrain: the base and crown of the embankment were calculated. This allowed us to control the change in the height of the embankment over time. The results of the calculations are shown in Table 1.

Table 1. Calculations of changes in embankment height over time

Section A-A	2012	2018	2021
Average base ordinate	271.35	269.98	269.16
Average crown height	277.83	276.32	275.29
Height of the embankment (m)	**6.48**	**6.34**	**6.13**

Calculations generated from the DTM of the cross sections show that the height of the embankment at cross section A-A is decreasing over time. This is certainly related to the ongoing mining operations. This decreasing height can be interpreted in this case as a sinking phenomenon of the embankment. The embankment has been in the zone of land deformation twice. During the first mining operation in 2014-16, the mining front passed under the embankment (Fig. 7a). During the second operation (Fig. 7b), the embankment was already on the edge of the basin, which, according to the theory [46], is a zone of horizontal tensile deformations, particularly dangerous due to the additional lowering of the embankment [14, 47, 48]. Comparing the lowering of the cross-sectional control points in the mesh generated, it is clear that the lowering of the points outside the embankment is slightly more than 2 meters, while the crown of the embankment lowered by 2.5 meters (Fig. 19 – middle zone).

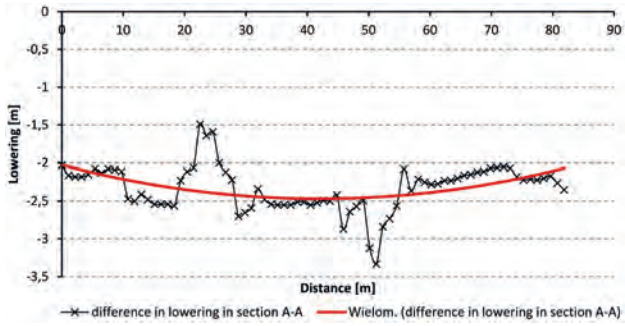

Fig. 19. Decrease in the characteristic points of cross-section A-A with DTM over time (2012-2021)

In addition to the subsidence, the influence of horizontal strain can also be seen in the graph (Fig. 19). The embankment has shifted in the direction of the exploited parcel (exploitation in 2018-2020) (Fig. 7b – to the left). Comparing the depressions, it can be seen that the points next to the embankment have suffered uplifts and others (to the right) have suffered strong depressions. In fact, these places are the slopes of the embankment. As a result of the horizontal shift, the embankment in 2014 is in a different place than in 2021. If the embankment moved only vertically, the graph of vertical strain would be undisturbed by the effect of the horizontal shift. Introducing the trend line into the obtained depressions, it is clear that its character is concave (parabolic), suggesting depressions greater in the middle zone of the section – at the site of the embankment. This result confirms the fact of depicting the sinking effect of the object.

8. SUMMARY

The extensive data set collected in GIS databases now offers new possibilities. DTM numerical terrain

models allow imaging of phenomena previously difficult to observe with classical techniques. One such issue is additional lowering of embankments in areas of active mining activity. Monitoring this phenomenon for the analyzed embankment would be difficult to implement based on classical techniques. Thanks to DTM analyses, the possibility of its recognition on a larger scale than before opens up. In the present study, the average error of height estimation from the digital terrain model relative to reference data in the form of precision leveling was about m_h = 0.05 m (Fig. 13). This result confirms the usefulness of DTM for observing phenomena in areas of mining activity when the area of analysis has little spatial variation.

The advantage of classical measurements is certainly accuracy. Consequently, the significant limitation of DTM comparative analyses is the obtained result accuracy and the variability over time of the height determination error components in the form of field, instrumental and environmental factors. Nevertheless, technological advances and increasingly widespread access to laser scanning systems for unmanned aerial vehicles are likely to address previous shortcomings related to the accuracy and repeatability of obtained observations from ALS [49]. The DTM verification presented in the paper gave satisfactory results in this regard. Of course, measurement errors at the level of a few cm are in many cases an unacceptable threshold. Nevertheless, in the case of capturing the phenomenon of additional lowering of embankments, the quantities sought can exceed the measurement error resulting from the quality of the DTM product.

It is worth mentioning that DTM comparative analyses can also be useful for imaging sinkholes and differential subsidence over time caused by a mechanism other than mining activity. This is because the data stored in GIS databases allows for backward analyses of so-called weak points, i.e. places where damage has occurred. The results of DTM comparative analysis can be an important input in research work aimed at determining the causes of failure of road embankments in the zone of deforming ground surface. The end products derived from ALS data can reveal masked sinkholes and identify the most active ones, which should be monitored in detail.

REFERENCES

[1] Kwiatek J., *Construction facilities on mining areas*. GiG Katowice 2007, pp. 266.

[2] Mrozek D., Mrozek M., Fedorowicz J., *The protection of masonry buildings in a mining area*. Procedia Engineering, 193, International Conference on Analytical Models and New Concepts in Concrete and Masonry Structures AMCM'2017, pp.184-191; https://doi.org/10.1016/j.proeng.2017.06.202.

[3] Kłosek K., *Motorway pavement and earthwork structures on mining Fields*, WUG 2006, bwmeta1.element.baztech-article-BSL9-0011-0003.

[4] Szojda L., Kapusta Ł., *Numerical analysis of the influence of mining ground deformation on the structure of a masonry residential building,* Archives of Civil Engineering, 2021, Vol. 67, no. 3, DOI: 10.24425/ace.2021.138054.

[5] Rusek J., Tajduś K., Firek K., Jędrzejczyk A., *Bayesian networks and Support Vector Classifier in damage risk assessment of RC prefabricated building structures in mining areas*. 2020 5th International Conference on Smart and Sustainable Technologies (SpliTech); DOI: 10.23919/SpliTech49282.2020.9243718.

[6] Blachowski J., *Application of GIS spatial regression methods in assessment of land subsidence in complicated mining conditions: case study of the Walbrzych coal mine (SW Poland),* Nat Hazards 84, 997–1014 (2016), https://doi.org/10.1007/s11069-016-2470-2.

[7] Suh J., *An Overview of GIS-Based Assessment and Mapping of Mining-Induced Subsidence*. Applied Sciences. 2020; 10(21):7845. https://doi.org/10.3390/app10217845.

[8] Malinowska A., Hejmanowski R., *Building damage risk assessment on mining terrains in Poland with GIS application*. International Journal of Rock Mechanics and Mining Sciences, Volume 47, Issue 2, 2010, pp. 238-245, https://doi.org/10.1016/j.ijrmms.2009.09.009.

[9] Kłosek K., *Discretization of the model of interaction of the track grid with its direct subgrade and the ground subgrade*, 1st Ministerial Problem Seminar of the Ministry of Science and Higher Education RI-18 entitled "Model bases for shaping and maintaining rail roads", IDiM Pol. Warsaw 1983, pp. 121-147.

[10] Szumierz W., *Development of methods for forecasting mining deformations in railway facilities*. COBiRTK works, No. 3098/16 part B (analytical), Katowice 1981.

[11] Szumierz W., *Analysis of the impact of mining terrain stretching on the stability of railway track slopes*. Materials for a scientific conference. Earth structures in mining areas, Katowice 1977.

[12] Litwinowicz L., Malcharek K., Rosikoń A., *The impact of mining exploitation on the stability of embankment slopes and earthen dikes*, OTG vol. 33/1975.

[13] Rosikoń A., Malcharek K., *The impact of mining exploitation on the railway track in the light of research work on experimental sites*. OTG Vol. 20/1972.
[14] Kłosek K., *The influence of deformations of the mining subsoil on the cooperation of the subgrade with the railway road surface*, Scientific journals of the Silesian University of Technology, Gliwice 1988.
[15] Kłosek K., Graftiaux M.F., *Interactions des fondations des ouvrages d'art et du sol d'assiseen terrain d'exploitationminiere*. "Industrie Minerale – Mines et Carrières – les Technijues", France - Juin 1986, s. 283-292.
[16] Fedorowicz J., *Building-soil contact issues. Part I. Criteria for modeling and analysis of basic contact issues between building structure and ground*. Scientific Journals of the Silesian University of Technology, Construction series, No. 1729, issue 107, Gliwice 2006.
[17] Fedorowicz J., *The issue of contact between the building and the ground. Part II. Criteria for creating and assessing computational models of building structure – mining substrate systems*. Scientific Journals of the Silesian University of Technology, Construction series, No. 1805, issue 114, Gliwice 2008.
[18] Fedorowicz L., Fedorowicz J., *Numerical modeling of in situ phenomena occurring in subsoil in areas of mining deformations*. Land, air and water routes, No. 11, 2009, pp. 63–67.
[19] Bzówka J., Chmielniak S., Sternik K., *The influence of mining impacts on the deformation of a road embankment based on numerical analyses*. 6th International Conference "Durable and safe road surfaces", Kielce, May 9-10, 2000, Volume 2, 23-32.
[20] Gryczmański M., Sternik K., *Failure of the high embankment of the A4 motorway between the "Wirek" – "Batorego" junctions*. XXII Scientific and Technical Conference Construction Failures 2005, Szczecin-Międzyzdroje 2005.
[21] Cała M., Cieślik J., Flisiak J., Kowalski M., *Errors in design, and not only mining, cause damage to the highway*. Modern Engineering Construction No. 5 (8), 2006, 26-31.
[22] Ostrowski J., *Deformations of the mining area*. AGH, Kraków 2015.
[23] Białek J., Mielimaka R., Orwat J., *Determination of regressive relation binding the theoretical and observed final values of curvatures for geological and mining conditions the one of JSW coal mines.* Journal of Sustainable Mining, vol. 14, issue 2, 2015, https://doi.org/10.1016/j.jsm.2015.08.011.
[24] Ochmański M., Modoni G., Spagnoli G., *Influence of the annulus grout on the soil-lining interaction for EBP tunneling, Geotechnical aspects of underground construction in soft ground.* Proceedings of the Tenth International Symposium on Geotechnical Aspects of Underground Construction in Soft Ground, IS-Cambridge 2022, Cambridge, United Kingdom, 27-29 June 2022 / Elshafie Mohammed, Viggiani Giulia, Mair Robert (*ed.*), 2021, Routledge, s. 350-356, ISBN 978-1-032-02769-2. DOI:10.1201/9780429321559-45.
[25] Popiołek E., *Protection of mining areas*, AGH Kraków, 2009.
[26] Pielok J., *Determination of the surface strain tensor in mining areas based on geodetic measurements*. University Scientific and Didactic Publishing House of the AGH University of Science and Technology, Kraków 2005.
[27] Kłosek K., Litwinowicz L., Zimnoch S., *Deformations of railway earth structures in mining areas in the light of model experiments and field tests*. Published Silesian University of Technology, Civil Engineering Faculty, Volume 61, pp. 37-46, Gliwice 1985.
[28] Góral W., Szewczyk J., *Application of GPS technology in precise deformation measurements*. AGH, Kraków 2004.
[29] Lipecki T., *Assessment of measurement accuracy in the context of determined terrain deformation indices*. Przegląd Górniczy, Vol. 67, no. 1-2, pp. 63-67, 2011 YADDA identifier bwmeta1.element.baztech-article-AGH8-0009-0026.
[30] Blezień J., Jaśkowski W., Jóźwik M., Lipecki T., *Preliminary results of using active geodesic net (ASG-PL) for mining surveying – Introductory results of using activegeodesic net (ASG) for surveying*. Geodesy: semi-annual of the AGH University of Science and Technology; ISSN 1234-6608. 2003, vol. 9, issue 2/1, pp. 299–309.
[31] Lipecki T., *Application of GPS-RTK technology in monitoring the deformation of the terrain surface and special objects under the influence of mining,* Przegląd Górniczy 11/1999.
[32] Hejmanowski R., Sopata P., Stoch T., Wójcik A., *Updating of mining area relief on the basis of GPS-RTK measurements,*Przegląd Górniczy; ISSN 0033-216X. 2012, vol. 68, No 8, pp. 154–159.
[33] Stoch T., *Precision of determinantion of the indicato svalues of surface deformation on the spatial observation network using GPS-RTK measurement,* 15th Mining Workshops from the series "Natural hazards in mining" Czarna 4–6 june 2012 : scientific conference materials.
[34] Sopata P., *Use of GPS-RTK method to measure the surface displacements of mining areas*, Przegląd Górniczy 2012, vol. 68, No. 7, pp. 104–109.
[35] Siejka Z., *The use of GNSS measurements to determine the coordinates of the basic implementation network in mining impact areas*. Archive of photogrammetry, cartography and remote sensing, vol. 19, 2009.
[36] Maciaszek J., Gawałkiewicz R., *The use of laser scanning in the diagnosis of objects affected by mining*, Geodesy (AGH semi-annual) 2006.
[37] Popiołek E., Sopata P., *Possibilities of using the InSAR method in hazard monitoring in mining areas*. 7th Scientific and Technical Conference "Environmental Protection in mining areas", Szczyrk 4-6.06.2008.

[38] Polanin P., *Monitoring land surface deformations using airborne laser scanning on the example of the city of Bytom*, Przegląd Górniczy, 2017, pp 22-30.
[39] Kuzia K., *Application of airborne laser scanning in monitoring of land subsidence caused by underground mining expoloitation*, Geoinform. Pol. 2016, pp. 7–13.
[40] Blachowski J., *Application of GIS spatial regression methods in assessment of land subsidence in complicated mining conditions: case study of the Walbrzych coal mine (SW Poland)*. Nat Hazards 84, 997–1014 (2016), https://doi.org/10.1007/s11069-016-2470-2.
[41] Suh J., *An Overview of GIS-Based Assessment and Mapping of Mining-Induced Subsidence*. Applied Sciences. 2020; 10(21):7845. https://doi.org/10.3390/app10217845.
[42] Malinowska A., Hejmanowski R., *Building damage risk assessment on mining terrains in Poland with GIS application*. International Journal of Rock Mechanics and Mining Sciences, Volume 47, Issue 2, 2010, pp. 238-245, https://doi.org/10.1016/j.ijrmms.2009.09.009.
[43] Tajduś K., Misa R., *Influence of underground mining operation on highways – domestic and foreign experience*, Przegląd Górniczy 2014, nr 5, s. 39-47 ISSN: 0033-216X.
[44] Kapusta Ł., Szojda L., *The role of expansion joints for traditional buildings affected by the curvature of the mining area*. Enginnering Failure Analisys, vol. 128, 10.2021, https://doi.org/10.1016/j.engfailanal.2021.105598.
[45] Jaśkowski W., *Measurement report: Deformation measurements in mining areas Bytom – IIIZG I Bobrek Miechowice I, report 28*, 08.2020.
[46] Knothe S., *Project of classification of mining areas from the point of view of suitability for construction purposes*. Przegląd Geodezyjny, R. 9. Nr 4, 1953.
[47] Tong L., Leo L., Amatya B. et al., *Risk assessment and remediation strategies for highway construction in abandoned coal mine region: lessons learned from Xuzhou, China*. Bull EngGeolEnviron 75, 1045–1066 2016. https://doi.org/10.1007/s10064-015-0760-7.
[48] Pilecka E., Szwarkowski D., Stanisz J., Blockus M., *Analysis of a Landslide on a Railway Track Using Laser Scanning and FEM Numerical Modelling*. Appl. Sci. 2022, 12, 7574. https://doi.org/10.3390/app12157574.
[49] Sobura S., *Calibration of the low-cost UAV camera on a spatial test field*, Geodesy and Cartography, Volume 48 Issue 3, pp. 134–143, https://doi.org/10.3846/gac.2022.16215.

Wiktor Wciślik
Structure and Environment 2024, vol. 16, (2), pp. 97-110, Article number: el 009
https://doi.org/10.30540/sae-2024-009

Structure and Environment
ISSN 2081-1500
e-ISSN 2657-6902
https://content.sciendo.com/sae
https://sae.tu.kielce.pl

sciendo

Kielce University of Technology

DOI: 10.30540/sae-2024-009

SELECTED MICROSTRUCTURAL PHENOMENA IN FSW JOINTS

WYBRANE ZAGADNIENIA MIKROSTRUKTURY SPOIN WYKONANYCH W TECHNOLOGII FSW

Wiktor Wciślik
Kielce University of Technology, Poland

Abstract

The article is a literature review on selected phenomena leading to microstructural changes in material welded using the friction stir welding (FSW) method. Particular attention was paid to the phenomena of grains recrystallization, as well as dissolution and reprecipitation of second phase particles, resulting from temperature changes during FSW. Temperature transformations in different zones of the FSW joints were characterized. The role of base material phase transformation in the formation of new particles is discussed. In the tested aluminum alloys and stainless steels, this process was particularly intensified in the heat affected zone (HAZ). In areas subjected to high temperature and significant plastic deformation (nugget zone and thermomechanically affected zone), this phenomenon did not occur or was characterized by small intensity. It was indicated that the phenomenon of particle formation clearly affects the strength parameters of the joint.

Keywords: Friction Stir Welding (FSW), microstructure, grain, recrystallization, precipitation, strengthening particle

Streszczenie

W artykule przedstawiono przegląd literatury dotyczący wybranych zjawisk prowadzących do zmian mikrostrukturalnych w metalach spawanych metodą zgrzewania tarciowego (FSW). Szczególną uwagę zwrócono na zjawiska rekrystalizacji ziaren oraz rozpuszczania i ponownego wytrącania cząstek drugiej fazy, zachodzące jako efekt zmian temperatury podczas FSW. Scharakteryzowano zmiany temperatury w różnych strefach złączy FSW. Omówiono rolę przemian fazowych materiału podstawowego w powstawaniu nowych cząstek. W badanych stopach aluminium i stalach nierdzewnych proces ten był szczególnie nasilony w strefie wpływu ciepła (SWC). W obszarach narażonych na działanie wysokiej temperatury i znacznych odkształceń plastycznych (jądro zgrzeiny i strefa uplastycznienia termomechanicznego) zjawisko to nie występowało lub charakteryzowało się niewielkim natężeniem. Wykazano, że zjawisko tworzenia cząstek wyraźnie wpływa na parametry wytrzymałościowe złącza.

Słowa kluczowe: zgrzewanie tarciowe (FSW), mikrostruktura, ziarno, rekrystalizacja, wydzielenie, utwardzanie wydzieleniowe

1. INTRODUCTION

Friction stir welding (FSW) is described in the literature as a modern welding technique, although its history dates back over 30 years. Originally developed for aluminum and other soft metals, it has been greatly developed in recent years [1] and is also used for various metals (magnesium, titanium, copper, nickel, steel), polymers [2] and others, including dissimilar components [3]. Ease of use, simplicity and universality result in its wide application in the industry, primarily in the automotive, civil engineering, aviation, shipbuilding, chemical and others.

FSW involves introducing a non-consumable tool between the edges of the welded elements and its

*Kielce University of Technology, Poland, e-mail: wwcislik@tu.kielce.pl

uniform movement. The tool consists of a shoulder, whose main task is to generate heat and soften the material, and a pin, intermixing the materials and leading to a permanent joining of both elements. Importantly, during FSW there is no material melting, therefore it is a solid state process. The schematic diagram of FSW is presented in Figure 1.

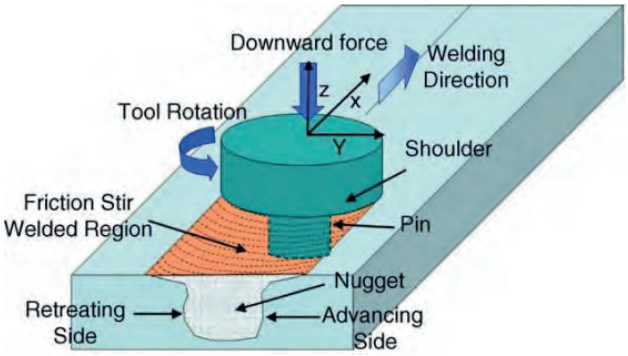

Fig. 1. Scheme of FSW technology [4]

Compared to traditional welding methods, FSW has many advantages that can be divided into 3 basic groups [4]:

1. Metallurgical – slight deformation of welded elements, repeatability and dimensional stability, high metallurgical quality of the joint, no cracking, no loss of alloying elements, fine microstructure.
2. Environmental – no need for special preparation of the welded surfaces and the use of protective gases, no need for additional consumable materials.
3. Energetic – low energy consumption, low structure weight.

The great advantage of FSW is its versatility and the ability to make various types of joints (Fig. 2).

In recent years, FSW technology has undergone tremendous development. This applies primarily to the patenting of various types of tools and additional material processing, which can be classified as new subtypes of FSW. Technologies derived from typical FSW are used not only for welding elements, but also for modifying the surface properties of a single element, repairing material defects etc.

For instance, Friction Stir Processing (FSP) is a technology derived from FSW. As in FSW, a rotating tool (pin and shoulder) is used, but not for welding elements, but for surface material modification of a single workpiece [6, 7]. FSP is a modern technology for the production of ultra-fine grain (UFG) materials. The effectiveness of FSP depends on the type of material in the delivery state, primarily on its microstructure and chemical composition.

Another technique based on FSW is Friction Stir Alloying (FSA), which, similarly to FSP, involves modification of material properties, but with the addition of a consumable material. As a result, a composite is formed, consisting of the basic (modified) material and the second phase dispersed in it. In practice, due to the difficulty of dispersing the filler uniformly in the volume of the base material, usually the material modification covers only its thin near-surface layer, which, however, significantly improves such properties as hardness or corrosion resistance [8].

An extensive and detailed description of technologies derived from FSW can be found in [9].

The present article discusses selected issues related to microstructural changes occurring in material during FSW/FSP, with particular emphasis on steel and aluminum alloys. Chapter 2 describes

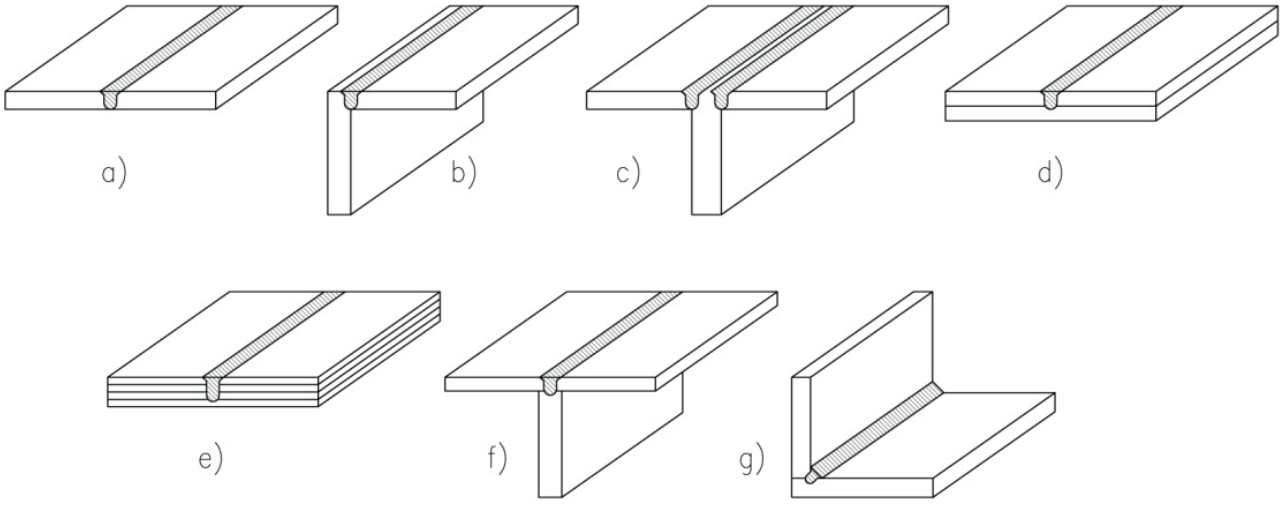

Fig. 2. Different types of FSW joints: a) square butt; b) edge butt; c) T butt joint; d) lap joint; e) multiple lap joint; f) T lap joint; g) fillet joint, based on [4, 5]

the FSW joint zones in which, due to the different thermomechanical history, various processes occur. The issues of recrystallization (Chapter 4) and the phenomena related to the reinforcing particles (primarily dissolution, reprecipitation and coarsening) are discussed (Chapter 5). Considering that these issues are closely related to temperature changes, in Chapter 3 a brief description of thermal phenomena in FSW/FSP is provided.

This article focuses on microstructural transformations during FSW, but its scope does not include the characteristics of thermomechanical processes occurring during welding, as well as unsteady heat flow and phase transformations. These issues are discussed, for example, in [10-12]. The influence of welding parameters on the physical and strength properties of joints is discussed, for example, in [13].

The results of experimental studies and observations of the material microstructure are described. The wide range of analytical and numerical models, which in recent years have contributed to a better understanding of the physical phenomena occurring during FSW/FSP, is not discussed. A comprehensive review can be found in [5, 14].

2. OVERVIEW

Depending on the position with respect to the tool, the material experiences various types of thermomechanical transformations that determine its subsequent microstructure and, consequently, also its strength properties. For this reason a typical FSW joint cross section consists of nugget zone (NZ, or stirred zone – SZ), thermomechanically affected zone (TMAZ) and heat affected zone (HAZ, Fig. 3).

The joining of elements takes place in NZ. This is the zone of direct impact of the tool pin and therefore experiences significant deformation and high temperature. For this reason, recrystallization and formation of fine, equalized grains occur in NZ. The TMAZ, on the other hand, can be defined as a transition zone in which the deformation is smaller and complete recrystallization does not occur. No plastic deformation is observed in HAZ, so its microstructure (except for strengthening particles) is very similar to the base material. The size of each of these zones depends on the type of material, tool and welding technological parameters [16].

The quality and parameters of the entire joint depend on the microstructure of each of these zones. To assess the quality of joints made with the FSW technique, transmission electron microscopy (TEM), optical microscopy and X-ray diffraction are most often used [5].

In turn, to understand the formation and properties of FSW joints, it is crucial to determine the flow of material during welding. For this purpose, various flow visualization techniques are used, such as placing a marker (contrast material) [17-20], or combining different alloys [21, 22]. It should be borne in mind that the flow of material is highly dependent on the shape of the tool [4].

3. EFFECT OF TEMPERATURE

In the FSW process material experiences both significant plastic deformation and high temperature. In the first phase of inserting the tool, heat is generated primarily by friction at the contact point between the pin and the welded material. Already during the welding itself (after the tool is fully inserted), heat is generated primarily by friction at the contact surface between the shoulder and the welded material. A certain amount of heat is also the result of the material deformation [23]. Higher rotational speed of the tool results in higher temperature generation, which in turn translates into better mixing of the

Fig. 3. Typical cross section of a FSW joint [15]

material. The intensity of heating is also related to the type of tool. In addition, the preheating of the workpiece results in local material softening, reduction in the friction coefficient and the associated reduction in heat generation [24]. On the other hand, the change in travel speed does not significantly affect the peak temperature [25, 26].

Depending on the thermal conductivity of the welded material, peak temperature asymmetry between the advancing side (on which the direction of rotation and movement of the tool are consistent) and retreating side can be observed. For example, as observed in [27], the temperature of the 304L stainless steel on the advancing side was about 100K higher. However, such a large scale of this phenomenon occurs quite rarely. The authors attributed this significant difference to the low, compared to other FSW joined materials, thermal conductivity of the tested alloy.

In the stirred zone (SZ) the temperature oscillates around 0.75-0.9T_m (T_m – melting temperature) [28]. In the thermo-mechanically affected zone (TMAZ), the temperature was estimated at 0.6-0.7T_m [29, 30].

Additionally, in some cases (materials characterized by high melting temperature), the heat generated by friction in FSW is not sufficient to soften and thoroughly mix the material, which makes it necessary to provide additional heat from an external source.

On the other hand joint cooling can be also used (especially for soft materials) to prevent excessive growth of recrystallized grains and dissolution of reinforcing particles [4, 26].

In general, the temperature distribution depends on the type of tool used and technological parameters, namely:

- Heat is generated primarily by the shoulder – it is commonly believed that the shoulder produces about 80% of the heat released [31, 32].
- With constant tool travel speed, the maximum temperature increases as the rotation speed increases.
- The maximum temperature increases with the increase of rotation speed/travel speed ratio [4].

The above mentioned thermal effects, regardless of plastic deformation, cause changes in the microstructure of the welded material (grain size and boundaries, dissolution and coarsening of the second phase particles, change in texture, etc.). Thus, temperature measurement can be used as an auxiliary tool that allows for an indirect assessment of the joint quality [33].

To understand these relationships, it is important to measure the temperature distribution in the weld area and its surroundings. Measuring the temperature of the material, due to its plastic deformation, is technically difficult. The use of a thermal imaging camera, although not problematic, does not provide insight into the interior of the material. Due to the impossibility of placing the measuring instruments directly in the welding zone, measurements are made in its vicinity, then the obtained results are extrapolated [14, 34]. One of the measurement possibilities is to embed a thermocouple in the welded material in the vicinity of the tool [4]. High measurement accuracy is obtained when thermocouples are embedded in several holes of different depths [35]. Moreover, thermocouples embedded inside the tool, as well as tool-workpiece thermocouple (measurement based on thermoelectric effect between tool and workpiece) are used [14]. The temperature distribution can be also assessed indirectly, based on the analysis of the weld microstructure.

Regardless of measurements and observations, many thermomechanical models combining friction and plastic deformation with thermal effects have been developed. As already mentioned, modeling issues is beyond the scope of this paper. A comprehensive review of the thermomechanical models related to FSW/FSP can be found, for example, in [24].

4. GRAIN RECRYSTALLIZATION AND REFINEMENT

As a result of plastic deformation, grain size is reduced [36, 37], which, according to the Hall-Petch relationship, directly translates into an increase in the material strength. Grain refinement occurs first of all by dynamic recrystallization, which is the dominant mechanism in SZ and TMAZ. Especially in the SZ fine, equiaxed recrystallized grains are observed. Three basic submechanisms can be distinguished [38, 39]:

- Discontinuous dynamic recrystallization (DDRX) – nucleation and growth of new grains, characteristic for materials of low and medium stacking fault energy (SFA).
- Continuous dynamic recrystallization (CDRX) – formation of low angle boundaries, gradual increase in boundary misorientation and continuous accumulation of the dislocations introduced by plastic deformation.
- Geometric dynamic recrystallization (GDRX) – grain refinement occurs through a process of grain elongation and thinning leading to an increase in grain boundary area [40].

The dynamic recrystallization mechanism that occurs in the material during FSW/FSP depends on temperature and strain. DDRX occurs at high temperature and low strain while CDRX occurs at medium temperature and high strain [41, 42].

Due to the fact that after passing the FSW/FSP tool, material is subjected to high temperature for some time, especially in the nugget zone, one more recrystallization mechanism is observed, namely metadynamic recrystallization (MDRX). MDRX results from the post deformation annealing in the SZ [41].

The homogeneity of the microstructure increases with increasing temperature and decreasing strain rate. In practice, a homogeneous structure is formed in SZ, while partial recrystallization is observed in TMAZ [43].

Another mechanism is static recrystallization, which involves the nucleation of new, undeformed grains and their subsequent growth. Material recrystallized in this way gradually replaces the microstructure of the parent material. The recrystallized and non-recrystallized areas are clearly separated.

Static recrystallization can also be divided into two separate submechanisms, namely discontinuous static recrystallization (DSRX) and continuous static recrystallization (CSRX). DSRX is characteristic of low SFE materials and occurs at temperatures above $0.5T_m$. Recrystallization occurs by migration of the high-angle grain boundary (HAGB) existing in material into the deformed matrix in a heterogeneous manner.

For materials with high SFE, static recrystallization most often takes the form of CSRX. In this case, sites of grains nucleation consist partly of high-angle grain boundaries (HAGBs) and low-angle grain boundaries (LAGBs). In terms of CSRX, two additional submechanisms can be distinguished:

- Migration of LAGBs – growth of subgrains in the presence of an orientation gradient resulting from geometrically necessary dislocations.
- Coalescence of neighboring subgrains through the decomposition of a low misorientation LAGB [41, 44].

Important factor affecting grain refinement is the need for efficient and quick heat dissipation [38]. Various liquid cooling systems (water, nitrogen and others) are used for this purpose.

The efficiency of FSW/FSP in grain size reduction and increase in material strength also depend on the shape of the tool. For example, Prabhu et al. [45] demonstrated that in aluminum AA6061-rutile composite the square pin produced finer grains than the cylindrical threaded one.

The effect of the type of tool on the material thermomechanical transformation is particularly clear when using a bobbin tool (BT, 2 shoulders on both sides of the joined workpieces). The amount of heat generated by the friction of two shoulders is greater than in the case of classic tools. In addition, energy dissipation and joint cooling are difficult. This obviously affects the microstructure of the weld and its properties. The impeded heat outflow causes that the grains affected by the both shoulders are larger than in the nugget zone (NZ) [9]. In addition, grains in NZ and HAZ are larger than for single shoulder tools [46]. As discussed in the literature, the use of BT for Al and Mg alloys, due to grain coarsening, results in low strength parameters of the joints.

Another possibility to increase the efficiency of FSW/FSP in grain refinement is the multipass technique. Each time the tool is passed through the material, the grain size gradually decreases.

For some materials, recrystallization is preceded by static recovery, which is associated with a change in the dislocation arrangement. It may result from:

- dislocation annihilation;
- dislocations rearrangement towards lower energy systems;
- subgrains growth [44].

In most pure materials, static recovery occurs at temperatures greater than $0.3T_m$, while recrystallization itself occurs at higher temperatures, above $0.4T_m$. Material ability for static recovery depends on stacking fault energy [41].

The above described microstructural changes occurring during FSW/FSP also result in changes in the mechanism of material failure. Metals used in technology, under normal conditions, crack through nucleation and the development of microvoids. The course of this phenomenon depends to a large extent on the structure of the material, its chemical composition and the presence of foreign phase particles [47-49].

In the case of FSA, grain size reduction and the introduction of an additional material affect the process of voids development. For example, in [50], fracture surfaces of pure (99.9%) aluminum and aluminum-graphene composite, obtained in the FSA process, were compared. The both types of specimens were subjected to tension. Example photographs of fracture surfaces, obtained with the use of transmission electron microscopy (TEM), are shown in Figure 4. Both fractures are ductile in nature, the voids formed as a result of plastic deformation are clearly visible.

However, the significantly smaller diameter of the voids in the composite material is observed.

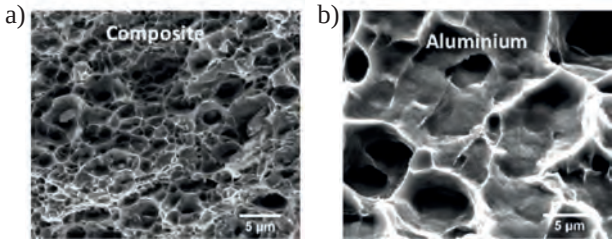

Fig. 4. Fracture surfaces of aluminum-graphene composite made by FSA (a) and pure aluminum (b), [50]

In recent years, many papers have been devoted to the properties of FSW joints made in super duplex (ferritic-austenitic) stainless steels, both in terms of strength properties and microstructure [51]. At the welding temperature of 1300°C, steels of this type change their structure to fully ferritic [52]. Depending on the technological parameters, at lower temperatures, the ferritic-austenitic structure is still observed in the weld zone, but the distribution and morphology of the austenite islands become heterogeneous. On the advancing side, the material experiences the greatest deformation, so that the austenite grains are broken up. As a result, the austenite grains in this area become finer. Moreover, typically for the FSW, grains in the joint area (both ferrite and austenite) are characterized by smaller sizes than in the base material.

The grain size after FSW is also dependent on the technological parameters: the grain size decreases when the tool rotational speed [53, 54] and the rotational speed/travel speed ratio [55] are reduced. This effect is attributed to the lower heat input and its faster dissipation at higher welding speeds.

An example of the analysis of the microstructure and strength parameters of an FSW joint in AISI321 steel is discussed in [56]. The change in the structure and refinement of grains in the stir zone (SZ) was the result of discontinuous dynamic recrystallization (formation and growth of new grains). The course of this phenomenon depended on the welding temperature, which in turn changed with the travel speed of the tool. At the lowest welding speed (25 mm/min), the temperature in SZ reached approximately 80% of the melting temperature of the alloy. The large amount of heat generated resulted in the formation of relatively large grains in the SZ. In the case of a higher welding speed (50 mm/min), the amount of heat supplied was lower (temperature of the order of 67% of the melting temperature) at higher strain rates, which led to a reduction in grain size.

Similar conclusions were drawn from the analysis of the microstructure of FSW joints in 316L stainless steel [57]. Microscopic observations revealed the presence of ultrafine grains in SZ and enlarged reoriented grains in the TMAZ. However, the authors point out that when changing the welding speed, the dominant mechanism influencing the grain size is not the temperature but the strain rate. At higher welding speeds there is less time for dislocation movement and grain boundary relocation, which ultimately results in a reduction in grain size. The dominance of the influence of strain rate over the influence of temperature was also indicated in [58]. The authors of [57] additionally analyzed the weld structure in the TMAZ. In this area, due to the lower temperature than SZ, grain dislocation was the dominant phenomenon. It was further noted that the combination of high tool rotation speeds and low welding speeds resulted in excessive material heating and defect formation.

The authors of [59] analyzed the microstructural changes in SZ in 2205 DSS steel (duplex stainless steel) using quantitative metallography methods. The FSW welding process resulted in a reduction in the ferrite grain size from 8.8 micrometers (in the case of the base material) to 2.71 micrometers. The average austenite grain size decreased from 13.3 micrometers to 2.24 micrometers. At the same time, the authors of [59] emphasize the great importance of the value of the force pressing the tool and its impact on the possibility of making a defect-free joint.

Based on a detailed analysis of the microstructure of 304L austenitic stainless steel, the authors of [60] distinguished 4 stages of the microstructural transformation of the material: compression deformation, rotation deformation, forge and torsion deformation, annealing. In the first phase, LAGB segments are formed in the compression zone, and then partially evolve into HAGBs. Then (the second phase) the coarse grains are transformed into finer ones by DDRX and twinning. In the third phase, after the material is deposited behind the tool, the resulting grains grow and the rotating shoulder introduces forge and torsion deformation. The fourth phase includes the state in which the tool has passed the material and the evolution of the structure is the result of the influence of temperature. Under these conditions, the density of LAGBs decreased and new twin boundaries developed.

5. PRECIPITATION PHENOMENA

5.1. General remarks

Alloys for technical applications are often strengthened by dispersing second phase particles in their structure (e.g. aluminum alloys, metal matrix composites – MMC). It is commonly believed that under the influence of thermomechanical history, the distribution, size and shape of particles changes [61], which directly affects material properties. The particle phase transformation also depends on the chemical composition and temper condition of the base material.

Therefore, a separate problem, relatively often discussed in the literature, is the effect of the temperature and deformation generated during FSW on inclusions and precipitates phenomena [62]. Due to the complex history of thermomechanical changes, depending on the weld zone, pre-existing precipitations are subjected to different processes during FSW. In areas with relatively low temperatures, the existing precipitates coarsen or transform into a more stable phase. In areas with higher temperatures (mainly SZ and TMAZ), the second phase particles dissolve and then reprecipitate. This process depends on the cooling rate, and therefore indirectly also depends on the technological parameters (rapid cooling prevents the formation of new particles). In general, reprecipitation of second phase particles and their growth is often heterogeneous. Depending on the welded material and technological parameters, nucleation and growth of new precipitates is also possible.

Regardless of the stationary processes of reprecipitation, dynamic precipitation (DP) is observed during FSW/FSP, in which particle nucleation and growth are accelerated by plastic deformation. The following mechanisms are possible [63]:

- Particle nucleation acceleration related to the presence of dislocations (heterogeneous nucleation sites).
- Particle growth assisted by pipe diffusion and solute transport by dislocation sweeping.
- Particle coarsening induced by non-equilibrium vacancy concentration.

Particle dissolution is also affected by plastic strain. In general, the mechanism of DP is strongly dependent on temperature, exposure time [64] and plastic strain [65], i.e. variables directly affected by the technological parameters of FSW/FSP. Nowadays deformation induced evolution of second-phase particles is not recognized completely. This refers especially to unstable particles [63].

5.2. Precipitation transformation in steels

Although most of the published works concern the use of FSW for aluminum alloys, the issue of microstructural changes has also been analyzed for various steels.

The paper [66] describes an example of the formation of material discontinuities in the area of the FSW joint of super duplex stainless steel. Particles were not observed neither at the center of the stir zone (SZ) nor at the interface of the SZ and the thermomechanically affected zone (TMAZ). However, microstructural studies showed the presence of a σ-phase in the area of the heat affected zone (HAZ). This phase is defined as the tetragonal intermetallic phase described as Fe-Cr(-Mo). The σ-phase is formed at the boundary of δ-Fe (ferrite) and γ-Fe (austenite) grains. The precipitation of the σ-phase was explained by the effect of heat.

Slightly different conclusions were drawn from the observations of the SZ, primarily on the advancing side. A structure of bright bands was observed at the microscale. The analysis revealed that the bands consist almost entirely of γ-Fe. The δ-Fe phase, which forms the parent material, was not observed in this zone. Moreover, the Cr_2N particles (hexagonal nitride) were also precipitated on the boundaries of γ-Fe grains. Another precipitate was present between the Cr_2N particles (at the triple junction of the γ-Fe grains). As shown by EDX (energy dispersive X-ray spectrometry) analysis, the precipitation was composed of the so called χ-phase ($Fe_{36}Cr_{12}Mo_{10}$).

Moreover, an attempt was made to explain the origin of the observed precipitations. Using the JMatPro software, time-temperature-transformation (TTT) diagrams of the analyzed alloy were developed. It was found that the σ-phase is most intensively formed when the material is exposed to the temperature of 950°C for at least 1 minute. The highest temperature during welding was estimated at about 1100°C, but in the HAZ, where the σ-phase was observed, lower values, of the order of 950°C, should be expected. Based on the simulations, it was also found that precipitation of Cr_2N particles and the χ-phase takes place faster than in the case of the σ-phase.

The authors of [67] studied the influence of tool rotation speed (and thus temperature and strain

rate) on the microstructure of Reduced Activation Ferritic Martensitic (RAFM) steel. Regardless of the rotational speed used (200 or 700RPM), Fe_3C and $M_{23}C_6$ particles were dissolved in SZ and TMAZ. In turn, coarsened and coalesced particles were observed in the HAZ. The use of post-weld direct tempering (PWDT) resulted in the reprecipitation of particles in SZ and TMAZ, and in the case of a lower rotational speed (200RPM), these particles had a more homogeneous character. In general, the authors recommend welding at low rotational speeds so that the temperature generated remains below the tempering temperature employed for base material (BM).

In turn, in [68] the transformations of precipitations in AISI 317L steel were analyzed in three stages: base material, immediately after FSW and after thermal aging at 550°C for up to about 400 hours. No intermetallic phases were observed immediately after welding. However, fine intermetallic precipitates uniformly distributed in the ferrite islands appeared in aged specimens. With increasing aging time and development of precipitation phenomena, the content of ferrite gradually decreased. Intermetallic precipitates formed Cr and Mo rich phases precursor to sigma phase.

A separate problem is the phase analysis of dissimilar joints. In one of the papers devoted to this issue [69], the joint of RAFM and 316L steel was analyzed. Ni diffusion from 316L to RAFM steel was observed in SZ. Excess of Ni in RAFM resulted in the formation of a dual-phase structure consisting of martensite/ferrite and austenite adjoining the bonding interface. Interestingly, it was found that from the point of view of the quality and strength of the joint, it was more advantageous to place 316L steel on the advancing side.

5.3. Aluminum alloys

Due to the widespread use of the FSW technology in the welding of aluminum alloys, a relatively large amount of work has been devoted to the problem of precipitation phenomena in this type of materials.

For example, Ma et al. [70] compared the microstructure of as cast A356 aluminum alloy and the same materials after FSP. A complex structure with needle-shaped Si particles, primary aluminum dendrites and voids/pores was observed in the as cast material (Fig. 5a).

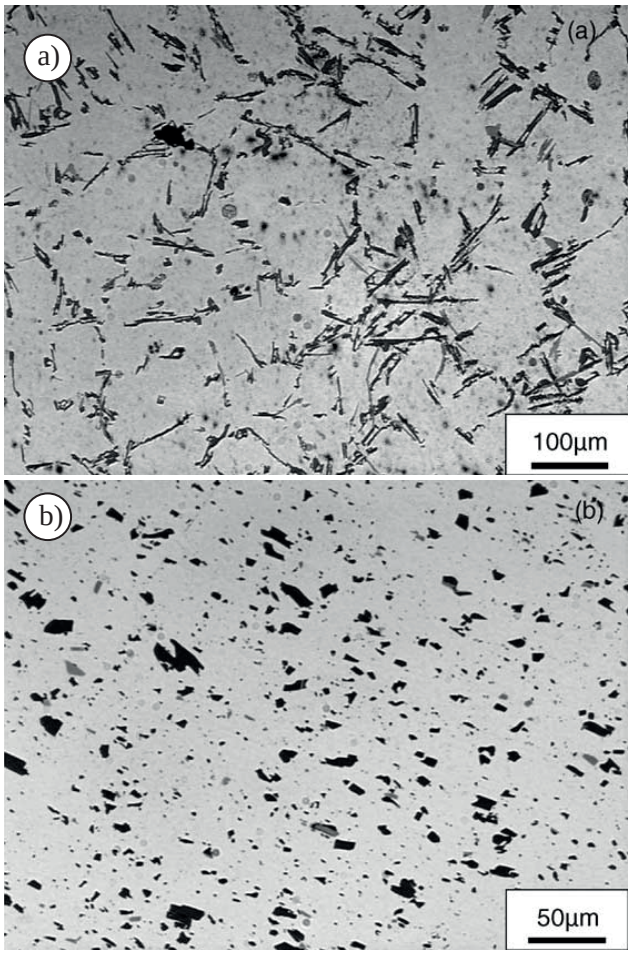

Fig. 5. Microstructure of A356 as cast aluminum alloy: a) microstructure of A356 as cast aluminum alloy, b) microstructure after FSW [4, 70]

The base material was then subjected to FSP at the tool rotation speed of 900RPM and a travel speed of 203 mm/min. As a result, the structure visible in Figure 5b was obtained. FSP resulted in the fragmentation of Si particles, aluminum dendrites and their uniform distribution in the material volume. In addition, a reduction in the material porosity was observed.

In [71], the distribution of precipitates in the cross section of the FSW joint was analyzed. Two types of the 7449 aluminum alloy ageing conditions were taken into account, namely: T3 (naturally aged) and T79 (over-aged). Plates with a thickness of 6.5 mm were welded at a constant tool rotational speed of 350RPM and at two linear speeds: 175 mm/min (low speed) and 350 mm/min (high speed). In the next stage, the structure of individual weld areas was examined using optical microscopy, transmission electron microscopy (TEM) and, above all, small-angle X-ray scattering (SAXS).

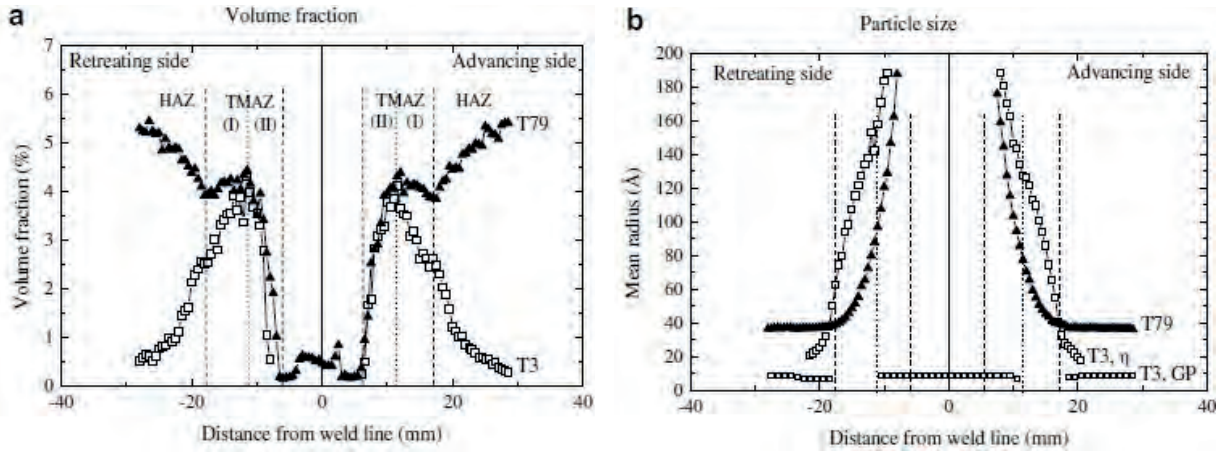

Fig. 6. Basic geometrical characteristics of precipitations in the FSW joint cross section for 7449 aluminum alloys in T3 (naturally aged) and T79 (over-aged) states: a) volume fraction; b) mean particle size [71]

In Figure 6 the volume fraction and mean particle size, obtained with SAXS, are presented. In terms of the analyzed parameters, no significant differences between retreating and advancing side were observed. However, the large difference in precipitates volume fraction between the T3 and T79 materials can be found. In the case of the T79 alloy, a rapid decrease in the precipitations fraction is observed in the HAZ, which is associated with the impact of heat and the accompanying dissolution of parent material hardening precipitates. As can be seen from Figure 6b, these processes were not accompanied by a significant change in particle size.

On the other hand, in TMAZ, on the HAZ side, a slight increase in the fraction of particles is observed, followed by a sharp decrease, to about 0%, close to SZ. A characteristic feature of TMAZ is also a constant increase in particle size with decreasing distance to SZ.

Precipitates in the SZ and TMAZ of the T3 alloy joints have similar characteristics. However, in HAZ, the weld showed a completely different behavior than before. With decreasing distance to the TMAZ, the volume fraction of particles increased rapidly. Their constant size, similar to the parent material, suggests the nucleation of new particles.

The analysis of the microstructure of FSW joints of aluminum 2024 T351 and 2024 T6 alloys, both in terms of grain structure changes and hardening precipitates, is discussed in detail in [72]. In the case of 2024 T351 alloy base material, all precipitations had the form of Guinier Preston Bagaryatskii (GPB) zones (age hardening with fully coherent metastable precipitates [73]). In HAZ, under the influence of temperature, GPBs dissolved and then were replaced by S'(S) (Al_2CuMg) precipitates. Susequently, the precipitates grew, which led to a decrease in the hardness of the material at the HAZ/TMAZ border. A similar phenomenon occurred in TMAZ. On the other hand, in nugget, high temperature resulted in a small number of coarse S'(S) phase, while a large amount of solute enabled nucleation of GPB zones.

Similar phenomena occurred in 2024 T6 alloy, although in the HAZ area, in the vicinity of the base material, the S'(S) particles were characterized by smaller sizes, which directly translated into a slightly higher hardness than in the case of 2024 T351 alloy.

The aforementioned decrease in the hardness of the 2024 T351 alloy in HAZ was also observed in [74]. The authors, however, compared the properties of welds made by the traditional FSW method and those made by impulse friction stir welding (IFSW). The characteristic feature of IFSW is the additional, vertical movement of the tool, which causes a sinusoidal change in the vertical force. In the case of IFSW joints, a higher hardness in the HAZ zone was observed than in the case of FSW. The authors [74] attribute this phenomenon to additional deformations caused by mechanical impulses, which in combination with the influence of temperature promoted reprecipitation of fine S particles at the dislocations and low angle grain boundaries. The presence of fine S particles had a positive effect on the strength of the material in HAZ.

A detailed analysis of the microstructural changes of both alloys (2024 T351 and 2024 T6) during friction surfacing (FS) was also conducted in [75]. In this case, FS involved the deposition of AA2024 T6 coating with the friction method on a substrate in the form of a sheet of AA2024 T351 aluminum alloy. A detailed analysis of temperature changes and associated phase transitions

in the HAZ was carried out using DSC (differential scanning calorimetry), TEM and SAXS techniques. The theoretical description of phase transformations in 2024 alloy, according to [76], was compared with the results of heat flux assessed by DSC. This allowed the estimation of changes in the microstructure during FS, depending on the range of process temperatures. Between 160°C and 210°C dissolution of GP(I)/GPB zones and θ”/S” phase was observed. In the next stage, exothermic transformations occurring in the range of 250-300°C were assigned to the precipitation of θ’/S’ phase. Between 300°C and 470°C θ’/S’ phases dissolved or transformed into a stable θ (Al_2Cu)/S (Al_2CuMg) phase.

The occurrence of microstructural changes including precipitates dissolution and reprecipitation depends on both the material chemical composition and the temperature related to the type of tool used and technological parameters. For example, in [77], microstructural changes of aluminum alloys Al-Mg-Si (6061 AA) and Al-Mg-Sc were compared. In the case of the first alloy, the rotational speed of the tool was 400RPM and travel speed was 2 mm/s. The analogous values for the second alloy were 500RPM and 1 mm/s. With similar welding parameters, different nugget zone microstructures were obtained. In the case of the Al-Mg-Si alloy, almost complete dissolution of the β” phase was observed, which in turn resulted in a significant decrease in the hardness in the nugget zone. The ageing treatment allowed reprecipitation to some extent and improved material properties.

In turn, in the case of the Al-Mg-Sc alloy, no dissolution or coarsening of the Al_3Sc strengthening phase was observed. The decrease in hardness of the material compared to the parent material was therefore small. It was also found that the Al_3Sc particles interacted with the boundaries of recrystallized grains, which in turn limited grain growth. Microstructural studies showed the presence of both coherent and incoherent Al_3Sc particles in the nugget zone.

In the work [65], the microstructure and mechanical properties of 2219Al T6 aluminum alloy joints were compared for different rotational and linear speeds of the tool. The joint properties depended on the Al_2Cu phase transitions. The growth of these particles was dependent on the overaging time (duration above the aging temperature of 190°C), which in turn was dependent on the linear speed and was independent on the rotational speed. Increasing the linear speed from 100 mm/min to 400 mm/min shortened the overaging time, limited particle growth, and consequently increased hardness and strength in the low hardness zone (LHZ). However, a further increase in the linear welding speed (up to 800 mm/min) did not result in an increase in these parameters.

The analysis of phase transformations during FSW can also be carried out by numerical analysis or a methodology combining experimental research and finite element method (FEM) simulation. For example, in [78], a multi-stage microstructural analysis of joints of aluminum alloys 2017A-T451 and 7075-T651 was performed. Using the DSC technique, changes in the heat flux in the weld were determined, which allowed the detection of areas of phase transitions in the welded material. Then, the results obtained in this way were included into the computational model [15], which enabled the numerical determination of maps of phase transformations occurring in the material during welding. It was shown that the temperature generated near the weld center was sufficient to completely dissolve the equilibrium η phase in 7075-T651 alloy and partially dissolve the equilibrium S phase in 2017A-T451 alloy. Gradual cooling of the weld led to Guinier-Preston (GP) and Guinier-Preston-Bagaryatskii (GPB) zones reprecipitation, which led to an increase in the material hardness.

The obtained results were subjected to indirect verification, based on the measurement of hardness changes in individual areas of the weld and positron lifetime curves across the weld. Changes in both of these parameters turned out to be well correlated with the phase transitions predicted in the numerical model.

Another technique that enables the study and description of changes in the microstructure of the material during FSW is the measurement of the electrical conductivity of individual areas of the weld. An example of using this technique to test joints of aluminum alloys AA 7075 T6 and AlMgSc is described in [79]. However, it was indicated that in the case of the tested alloys, the change in conductivity is primarily the result of the grain size, and is not dependent on the presence of precipitates. Therefore, their assessment is difficult.

As mentioned in the previous section, the use of the bobbin tool (BT) results in high welding temperatures and poor heat dissipation. Therefore, dissolution and coarsening of second phase particles is more intense, which is not favorable from the point of view of weld strength, especially in the case of high rotational speeds of the tool [80]. These disadvantages can be reduced to some extent by spraying/water cooling the workpieces [81] or postweld heat treatment.

6. CONCLUSIONS

FSW, despite its relatively short history, turned out to be an excellent tool for joining metal alloys used in industry (primarily aluminum). The great success of this technology is evidenced by a wide range of applications, a huge number of scientific publications on it (also in recent years), as well as numerous derivative technologies (such as FSP/FSA).

Although a significant number of studies and publications have been devoted to the properties of FSW joints, there are still many unexplored issues regarding the impact of technological parameters on the microstructure of welds. Since microstructural changes greatly affect the strength properties, understanding them is crucial to ensuring the safety of the structure.

In general, the structure of individual weld areas depends on the temperature, which is influenced by the type of welded material, the tool and technological parameters (mainly rotational speed and travel speed).

The history of plastic deformation and heating/cooling conditions determine the course of grain recrystallization, which is particularly intense in SZ. As a result of these changes, the grains are refined, which directly affects the improvement of mechanical properties in this zone.

As described above, several recrystallization mechanisms are possible, which depend on the crystal structure of the base material and its stacking fault energy (SFA).

The second factor determining the properties of the weld, especially in particle strengthened aluminum alloys, are precipitation phenomena, which in turn depend on thermal history. In areas with relatively low temperatures, existing particles coarsen or transform into more stable phases. On the other hand, in areas with higher temperatures (primarily SZ), the particles partially or completely dissolve. Depending on the cooling rate, the resulting solute may form new precipitates. Since the material contains the crystal structure defects, which are sites of reprecipitation, the formation of these particles is heterogeneous.

REFERENCES

[1] Yang Y., Bi J., Liu H., Li Y., Li M., Ao S., Luo Z.: *Research progress on the microstructure and mechanical properties of friction stir welded Al–Li alloy joints*, Journal of Manufacturing Processes, 82 (2022), 230-244.
[2] Lambiase F., Derazkola H.A., Simchi A.: *Friction stir welding and friction spot stir welding processes of polymers-state of the art*, Materials, 13 (2020), 2291.
[3] Çam G., Javaheri V., Heidarzadeh A.: *Advances in FSW and FSSW of dissimilar Al-alloy plates*, Journal of Adhesion Science and Technology, 37(2) (2023), 162-194.
[4] Mishra R.S., Ma Z.Y.: *Friction stir welding and processing*, Materials Science and Engineering: R: Reports, 50 (2005), 1-78.
[5] He X., Gu F., Ball A.: *A review of numerical analysis of friction stir welding*, Progress in Materials Science, 65 (2014), 1-66.
[6] Li K., Liu X., Zhao Y.: *Research status and prospect of friction stir processing technology*, Coatings, 9(2) (2019), 129.
[7] Rhodes C.G., Mahoney M.W., Bingel W.H., Spurling R.A., Bampton C.C.: *Effects of friction stir welding on microstructure of 7075 aluminum*, Scripta Materialia, 36 (1997), 69-75.
[8] Morisada Y., Fujii H., Nagaoka T., Nogi K., Fukusumi M.: *Fullerene/A5083 composites fabricated by material flow during friction stir processing*, Composites Part A, 38 (2007), 2097-2101.
[9] Meng X., Huang Y., Cao J., Shen J., dos Santos J.F.: *Recent progress on control strategies for inherent issues in friction stir welding*, Progress in Materials Science, 115 (2021), 100706.
[10] Jemioło S., Gajewski M.: *Symulacja MES obróbki cieplnej wyrobów stalowych z uwzględnieniem zjawisk termo-metalurgicznych*, Część 1. Nieustalony przepływ ciepła z uwzględnieniem przejść fazowych, Zeszyty Naukowe, Budownictwo, z. 143, Oficyna Wydawnicza PW, Warszawa 2005.
[11] Jemioło S., Gajewski M.: *Symulacja MES obróbki cieplnej wyrobów stalowych z uwzględnieniem zjawisk termo-metalurgicznych*, Część 2. Przykłady numeryczne z zastosowaniem programu SYSWELD, Zeszyty Naukowe, Budownictwo, z. 143, Oficyna Wydawnicza PW, Warszawa 2005.
[12] Jemioło S., Gajewski M.: *Zastosowanie programu SYSWELD w modelowaniu resztkowych naprężeń pospawalniczych*, Zeszyty Naukowe, Budownictwo, z. 143, Oficyna Wydawnicza PW, Warszawa 2005.
[13] Kossakowski P.G., Wciślik W., Bakalarz M.: E*ffect of selected friction stir welding parameters on mechanical properties of joints*, Archives of Civil Engineering, 65(4) (2019), 51-62.
[14] Jacquin D., Guillemot G.: *A review of microstructural changes occurring during FSW in aluminium alloys and their model-ling*, Journal of Materials Processing Technology, 288 (2021), 116706.

[15] Hamilton C., Dymek S., Dryzek E., Kopyściański M., Pietras A., Węglowska A., Wróbel M.: *Application of positron lifetime annihilation spectroscopy for characterization of friction stir welded dissimilar aluminum alloys*, Materials Characterization, 132 (2017), 431-436.
[16] Patel V., Li W., Vairis A., Badheka V.: *Recent development in friction stir processing as a solid-state grain refinement technique: microstructural evolution and property enhancement*, Critical Reviews in Solid State and Materials Sciences, 5 (2019), 378-426.
[17] Reynolds A.P.: *Visualisation of material flow in autogenous friction stir welds*, Science and Technology of Welding and Joining, 5(2) (2000), 120-124;
[18] Seidel T.U., Reynolds A.P.: *Visualization of the material flow in AA2195 friction-stir welds using a marker insert technique*, Metallurgical and Materials Transactions A, 32 (2001), 2879-2884.
[19] Colligan K.: *Material flow behavior during friction stir welding of aluminum*, Welding Journal, 78 (1999), 229-s-237-s.
[20] Schmidt H.N.B., Dickerson T.L., Hattel J.H.: *Material flow in butt friction stir welds in AA2024-T3*, Acta Materialia, 54 (2006), 1199-209.
[21] Ouyang J.H., Kovacevic R.: *Material flow and microstructure in the friction stir butt welds of the same and dissimilar aluminum alloys*, Journal of Materials Science, 11 (2002), 51-63.
[22] Li Y., Murr L.E., McClure J.C.: *Solid-state flow visualization in the friction-stir welding of 2024 Al to 6061 Al*, Scripta Materialia, 40(9) 1999, 1041-1046.
[23] Colegrove P.A., Shercliff H.R.: *3-Dimensional CFD modelling of flow round a threaded friction stir welding tool profile*, Journal of Materials Science, 169 (2005), 320-327.
[24] Nandan R., DebRoy T., Bhadeshia H.K.D.H.: *Recent advances in friction-stir welding – Process*, weldment structure and properties, Progress in Materials Science, 53 (2008), 980-1023.
[25] El-Sayed M.M., Shash A.Y., Mahmoud T.S., Abd-Rabbou M.: *Effect of friction stir welding parameters on the peak tem-perature and the mechanical properties of aluminum alloy 5083-O*, Advanced Structured Materials, 72 (2018), 11-25.
[26] El-Sayed M.M., Shash A.Y., Abd-Rabou M., ElSherbiny M.G.: *Welding and processing of metallic materials by using friction stir technique: A review*, Journal of Advanced Joining Processes, 3 (2021), 100059.
[27] Cho J.H., Boyce D.E., Dawson P.R.: *Modeling strain hardening and texture evolution in friction stir welding of stainless steel*, Materials Science and Engineering: A, 398 (2005), 146-163.
[28] Ma Z.Y.: *Friction stir processing technology: A review, Metallurgical and Materials Transactions A*, 39 (2008), 642-658.
[29] Prakash P., Jha S.K., Lal S.P.: *Numerical investigation of stirred zone shape and its effect on mechanical properties in friction stir welding process*, Welding World, 63 (2019), 1531-1546.
[30] Chen K., Liu X., Ni J.: *A review of friction stir–based processes for joining dissimilar materials*, The International Journal of Advanced Manufacturing Technology, 104 (2019), 1709-1731.
[31] Gallais C., Denquin A., Bréchet Y., Lapasset G.: *Precipitation microstructures in an AA6056 aluminium alloy after friction stir welding: characterisation and modelling*, Materials Science and Engineering: A, 496 (2008), 77-89.
[32] Hattel J.H., Schmidt H.N.B., Tutum C.: *Thermomechanical modelling of friction stir welding.* The 8th International Conference Trends in Welding Research, Pine Mountain, Georgia, USA, 2008.
[33] Imam M., Biswas K., Racherla V.: *On use of weld zone temperatures for online monitoring of weld quality in friction stir welding of naturally aged aluminium alloys*, Materials & Design, 52 (2013), 730-739.
[34] Jacquin D., De Meester B., Simar A., Deloison D., Montheillet F., Desrayaud C.: *A simple Eulerian thermomechanical modelling of friction stir welding*, Journal of Materials Processing Technology, 211(1) (2011), 57-65.
[35] Tang W., Guo X., McClure J.C., Murr L.E.: *Heat input and temperature distribution in friction stir welding*, Journal of Materials Processing and Manufacturing Science, 7(2) (1998), 163-172.
[36] Sharma V., Prakash U., Kumar B.V.M.: *Surface composites by friction stir processing: A review*, Journal of Materials Processing Technology, 224 (2015), 117-134.
[37] Rodrigues D.M., Loureiro A., Leitao C., Leal R.M., Chaparro B.M., Vilaça P.: *Influence of friction stir welding parameters on the microstructural and mechanical properties of AA 6016-T4 thin welds*, Materials & Design, 30 (2009), 1913-1921.
[38] Węglowski M.S.: *Friction stir processing – State of the art*, Archives of Civil and Mechanical Engineering, 18 (2018), 114-129.
[39] Givi M.K.B., Asadi P.: *Advances in friction stir welding and processing*. Woodhead Publishing, Amsterdam, 2014.
[40] Kassner M.E., Barrabes S.: *New developments in geometric dynamic recrystallization*, Materials Science and Engineering: A, 410 (2005), 152-155.

[41] Heidarzadeh A., Mironov S., Kaibyshev R., Çam G., Simar A., Gerlich A., Khodabakhshi F., Mostafaei A., Field D.P., Robson J.D., Deschamps A., Withers P.J.: *Friction stir welding/processing of metals and alloys: A comprehensive review on microstructural evolution*, Progress in Materials Science, 117 (2021), 100752.
[42] Dudova N., Belyakov A., Sakai T., Kaibyshev R.: *Dynamic recrystallization mechanisms operating in a Ni–20% Cr alloy under hot-to-warm working*, Acta Materialia, 58 (2010), 3624-3632.
[43] Liu H., Fujii H.: *Microstructural and mechanical properties of a beta-type titanium alloy joint fabricated by friction stir welding*, Materials Science and Engineering: A, 711 (2018), 140-148.
[44] Humphreys F.J., Hatherly M.: *Recrystallization and related annealing phenomena*, Elsevier, 2004.
[45] Prabhu S.R.B., Shettigar A.K., Herbet M.A., Rao S.S.: *Microstructure evolution and mechanical properties of friction stir welded AA6061/Rutile composite*, Materials Research Express, 6(8) (2019), 0865i7.
[46] Padmanaban G., Balasubramanian V., Sarin Sundar J.K.: *Influences of welding processes on microstructure, hardness, and tensile properties of AZ31B magnesium alloy*, Journal of Materials Engineering and Performance, 19 (2010), 155-165.
[47] Wciślik W.: *Experimental determination of critical void volume fraction f_F for the Gurson Tvergaard Needleman (GTN) model*, Procedia Structural Integrity, 2 (2016), 1676-1683.
[48] Wciślik W., Pała R.: *Some microstructural aspects of ductile fracture of metals*, Materials, 14(15) (2021), 4321.
[49] Wciślik W., Lipiec S.: *Void-induced ductile fracture of metals: experimental observations*, Materials, 15(18) (2022), 6473.
[50] Dixit S., Mahata A., Mahapatra D.R., Kailas S.V., Chattopadhyay K.: *Multi-layer graphene reinforced aluminum – Manufacturing of high strength composite by friction stir alloying*, Composites Part B: Engineering, (136) (2018), 63-71.
[51] Merah N., Azeem M.A., Abubaker H.M., Al-Badour F., Albinmousa J., Sorour A.A.: *Friction stir processing influence on microstructure, mechanical, and corrosion behavior of steels: a review*, Materials, (14) (2021), 5023.
[52] Sato Y.S., Nelson T.W., Sterling C.J., Steel R.J., Pettersson C.O.: *Microstructure and mechanical properties of friction stir welded SAF 2507 super duplex stainless steel*, Materials Science and Engineering: A, (397) (2005), 376-384.
[53] Kwon Y.J., Saito N., Shigematsu I.: *Friction stir process as a new manufacturing technique of ultrafine grained aluminium alloy*, Journal of Materials Science, (21) (2002), 1473-1476.
[54] Saeid T., Abdollah-zadeh A., Assadi H., Malek Ghaini F.: *Effect of friction stir welding speed on the microstructure and mechanical properties of a duplex stainless steel*, Materials Science and Engineering: A, (496) (2008), 262-268.
[55] Ma Z.Y., Mishra R.S., Mahoney M.W.: *Superplastic deformation behaviour of friction stir processed 7075Al alloy*, Acta Materialia, 50(17) (2002), 4419-4430.
[56] Johnson P., Murugan N.: *Microstructure and mechanical properties of friction stir welded AISI321 stainless steel*, Journal of Materials Research and Technology, 9(3) (2020), 3967-3976.
[57] Gain S., Das S.K., Sanyal D., Acharyya S.K.: *Exploring friction stir welding for joining 316L steel pipes for industrial applications: Mechanical and metallurgical characterization of the joint and analysis of failure*, Engineering Failure Analysis, 150 (2023), 107331.
[58] Li H., Yang S., Zhang S., Zhang B., Jiang Z., Feng H., Han P., Li J.: *Microstructure evolution and mechanical properties of friction stir welding super-austenitic stainless steel S32654*, Materials and Design, 118 (2017), 207-217.
[59] Ahmed M.M.Z., Hajlaoui K., El-Sayed Seleman M.M., Elkady M.F., Ataya S., Latief F.H., Habba M.I.A.: *Microstructure and mechanical properties of friction stir welded 2205 duplex stainless steel butt joints*, Materials, 14 (2021), 6640.
[60] Liu F.C., Nelson T.W.: *In-situ grain structure and texture evolution during friction stir welding of austenite stainless steel*, Materials and Design, 115 (2017), 467-478.
[61] Salih O.S., Ou H., Sun W., McCartney D.G.: *A review of friction stir welding of aluminium matrix composites*, Materials & Design, (86) (2015), 61-71.
[62] Zhang Z., Xiao B.L., Ma Z.Y.: *Effect of welding parameters on microstructure and mechanical properties of friction stir welded 2219Al-T6 joints*, Journal of Materials Science, (47) (2012), 4075-4086.
[63] Huang K., Marthinsen K., Zhao Q., Logé R.E.: *The double-edge effect of second-phase particles on the recrystallization behaviour and associated mechanical properties of metallic materials*, Progress in Materials Science, (92) (2018), 284-359.
[64] Kloc L., Spigarelli S., Cerri E., Evangelista E., Langdon T.G.: *Creep behavior of an aluminum 2024 alloy produced by powder metallurgy*, Acta Materialia, (45) (1997), 529-540.
[65] Deschamps A., Fribourg G., Bréchet Y., Chemin J.L., Hutchinson C.R.: *In situ evaluation of dynamic precipitation during plastic straining of an Al-Zn-Mg-Cu alloy*, Acta Materialia, (60) (2012), 1905-1916.

[66] Sugimoto I., Park S.H.C., Hirano S., Saito H., Hata S.: *Microscopic observation of precipitation behavior at friction stirring zone of super duplex stainless steel*, Materials Transactions, 60(9) (2019), 2003-2007.
[67] Manugula V.L., Rajulapati K.V., Reddy G.M., Mythili R., Bhanu Sankara Rao K.: *Influence of tool rotational speed and post-weld heat treatments on friction stir welded reduced activation ferritic-martensitic steel*, Metallurgical and Materials Transactions A: Physical Metallurgy and Materials Science, 48(8) (2017), 3702-3720.
[68] Farneze H.N., Tavares S.S.M., Pardal J.M., Londoño A.J.R., Pereira V.F., Barbosa C.: *Effects of thermal aging on microstructure and corrosion resistance of AISI 317L steel weld metal in the FSW process*, Materials Research, 18(2) (2015), 98-103.
[69] He B., Cui L., Wang D.P., Li H.J., Liu C.X.: *Microstructure and mechanical properties of RAFM-316L dissimilar joints by friction stir welding with different butt joining modes*, Acta Metallurgica Sinica (English Letters), 33 (2020), 135-146.
[70] Ma Z.Y., Sharma S.R., Mishra R.S., Mahoney M.W.: Unpublished results.
[71] Dumont M., Steuwer A., Deschamps A., Peel M., Withers P.J.: *Microstructure mapping in friction stir welds of 7449 alu-minium alloy using SAXS*, Acta Materialia, (54) (2006), 4793-4801.
[72] Genevois C., Deschamps A., Denquin A., Doisneau-Cottignies B.: *Quantitative investigation of precipitation and mechanical behaviour for AA2024 friction stir welds, Acta Materialia*, (53) (2005), 2447-2458.
[73] Bastow T.J., Hill A.: *Guinier-Preston and Guinier-Preston-Bagaryatsky zone reversion in Al-Cu-Mg alloys studied by NMR*, Materials Science Forum, (519-521) (2006), 1385-1390.
[74] Morozova I., Królicka A., Obrosov A., Yang Y., Doynov N., Weiß S., Michailov V.: *Precipitation phenomena in impulse friction stir welded 2024 aluminium alloy*, Materials Science and Engineering A, (852) (2022), 143617.
[75] Ehrich J., Staron P., Karkar A., Roos A., Hanke S.: *Precipitation evolution in the heat-affected zone and coating material of AA2024 processed by friction surfacing*, Advanced Engineering Materials, (24) (2022), 2201019.
[76] Ostermann F.: *Anwendungstechnologie aluminium*. Springer-Verlag, Berlin, 2014.
[77] Sauvage X., Dédé A., Cabello Muñoz A., Huneau B.: *Precipitate stability and recrystallisation in the weld nuggets of friction stir welded Al-Mg-Si and Al-Mg-Sc alloys*, Materials Science and Engineering A, (491) (2008), 364-371.
[78] Hamilton C., Dymek S., Kopyściański M., Węglowska A., Pietras A.: *Numerically based phase transformation maps for dissimilar aluminum alloys joined by friction stir-welding*, Metals, 8(5) (2018), 324.
[79] Santos T.G., Miranda R.M., Vilaça P., Teixeira J.P., dos Santos J.: *Microstructural mapping of friction stir welded AA 7075-T6 and AlMgSc alloys using electrical conductivity*, Science and Technology of Welding and Joining, 16(7) (2011), 630-635.
[80] Hou J.C., Liu H.J., Zhao Y.Q.: *Influences of rotation speed on microstructures and mechanical properties of 6061–T6 aluminum alloy joints fabricated by selfreacting friction stir welding tool*, International Journal of Advanced Manufacturing Technology, (73) (2014), 1073-1079.
[81] Zhao Y., Wang C., Dong C.: *Microstructural characteristics and mechanical properties of water cooling bobbin-tool friction stir welded 6063-T6 aluminum*, MATEC Web of Conferences, (206) (2018), 03002.


environment
environment

Anna Ciaciuch, Mariusz Sulewski
Structure and Environment 2024, vol. 16, (2), pp. 111-121, Article number: el 010
https://doi.org/10.30540/sae-2024-010

Structure and Environment
ISSN 2081-1500
e-ISSN 2657-6902
https://content.sciendo.com/sae
https://sae.tu.kielce.pl

sciendo

Kielce University of Technology

DOI: 10.30540/sae-2024-010

RECOVERY OF THE ORGANIC SOLVENTS FROM THE MULTICOMPONENT MIXTURE IN THE PROCESS OF THE FRACTIONAL DISTILLATION AND THE VACUUM DISTILLATION

ODZYSKIWANIE ROZPUSZCZALNIKÓW ORGANICZNYCH Z MIESZANINY WIELOSKŁADNIKOWEJ W PROCESIE DESTYLACJI FRAKCYJNEJ I DESTYLACJI PRÓŻNIOWEJ

Anna Ciaciuch, Mariusz Sulewski*
Bydgoszcz University of Science and Technology, Poland

Abstract

In these times of sustainability, the purification and regeneration of used solvents is attracting a lot of interest for environmental reasons and to reduce production costs. The article presents research on the separation of organic solvents such as acetonitrile, methanol, acetone, and toluene from a multicomponent mixture of liquid organic waste. This is an element of the circular economy and prevents the emission of volatile organic compounds into the environment. In order to separate the mixture and recover the solvents, fractional distillation and vacuum distillation were used together with pre-treatment of the waste using sorption on silica gel and calcium oxide. The analysis of the waste composition and the mixture after the separation was performed by gas chromatography coupled with a mass spectrometer (GC-MS). As a result of the research, the acetonitrile concentration increased to 90.7% after fractional distillation.

Keywords: fractional distillation, vacuum distillation, organic solvents, acetonitrile

Streszczenie

Aktualnie w czasach zrównoważonego rozwoju oczyszczanie i regeneracja zużytych rozpuszczalników cieszy się dużym zainteresowaniem ze względów środowiskowych i w celu obniżenia kosztów produkcji. W artykule przedstawiono badania nad wydzielaniem rozpuszczalników organicznych takich jak acetonitryl, metanol, aceton i toluen z wieloskładnikowej mieszaniny ciekłych odpadów organicznych. Jest to element gospodarki o obiegu zamkniętym i zapobiega emisji lotnych związków organicznych do środowiska. W celu rozdzielenia mieszaniny i odzyskania rozpuszczalników zastosowano destylację frakcyjną i destylację próżniową wraz z wstępną obróbką odpadów metodą sorpcji na żelu krzemionkowym i tlenku wapnia. Analizę składu odpadów oraz frakcji po rozdziale mieszaniny przeprowadzono metodą chromatografii gazowej sprzężonej ze spektrometrem mas (GC-MS). W wyniku przeprowadzonych prób stężenie acetonitrylu po destylacji frakcyjnej wzrosło do 90,7%.

Słowa kluczowe: destylacja frakcyjna, destylacja próżniowa, rozpuszczalniki organiczne, acetonitryl

1. INTRODUCTION

Organic solvents are widely used in many branches of industry (the greatest demand for solvents is recorded in the production of paints and coatings, inks, and adhesives. chemical, pharmaceutical, paints, and varnishes) and laboratories due to their valuable properties, as it was described [1]. These include, first of all, the ability to dissolve other substances

*Bydgoszcz University of Science and Technology, Poland, e-mail: mariusz.sulewski@pbs.edu.pl

without changing their chemical structure. Desirable characteristics of solvents are also transparency and lack of colour, volatility, appropriate viscosity depending on the type of use, resistance to chemicals, non-corrosive to apparatus, anhydrousness, chemical, and physical stability, and cost. Since sustainable development also applies to solvent management, more and more attention is paid to the fact that solvents are non-toxic, biodegradable, odour-free, and regenerable, to minimize the exposure of workers during production and use of solvents to their harmful effects and to reduce the emission of volatile organic compounds (VOC) to the atmosphere, what was studied [2].

In recent years, the development of two directions in the economy of solvents can be noticed. The first is to replace traditional solvents, the so-called ”green solvents”. This direction was widely described [3-5], and the second is the regeneration of used solvents after various industrial processes. The so-called ”green solvents” can be successfully used, inter alia, in the paints and varnishes sector, because it is in this production sector that the transition from solvent-based to water-based products can be observed. The development of the biological solvents production was widely described, such as bioethanol [6], butane 1-ol [7], acetic acid [8], 1-octanol [9], 1,3-diol butane, glycerol [1] were widely described. However, many branches of the chemical industry do not allow this type of solvents to achieve the desired product characteristics and classic solvents will still be used due to their chemical properties. The way to manage used organic solvents, which, mainly due to their volatility, pose a threat to the environment is their recovery. This allows not only the multiple use of solvents but also an ecological and environmentally safe method of disposal. Solvents used in chemical reactions, chemical analysis, or the pharmaceutical industry must meet high standards in terms of purity. This often requires the use of advanced and complex cleaning methods. The method that will be used to purify the solvents depends on the solvent itself and the type of impurities present in the mixture. The most commonly used and described are simple and fractional distillation techniques, membrane processes, and ion exchange [11-14]. Depending on the amount of waste, the nature of the mixture, and the process economy, the regeneration process is optimized, taking into account the technical possibilities, the scale of the process, and the required purity of the solvent. The solvent recovery process typically takes place in several steps, starting with the removal of solids that may be present in the waste stream, followed by a recovery, purification, and refinement step where higher purity solvents are required, these steps were presented [15]. Methods of purifying a mixture of organic solvents are discussed in the literature [10-12, 15]. The most commonly used distillation methods involve a multi-stage purification process or the use of recycl of the distillation stream for repeated distillation. The basic difficulties encountered during the purification of solvents include the need to separate substances from a multicomponent mixture of organic solvents and other impurities, flammability and explosiveness. Another problem is the presence of water in the mixture, which promotes the formation of azeotropic mixtures [16-20].

Undoubtedly, a very important aspect is the energy consumption of the solvent recovery process, because the process of separating the mixture and purifying solvents requires energy in the form of heat. Of course, due to the scale of the process and the required final purity of the solvents, this parameter will vary. Technical and economic indexes of distillation processes were compared in [21] such as conventional single column distillation process, conventional single column mechanical vapour recompression (MVR), heat pump distillation process, split heat pump distillation (SHPD) with single-state compression and SHPD with two-stage compression in process of the separation of acetone and water mixture. It was shown, that the conventional single-column distillation process compared with the conventional single-column MVR heat pump distillation process can save energy by 43.56%. The energy of SHPD with single-stage compression and the SHPD with two-stage compression was saved by 56.31% and 69.78%, respectively. Additionally, the SHPD process provides an effective energy-saving method for the separation of mixtures with large temperature differences and constant concentration.

One of the most widely used solvents is acetonitrile. Due to its low viscosity, high stability and high elution power, it has been widely used, among others, as a polar aprotic solvent in organic synthesis, fabric dyeing, lighting, and as an eluent in chromatographic techniques [18]. The leader in consumption is the Asia-Pacific region, where the annual growth rate of consumption will be 5% per year, while Europe and North America will show a more moderate growth of 4% per year [10].

Currently, many enterprises strive to optimize their production processes, minimize the impact of industrial activities on the environment and sustainably manage production. This results in the need to use solvent recovery systems that enable effective removal of a wide range of contaminants from the waste stream.

The solutions most often chosen by companies include solvent purification systems in evaporation processes using distillers and evaporators to regenerate contaminated solvents at atmospheric pressure and vacuum. These systems can be easily adapted to the individual needs of enterprises taking into account the nature of production, including daily efficiency, automation and ease of use. Additionally, these systems can be easily combined with a heat recovery system (heat exchangers) or coupling the solvent recovery system with the distillate purification system when high solvent purity is required, e.g. in the ion exchange process. The use of a system for recycling used solvents and their mixtures in the company not only reduces production costs, but also complies with the principles of "green chemistry" by saving raw materials and the principles of a closed-loop economy.

The aim of the work was to optimize the separation process of components of a waste mixture of volatile organic solvents, the dominant component of which was acetonitrile. The research was carried out on a laboratory scale and included five experiments where fractional distillation at atmospheric pressure and vacuum distillation were used to separate a multi-component mixture of organic solvents. The raw material for the tests was liquid waste, which was a mixture of volatile organic compounds with an admixture of water. The volatile components of a mixture of liquid organic waste were identified by using gas chromatography coupled with a mass spectrometer (GC-MS).

2. MATERIALS AND METHODS

The research material was liquid waste, which is a mixture of organic solvents, from research and development laboratories in the polyurethane adhesives and foams industry.

Qualitative and quantitative analysis of the mixture components were performed by GC-MS and gas chromatography coupled with a flame ionization detection (GC-FID). The qualitative GC-MS analysis was performed on an Agilent 7890B apparatus with an MS 5977B detector. The DB-23 capillary column 60 meters long, 0.250 mm internal diameter from Agilent was used. Helium was used as the carrier gas at a pressure of 20 psi. The temperature program started at 50°C for 7 minutes and the temperature was programmed to increase at a rate of 20°C/min to 250°C. Identification of volatile organic compounds present in the samples was carried out based on the NIST mass spectral database updated in 2019.

Chromatographic quantitative analysis of raw material and collected fractions was carried out on an HP 5890 Series II apparatus equipped with a flame ionization detector under analogous conditions. The concentrations of individual components were determined using the standard curve method. The volatile organic compounds of p.a. quality were used as standards.

Figure 2 shows the chromatogram of raw material with fourteen identified components.

Infrared analysis was performed on the FT-IR Bruker Alpha spectrometer by ATR (Attenuated Total Reflectance, Germany) on a diamond P-type attachment.

In order to separate the components of the raw material, the following experiments were carried out. Figure 1 shows the fractional and vacuum distillation sets used for the experiments:

Experiment 1. The fractional distillation of raw waste. Fractional distillation was performed on

Fig. 1. Distillation sets used in experiments: a) BUCHI vacuum evaporator, b) fractional distillation set

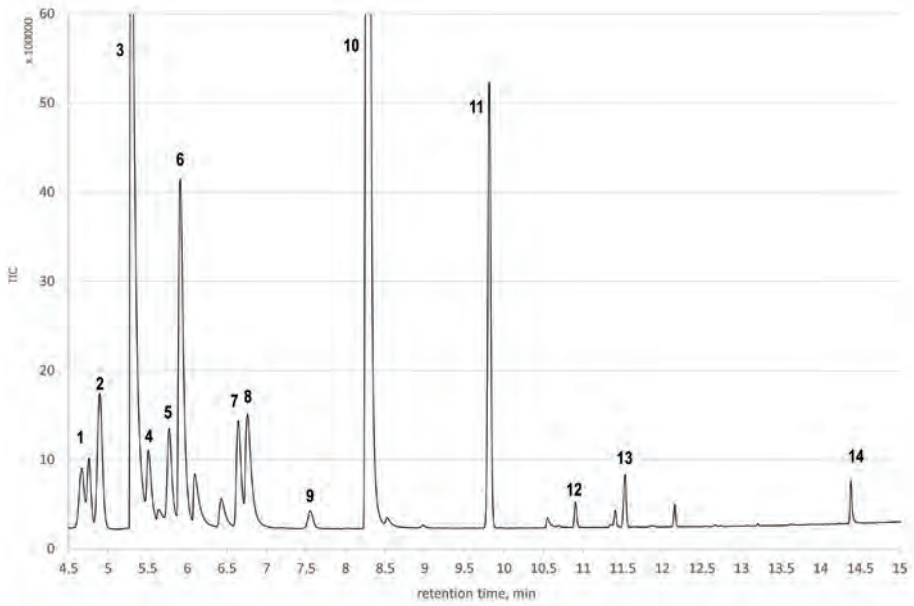

Fig. 2. Chromatogram of the raw material obtained by the GC-MS method. Peak numbering according to the compound numbers described in Table 1

a borosilicate glass column (800 mm, Simax). The individual fractions were collected in the temperature range of 50-80°C.

Experiment 2. Fractional distillation preceded by drying over silica gel (desiccant 2-5 mm, Merck, Germany). The crude waste was passed through a silica gel column to separate the water. Then, fractional distillation was performed as in experiment 1.

Experiment 3. Vacuum distillation. A rotary evaporator (ROTAVAPOR R-300, Buchi Labortechnik AG, Switzerland) was used. The process was carried out at a temperature of 50°C. The pressure was reduced gradually over the range of 410-290 mbar while collecting the individual fractions.

Experiment 4. Vacuum distillation followed by drying over silica gel. The crude material stream was passed through a silica gel column as in experiment 2. Then the procedure was as in experiment 3.

Experiment 5. Vacuum distillation followed by drying with calcium oxide CaO (Chempur, Poland). Anhydrous calcium oxide in an amount of 65 g/l was added to the raw material and mixed for 1 hour. After CaO was filtered off, distillation was carried out as in experiment 3.

3. RESULTS

3.1. Analysis of raw waste

After the quantitative analysis by the GC-FID method, it was found that raw waste contained acetonitrile methanol toluene and acetone in amounts of 55.4%, 22.4%, 4.13% and 2.04% by volume (Fig. 2). The water content in the mixture was 4% v/v. The remaining ten components of the mixture are in the range from 0.3 to 2% v/v. A detailed list of concentrations is presented in Table 1.

Table 1. The content of organic solvents in raw material

No.	Compound	Conc., % v/v	Boiling pt (°C)	No.	Compound	Conc., % v/v	Boiling pt (°C)
1.	1-methoxy-2-propanol	0.31	119.6	8.	ethyl acetate	1.38	77.1
2.	cyclohexane	0.80	80.7	9.	tetrahydrofuran	1.90	66.0
3.	methanol	22.45	65.0	10.	acetonitrile	55.41	81.6
4.	methyl acetate	0.50	57.0	11.	toluene	4.13	110.6
5.	hexane	0.40	68.7	12.	butyl acetate	0.38	125.0
6.	acetone	2.04	56.3	13.	xylene	0.64	139.0
7.	2-propanol	1.33	82.3	14.	N,N-DMF	1.12	153.0

3.2. Fractional distillation

Fractional distillation was carried out for raw material and material after prior drying. Drying was accomplished by passing the crude solvent mixture through a column containing silica gel. The distillate samples were collected at defined temperatures and subjected to chromatographic analysis.

The infrared spectroscopy analysis of the collected fractions was performed. It has been shown that during the temperature increase, the acetonitrile content increases, which was confirmed by an increase in the intensity of absorption band in the range of 2200-2400 cm^{-1}. At the same time, an increase in the intensity of the band coming from the C = O groups in the range of 1650-1780 cm^{-1} can be noticed. As the temperature increases, the methanol content in the obtained fractions decreases, which is confirmed by the reduction of the band intensity in the range of approx. 1100 cm^{-1}. A comparison of the infrared spectra of selected fractions is shown in Figure 3.

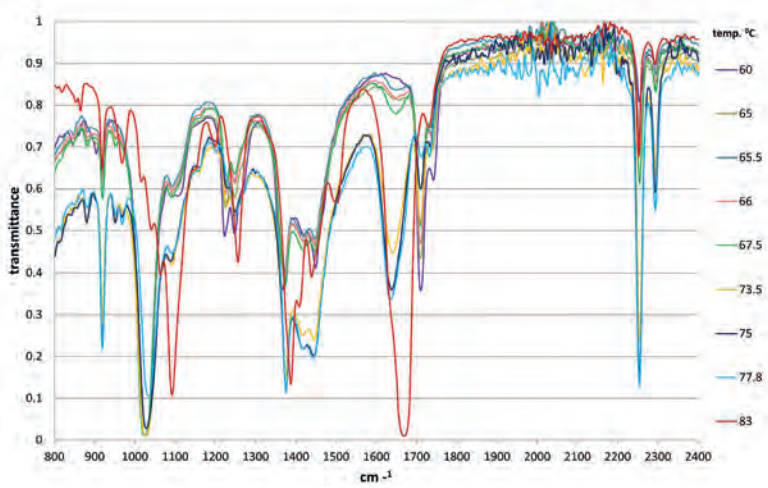

Fig. 3. Comparison of IR spectra of fractions obtained during fractional distillation

Table 2. The content of organic solvents (% v/v) depending on fractional distillation temperature

Temperature, °C	60.0	64.4	65.0	65.4	66.5	67.5	68.9	71.7	73.5	75.0	77.8	83.0
	Concentration, % v/v											
1-methoxy-2-propanol	–	–	–	–	–	–	–	–	–	0.49	0.99	8.76
2-propanol	1.33	0.51	0.58	0.63	0.79	0.97	1.10	1.38	1.42	1.28	0.93	–
acetone	10.4	9.68	9.52	9.27	7.98	6.34	5.45	3.35	2.13	1.15	0.45	–
acetonitrile	20.5	39.0	42.6	44.7	48.8	54.1	57.7	69.6	78.9	85.6	90.7	56.7
butyl acetate	–	–	–	–	–	–	–	–	0.61	0.86	1.25	3.52
cyclohexane	22.3	5.22	2.42	1.02	–	–	–	–	–	–	–	–
ethyl acetate	1.33	1.70	1.75	1.77	1.73	1.57	1.47	1.12	0.84	0.56	–	–
hexane	9.19	2.11	1.18	0.55	–	–	–	–	–	–	–	–
methanol	25.4	30.3	30.8	31.1	29.8	26.5	24.8	16.5	10.7	5.62	2.13	–
methyl acetate	2.03	1.34	1.21	1.03	0.79	0.56	0.43	–	–	–	–	–
N,N-DMF	–	–	–	–	–	–	–	–	–	–	–	29.9
tetrahydrofuran	3.58	3.41	3.34	3.23	2.69	2.01	1.63	0.84	–	–	–	–
toluene	3.13	5.16	5.39	5.53	5.52	5.06	4.69	3.43	2.44	1.62	0.96	–
xylene	–	–	–	–	0.46	0.57	0.65	0.87	0.98	1.03	1.04	1.35

The chromatographic analysis has shown, that changes in the composition of the individual fractions were temperature-dependent. This is particularly evident in the case of methanol and acetonitrile. With the increase in the boiling point of individual fractions, the content of acetonitrile increased until it reached almost 90% of the content. At the same time, the content of methanol was the highest around the boiling point (approx. 65°C), and then it systematically decreased to the level of approx. 2%. However, it is noteworthy, that due to the formation of azeotropes, it was not possible to separate all methanol at its boiling point and it appeared in higher-boiling fractions. Only above 70°C did its content drop significantly. Detailed results are presented in Table 2.

Experiment 2. Was performed by subjecting the raw waste to prior drying on a silica gel column. It is noteworthy that after drying the raw waste with silica gel, some components present in crude material in small amounts, such as butyl acetate (No. 5 Table 1), 1-methoxy-2-propanol (No. 1 Table 1) or 2-propanol (No. 2 Table 1), didn't appear in the fractions obtained later during distillation. The content of low-boiling waste components such as cyclohexane and hexane, which constitute nearly 30% of the fraction obtained at 60°C for raw waste, has also significantly decreased (Table 2). After drying, the content of these compounds in the lowest boiling fraction dropped to 11%, and in the remaining fractions, they were practically absent. It should be assumed that these components were adsorbed on a bed of silica gel. As in the case of the raw waste, a significant content of N,N-dimethylformamide can be observed in the residue, with a simultaneous decrease in the content of acetonitrile (Table 3).

The comparison of the content of the main components of the mixture for both experiments using the fractional distillation process depending on the boiling point is shown in Figure 4.

Table 3. Composition of the fractions obtained after fractional distillation of dried material

Temperature, °C	63	65	67	68.2	70.5	72.8	75	83
	Concentration, % v/v							
2-propanol	–	2.43	2.20	–	2.64	2.48	2.31	–
acetone	10.54	8.98	7.93	7.35	5.20	3.47	2.03	–
acetonitrile	38.20	46.26	52.65	58.44	65.42	71.83	83.72	71.75
cyclohexane	8.30	1.57	–	–	–	–	–	–
ethyl acetate	–	–	–	–	–	1.24	–	–
hexane	3.48	–	–	–	–	–	–	–
methanol	30.74	30.99	28.76	28.34	22.03	15.93	9.73	–
methyl acetate	–	1.65	–	–	–	–	–	–
N.N-DMF	–	–	–	–	–	–	–	22.36
tetrahydrofuran	3.54	1.93	2.63	–	–	0.88	–	–
toluene	5.19	6.19	5.83	5.86	4.72	3.27	2.20	5.89
xylene	–	–	–	–	–	0.91	–	–

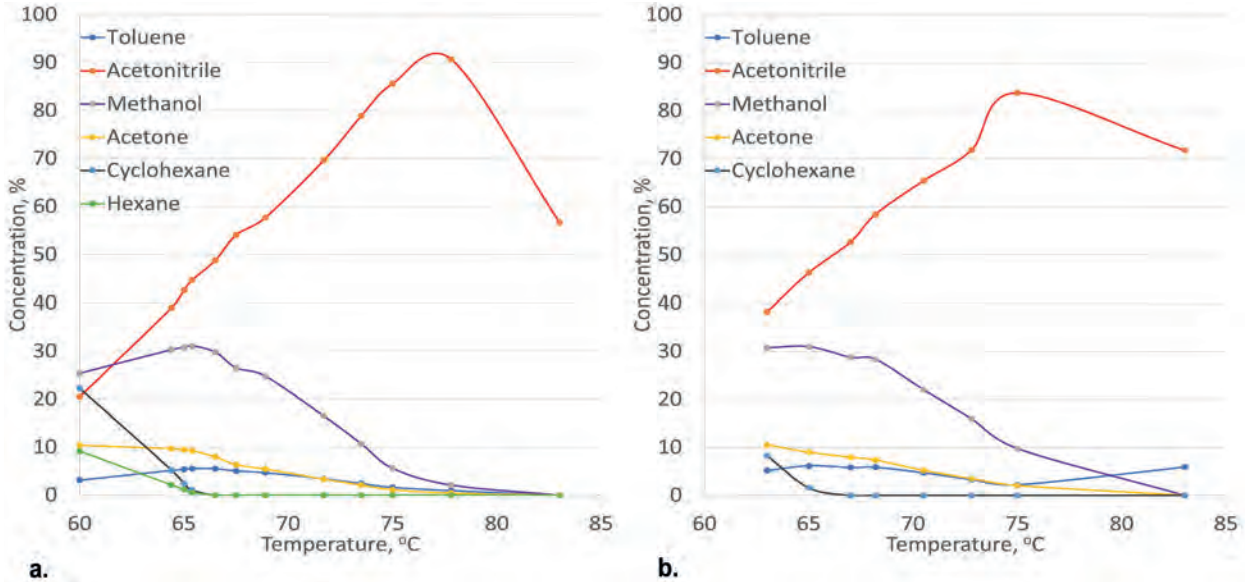

Fig. 4. The content of the main components of the fractions obtained: a) raw material, b) material after drying

3.3. Vacuum distillation

The process was carried out at a constant temperature of 50°C, gradually reducing the pressure. The collected fractions were subjected to chromatographic analysis and infrared spectroscopy. The differences in the pressures at which the fractions were collected for individual experiments result from the efficiency of the condensate streams, which for different samples allowed for collecting of appropriate volumes of distillate at different pressures.

The analysis of the IR spectra showed that as the pressure decreased, the acetonitrile content in the obtained fractions increased. The comparison of the spectra of selected fractions is shown in Figure 5.

The results of quantitative determinations of the components of individual fractions are presented in Table 4. It can be seen that the separation of the substance when the pressure decreases is similarly to the increase in temperature during fractional distillation. Important for the separation of the main components is the much lower acetonitrile content – c.a 73% v/v (Table 4) in the richest fraction, while in the case of fractional distillation near 91% v/v (Table 2, Fig. 3) of acetonitrile content was achieved.

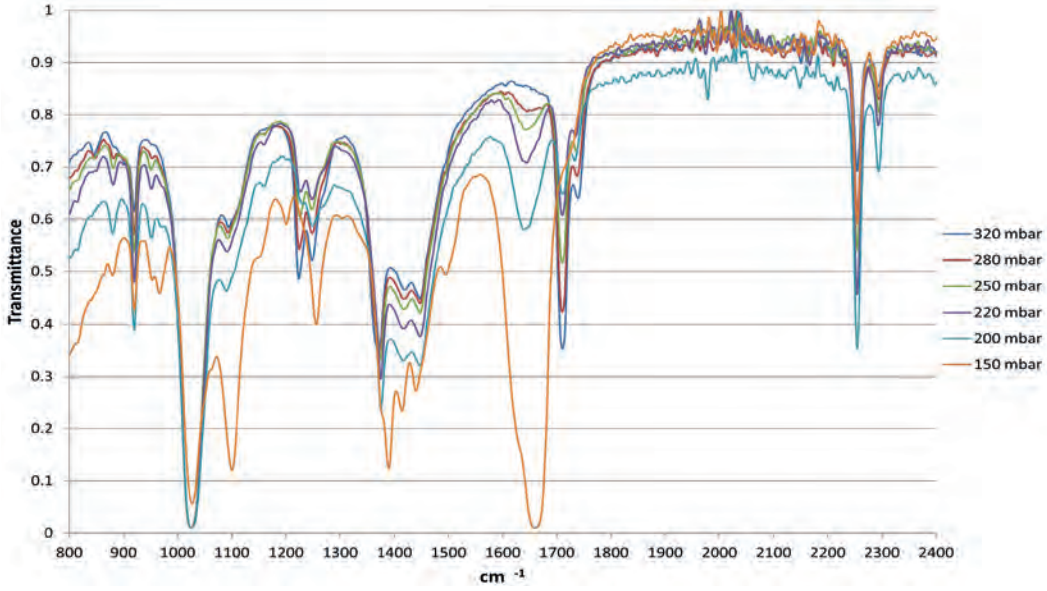

Fig. 5. Comparison of the IR spectra of the fractions obtained by vacuum distillation

Table 4. Composition of the obtained fractions of raw waste after vacuum distillation

Pressure, mbar	320	280	250	220	200	100
	Concentration, % v/v					
1-methoxy-2-propanol	–	–	–	–	–	5.48
2-propanol	0.94	1.48	1.99	2.52	3.14	4.08
acetone	11.33	8.81	5.55	3.03	1.35	–
acetonitrile	39.04	50.84	59.34	67.34	73.31	54.51
butyl acetate	–	–	–	0.49	1.05	2.22
cyclohexane	6.44	0.71	–	–	–	–
ethyl acetate	1.75	1.72	1.46	1.11	0.71	–
hexane	3.15	–	–	–	–	–
methanol	26.86	26.63	23.36	19.21	8.28	3.71
methyl acetate	1.52	0.96	0.44	–	7.48	7.77
N,N-DMF	–	–	–	–	–	17.58
tetrahydrofuran	3.93	2.96	1.74	0.85	–	–
toluene	5.05	5.31	4.69	3.31	1.79	–
xylene	–	–	0.63	0.93	1.26	2.14

The next experiments were carried out after preliminary drying of the raw material with the use of silica gel (experiment 4) and calcium oxide (experiment 5).

As in the case of fractional distillation, drying with both silica gel and calcium oxide resulted in a significant reduction in the amount of some components in the obtained fractions. This is especially true of hexane and cyclohexane. However, no butyl acetate and 1-methoxy-2-propanol were found in any of the fractions obtained. The results of the chromatographic analysis of the obtained fractions are summarized in Table 5.

Table 5. Composition of the obtained fractions of raw waste after drying and vacuum distillation

Sample	after silica-gel drying						after CaO drying					
Pressure, mbar	425	390	360	330	290	150	430	410	390	370	330	180
	Concentration, % v/v											
2-propanol	–	2.12	2.54	2.81	3.03	3.42	1.72	2.03	2.37	2.71	2.99	–
acetone	10.6	6.23	4.19	2.37	1.09	–	8.95	7.16	5.42	3.91	2.99	3.43
acetonitrile	41.8	55.9	62.9	71.7	78.5	80.9	49.3	54.4	59.3	65.1	70.1	78.0
cyclohexane	2.68	–	–	–	–	–	–	1.46	–	–	–	–
ethyl acetate	1.79	1.59	1.34	0.97	–	–	1.66	1.51	1.33	1.11	0.89	–
hexane	1.45	–	–	–	–	–	–	–	–	–	–	–
methanol	29.6	26.6	22.6	17.6	12.7	7.86	28.9	25.6	24.3	21.2	17.7	10.9
tetrahydrofuran	3.57	1.99	1.22	–	–	–	3.03	2.30	1.67	1.11	–	–
toluene	5.58	5.06	4.05	2.62	1.24	0.34	5.21	4.79	4.34	3.60	2.66	1.20
xylene	–	–	–	0.99	1.12	0.90	–	-–	–	–	1.10	1.09

A graphical comparison of the composition changes of the main components of raw waste in the vacuum distillation process is shown in Figures 6 and 7.

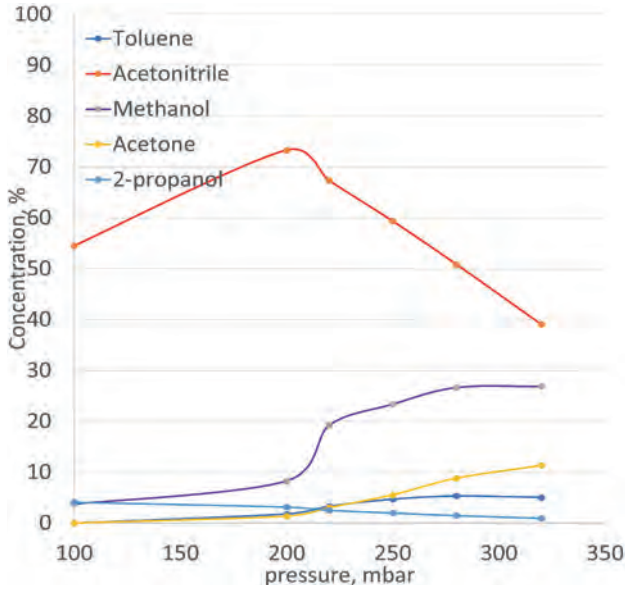

Fig. 6. The content of the main components of the fractions obtained in vacuum distillation

None of the analyzed methods resulted in obtaining a solvent fraction of analytical purity, but for many industrial applications such purity is not required. A fraction containing approximately 90% acetonitrile may meet the necessary requirements depending on the technological process for which it is to be used. The choice of method should depend on the specific composition of the mixture of volatile organic solvents, which, as we know, depends on the source of waste origin.

4. CONCLUSIONS

Global trends indicate an increase in the consumption of acetonitrile in the coming years. So we can expect the prices of organic solvents to increase. It will be beneficial for production plants to use solvent recovery, which is in line with the principles of sustainable development and green chemistry.

This article presents effective and cheap methods of recovering organic solvents from waste. Volatile organic components were separated by fractional distillation and distillation under reduced pressure.

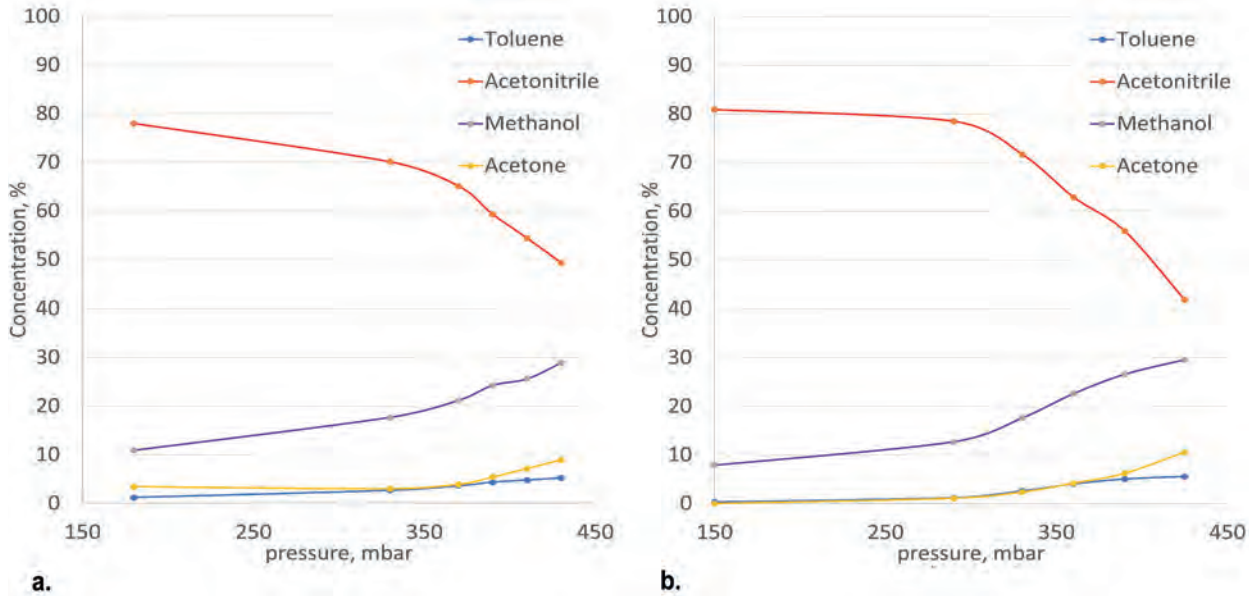

Fig. 7. The content of the main components of the fractions obtained in vacuum distillation: a) material dried on CaO, b) material dried on silica-gel

Comparing the methods used, fractional distillation turned out to be more effective in the recovery of acetonitrile. However, taking into account the energy efficiency of the process and the small difference between the achieved results, vacuum distillation can also be considered worth using for the waste tested.

In analyzed waste the main components of the volatile organic compounds were acetonitrile, methanol and toluene in amounts of 55%, 22.5% and approx. 4%, respectively. The mixture was also dried using cheap and easily available agents, such as silica gel and CaO. Initial drying of raw material

with silica gel and calcium oxide caused the sorption of some components present in low concentrations in the raw waste. As a result, the input stream to the next fractional distillation process was free from some impurities. The amounts of acetonitrile was 90.7% v/v after fractional distillation process (at a temperature of 77.8°C) (Table 2). This means that the concentration of acetonitrile after fractional distillation relative to the raw material increased by about 36%. In the process of vacuum distillation acetonitrile concentration in the obtained fractions was observed at a maximum of 80.9%, which is a value nearly 10% lower than in the case of fractional distillation.

The analyzed methods, such as fractional and vacuum distillation, are relatively simple and cheap processes. It is worth emphasizing that the analyzed methods work well on a laboratory and semi-technical scale, which is a sufficient scale for many laboratories and small production companies. Due to differences in the design of the equipment, scaling the process to an industrial scale requires extensive optimization research. It should also be noted that the tested liquid waste had a specific composition, characteristic of the production industry. The recovery of organic solvents requires an individual approach depending on the quantitative and qualitative composition of waste generated in a given production process.

This research did not receive any specific grant from funding agencies in the public, commercial, or not-for-profit sectors.

REFERENCES

[1] Calvo-Flores F.G., Monteagudo-Arrebola M.J., Dobado J.A., Isac-García J., 2018. *Green and Bio-Based. Green and Bio-Based Solvents*. Top Curr Chem (Z), 18, 376:18. DOI: 10.1007/s41061-018-0191-6.
[2] Clark J.H., Farmer T.J., Hunt A.J., Sherwood J., 2015. *Opportunities for Bio-Based solvents created as petrochemical and fuel products transition towards renewable resources*. Int. J. Mol. Sci., 16, 17101-17159. DOI:10.3390/ijms160817101.
[3] Brouwer T., Schuur B., 2020. *Bio-based solvents as entrainers for extractive distillation in aromatic/aliphatic and olefin/paraffin separation*. Green Chem., 22, 5369-5375. DOI: 10.1039/D0GC01769H.
[4] Chaudhary A., Dwivedi A., Upadhyayula S., 2021. Chapter 28 – *Supercritical fluids as green solvents.* Handbook of Greener Synthesis of Nanomaterials and Compounds, 1, 891-916. DOI: 10.1016/B978-0-12-821938-6.00028-1.
[5] Dolzhenko A.V., 2021. *Green solvents for eco-friendly synthesis of bioactive heterocycles*, 2021. Green Synthetic Approaches for Biologically Relevant Heterocycles (Second Edition). 2, 393-470. DOI: 10.1016/B978-0-12-820792-5.00007-X.
[6] Manochio C., Andrade B.R., Rodriguez R.P., Moraes B.S., 2017. *Ethanol from biomass: A comparative overview*. Renew Sustain Energy Rev 80, 743-755. DOI: 10.1016/j.rser.2017.05.063.
[7] Ndaba B., Chiyanzu I., Marx S., 2015. *n-Butanol derived from biochemical and chemical routes: A review*. Biotechnol Rep, 8, 1-9. DOI: 10.1016/j.btre.2015.08.001.
[8] Clark J.H., Hunt A., Topi C., Paggiola G., Sherwood J., 2017. *Sustainable solvents. CHAPTER 6: an appendix of solvent data sheets*. Royal Society of Chemistry, Green Chem Ser No. 49. DOI: 10.1039/9781782624035.
[9] Akhtar M.K., Dandapani H., Thiel K., Jones P.R., 2015. *Microbial production of 1-octanol: A naturally excreted biofuel with diesel-like properties*. Metab. Eng. Commun., 2, 1-5. DOI: 10.1016/j.meteno.2014.11.001.
[10] Acrylonitrile (ACN): 2023, *World Market Outlook up to 2032,* Report, Merchant Research and Consulting Ltd.
[11] Aboagye E.A., Chea J.D., Yenkie K.M., 2021. *Systems level roadmap for solvent recovery and reuse in industries*. iScience, 24, 10, 1-29. DOI: 10.1016/j.isci.2021.103114.
[12] Godbole S.P., Wappelhorst R.L., Jacobson P.A., 2001. *Purification and recovery of acetonitrile*, United States Patent 6326508, Application Number: 09/654631.
[13] Ohba K., Takano K., Iida M., Abe S., Masudo T., Kishizaki O., Ishibashi R., Yamashita Y., 2019. *Purification process for hydrolysable organic solvent*. United States Patent Application Publication, Pub . No US 2019 / 0009267 A1.
[14] Clarke C.J., Tu W-Ch., Levers O., Bröhl A., Hallett J.P., 2018. *Green and Sustainable Solvents in Chemical Processes.* Rev., 118, 2, 747–800. DOI: 10.1021/acs.chemrev.7b00571.
[15] Chea J.D., Lehr A.L., Stengel J.P., Savelski M.J., Slater C., Yenkie K.M., 2020. *Evaluation of Solvent Recovery Options for Economic Feasibility through a Superstructure-Based Optimization Framework*. Ind. Eng. Chem. Res., 59, 13, 5931-5944. DOI: 10.1021/acs.iecr.9b06725.
[16] Wang Y., Cui P., Ma Y., Zhang Z., 2015. *Extractive distillation and pressure-swing distillation for THF/ethanol separation. J Chem Technol Biotechnol*., 90, 1463-1472. DOI: 10.1002/jctb.4452.
[17] Frolkova A., Frolkova A., Gaganov I., 2021. *Extractive and auto-extractive distillation of azeotropic mixtures*. Chem. Eng. Technol. 44, 8, 1397–1402. DOI: 10.1002/ceat.202100024.

[18] Jun Qi, Yafang Li, Jiaxing Xue, Ruiqi Qiao, Zhishan Zhang, Qunsheng Li, 2020. *Comparison of heterogeneous azeotropic distillation and energy-saving extractive distillation for separating the acetonitrile-water mixtures*. Separation and Purification Technology, 238, 116487, ISSN 1383-5866, https://doi.org/10.1016/j.seppur.2019.116487.
[19] Lu Qi, Jinlong Li, Ao Yang, Xiuguang Yi, and Weifeng Shen, 2022. *Toward a Sustainable Azeotrope Separation of Acetonitrile/Water by the Synergy of Ionic Liquid-Based Extractive Distillation*, Heat Integration, and Multiobjective Optimization. Industrial & Engineering Chemistry Research 61 (27), 9833-9846. DOI: 10.1021/acs.iecr.2c01285.
[20] Yasen Dai, Xiangyu Zhou, Xiaojun Chu, Chen Li, Zihao Su, Zhaoyou Zhu, Peizhe Cui, Jianguang Qi, and Yinglong Wang, 2022. *Effect of Entrainer Thermodynamic Properties on the Separation of Ternary Mixtures Containing Two Minimum Boiling Azeotropes by Extractive Distillation*. Industrial & Engineering Chemistry Research 61 (41), 15273-15288. DOI: 10.1021/acs.iecr.2c02306.
[21] Yang D., Li M., Lou Ch., Wan D., Yun Y., 2022. S*plit heat pump distillation based on two-stage compression for separating an acetone-water mixture*. Chem. Eng. Technol. 45,1, 159-166. DOI: 10.1002/ceat.202100289.

IMPORTANCE OF HISTORICAL BACKGROUND OF THE PLACE AND CULTURAL AWARENESS IN DESIGNING COMPETITION PROJECTS DURING STUDENTS' WORKSHOPS

ZNACZENIE TŁA HISTORYCZNEGO DANEGO MIEJSCA I ŚWIADOMOŚCI KULTUROWEJ W TWORZENIU PROJEKTÓW KONKURSOWYCH PODCZAS WARSZTATÓW STUDENCKICH

Apolonia Kuc
Jagiellonian University, Poland

Structure and Environment vol. 16, No. 2/2024, p. 67 DOI: 10.30540/sae-2024-006

Abstract

This article's primary objective is to illustrate how an understanding of the historical and cultural context of a location can significantly enhance students' academic workshops, fostering interdisciplinary knowledge acquisition and aiding them in designing projects for international architectural competitions. Frequently, such projects tend to conform to global trends, often imitating fashionable patterns without regard for the local context, traditions, or cultural nuances.

The first section of this article describes the methodology employed in international student workshops. The second section delves into the application of the problem-based learning method (PBL) when conceiving projects for architectural competitions, emphasizing the importance of factoring in historical and cultural heritage when selecting design concepts. The third section provides a comprehensive analysis of the workshop outcomes and initiates a discussion on the pivotal role of historical context and the significance of cultural awareness in this educational context.

Streszczenie

Ten artykuł ma na celu pokazanie, w jaki sposób zrozumienie historycznego i kulturowego kontekstu danego miejsca może znacząco wzbogacić warsztaty akademickie dla studentów, sprzyjając interdyscyplinarnej akwizycji wiedzy i pomagając im w projektowaniu prac na międzynarodowe konkursy architektoniczne. Często takie projekty mają tendencję do podążania za globalnymi trendami, często naśladując modne wzorce bez uwzględnienia lokalnego kontekstu, tradycji czy kulturowych niuansów.

Pierwsza część tego artykułu opisuje metodykę stosowaną w międzynarodowych warsztatach studenckich. Druga część zagłębia się w zastosowanie metody nauki przez realizację projektów (PBL) poprzez tworzenie projektów na konkursy architektoniczne, podkreślając znaczenie uwzględniania dziedzictwa historycznego i kulturowego przy wyborze koncepcji projektowych. Trzecia część artykułu przedstawia szczegółową analizę wyników warsztatów i rozpoczyna dyskusję na temat kluczowej roli kontekstu historycznego oraz znaczenia świadomości kulturowej w tym kontekście edukacyjnym.

PROBLEMS OF CALCULATING THE CARBON FOOTPRINT IN SCOPE 3 USING BIM

PROBLEMATYKA OBLICZANIA ŚLADU WĘGLOWEGO W ZAKRESIE 3 Z WYKORZYSTANIEM BIM

Andrzej Szymon Borkowski, Marta Maroń,
Patrycja Olszewska, Krzysztof Wójcik
Warsaw University of Technology, Poland

Structure and Environment vol. 16, No. 2/2024, p. 76 DOI: 10.30540/sae-2024-007

Abstract

The article presents the requirements of the EU EPBD (Energy Performance of Buildings Directive) for counting the carbon footprint (especially in Scope 3) and including it in construction projects from 2030. The obligation to count the carbon footprint will burden mainly designers, who are increasingly using BIM (Building Information Modelling) in the design process. Performing analysis and calculation of the carbon footprint in BIM models is hampered by the lack of non-graphical information on the subject in library components. The paper explains the concept of CO_2 in 3 scope, also discusses currently available tools for counting the carbon footprint, and examines how many components available on the Internet already contain non-graphical information on emissions, as well as ideas for implementing this directive. The advantages and disadvantages of these approaches were presented from the perspective of various stakeholders in the planning and investment and construction processes. The aim of the paper was to present possible solutions, ensuring compliance with the EU directive by proposing specific techniques, enabling the calculation of the Scope 3 carbon footprint, using BIM. In addition to a review of existing ideas, an authorial proposal for a national repository of carbon footprint information taking into account all stakeholders was presented.

Streszczenie

W artykule przedstawiono wymagania unijnej dyrektywy EPBD (ang. Energy Performance of Buildings Directive) dotyczące liczenia śladu węglowego (zwłaszcza w zakresie 3) i uwzględniania go w projektach budowlanych od 2030 roku. Obowiązek liczenia śladu węglowego obciąży głównie projektantów, którzy coraz częściej wykorzystują BIM (ang. Building Information Modelling) w procesie projektowania. Przeprowadzanie analiz i obliczeń śladu węglowego w modelach BIM jest utrudnione ze względu na brak niegraficznych informacji na ten temat w komponentach bibliotecznych. W artykule wyjaśniono koncepcję liczenia CO_2 w tzw. zakresie 3, omówiono również obecnie dostępne narzędzia do liczenia śladu węglowego oraz zbadano, ile komponentów dostępnych w internecie zawiera już niegraficzne informacje na temat emisji, a także przedstawiono pomysły na wdrożenie tej dyrektywy. Zalety i wady tych podejść zostały zaprezentowane z perspektywy różnych interesariuszy procesów planistycznych i inwestycyjno-budowlanych. Celem artykułu było przedstawienie możliwych rozwiązań, zapewniających zgodność z dyrektywą UE poprzez zaproponowanie konkretnych technik umożliwiających obliczenie śladu węglowego z zakresu 3, z wykorzystaniem BIM. Oprócz przeglądu istniejących pomysłów przedstawiono autorską propozycję krajowego repozytorium informacji o śladzie węglowym z uwzględnieniem wszystkich interesariuszy.

ASSESING THE POTENTIAL OF DIGITAL TERRAIN MODELS FOR MONITORING ADDITIONAL SUBSIDENCE OF COMMUNICATION EMBANKMENTS IN MINING AREAS – A CASE STUDY

OCENA MOŻLIWOŚCI NUMERYCZNYCH MODELI TERENU DO MONITOROWANIA DODATKOWYCH OBNIŻEŃ NASYPÓW KOMUNIKACYJNYCH NA TERENACH GÓRNICZYCH – STUDIUM PRZYPADKU

Łukasz Kapusta, Szymon Sobura
Kielce University of Technology, Poland

Structure and Environment vol. 16, No. 2/2024, p. 84 DOI: 10.30540/sae-2024-008

Abstract

Today's technologies make it possible to capture certain phenomena that were very difficult or impossible to observe in terms of classical measurements. One of them is the so-called sinking of embankments. It is common in mining areas. It consists in the additional subsidence of the embankments into the ground, above the value of the lowering of the adjacent area. It takes place primarily in the zone of horizontal tensile deformations. The paper presents the results of comparative DTM (Digital Terrain Model) analyzes from 2001, 2014, 2018 and 2021. Their aim was to assess the usefulness of DTM data for monitoring the additional sinking of the communication embankment on the example of the northern bypass of Bytom. The authors analyzed digital terrain models generated in the process of rasterization of data from ALS (Airborn Laser Scanning).

Streszczenie

Dzisiejsze technologie pozwalają wychwycić pewne zjawiska, które w ujęciu pomiarów klasycznych były bardzo trudne lub też niemożliwe do zaobserwowania. Jednym z nich jest zjawisko tzw. tonięcia nasypów. Występuje ono powszechnie na terenach górniczych. Polega na dodatkowym zagłębianiu się budowli w podłoże, ponad wartość obniżenia terenu przyległego. Ma ono miejsce przede wszystkim w strefie poziomych odkształceń rozciągających. W pracy przedstawiono wyniki analiz porównawczych NMT z lat 2001, 2014, 2018 i 2021. Ich celem była ocena przydatności danych z NMT do monitorowania dodatkowego zagłębiania nasypu komunikacyjnego na przykładzie północnej obwodnicy Bytomia. Autorzy poddali analizom numeryczne modele terenu wygenerowane w procesie rasteryzacji danych pochodzących głównie z lotniczego skanowania laserowego ALS.

SELECTED MICROSTRUCTURAL PHENOMENA IN FSW JOINTS

WYBRANE ZAGADNIENIA MIKROSTRUKTURY SPOIN WYKONANYCH W TECHNOLOGII FSW

Wiktor Wciślik
Kielce University of Technology, Poland

Structure and Environment vol. 16, No. 2/2024, p. 97 DOI: 10.30540/sae-2024-009

Abstract

The article is a literature review on selected phenomena leading to microstructural changes in material welded using the friction stir welding (FSW) method. Particular attention was paid to the phenomena of grains recrystallization, as well as dissolution and reprecipitation of second phase particles, resulting from temperature changes during FSW. Temperature transformations in different zones of the FSW joints were characterized. The role of base material phase transformation in the formation of new particles is discussed. In the tested aluminum alloys and stainless steels, this process was particularly intensified in the heat affected zone (HAZ). In areas subjected to high temperature and significant plastic deformation (nugget zone and thermomechanically affected zone), this phenomenon did not occur or was characterized by small intensity. It was indicated that the phenomenon of particle formation clearly affects the strength parameters of the joint.

Streszczenie

W artykule przedstawiono przegląd literatury dotyczący wybranych zjawisk prowadzących do zmian mikrostrukturalnych w metalach spawanych metodą zgrzewania tarciowego (FSW). Szczególną uwagę zwrócono na zjawiska rekrystalizacji ziaren oraz rozpuszczania i ponownego wytrącania cząstek drugiej fazy, zachodzące jako efekt zmian temperatury podczas FSW. Scharakteryzowano zmiany temperatury w różnych strefach złączy FSW. Omówiono rolę przemian fazowych materiału podstawowego w powstawaniu nowych cząstek. W badanych stopach aluminium i stalach nierdzewnych proces ten był szczególnie nasilony w strefie wpływu ciepła (SWC). W obszarach narażonych na działanie wysokiej temperatury i znacznych odkształceń plastycznych (jądro zgrzeiny i strefa uplastycznienia termomechanicznego) zjawisko to nie występowało lub charakteryzowało się niewielkim natężeniem. Wykazano, że zjawisko tworzenia cząstek wyraźnie wpływa na parametry wytrzymałościowe złącza.

RECOVERY OF THE ORGANIC SOLVENTS FROM THE MULTICOMPONENT MIXTURE IN THE PROCESS OF THE FRACTIONAL DISTILLATION AND THE VACUUM DISTILLATION

ODZYSKIWANIE ROZPUSZCZALNIKÓW ORGANICZNYCH Z MIESZANINY WIELOSKŁADNIKOWEJ W PROCESIE DESTYLACJI FRAKCYJNEJ I DESTYLACJI PRÓŻNIOWEJ

Anna Ciaciuch, Mariusz Sulewski
Bydgoszcz University of Science and Technology, Poland

Structure and Environment vol. 16, No. 2/2024, p. 111 DOI: 10.30540/sae-2024-010

Abstract

In these times of sustainability, the purification and regeneration of used solvents is attracting a lot of interest for environmental reasons and to reduce production costs. The article presents research on the separation of organic solvents such as acetonitrile, methanol, acetone, and toluene from a multicomponent mixture of liquid organic waste. This is an element of the circular economy and prevents the emission of volatile organic compounds into the environment. In order to separate the mixture and recover the solvents, fractional distillation and vacuum distillation were used together with pre-treatment of the waste using sorption on silica gel and calcium oxide. The analysis of the waste composition and the mixture after the separation was performed by gas chromatography coupled with a mass spectrometer (GC-MS). As a result of the research, the acetonitrile concentration increased to 90.7% after fractional distillation.

Streszczenie

Aktualnie w czasach zrównoważonego rozwoju oczyszczanie i regeneracja zużytych rozpuszczalników cieszy się dużym zainteresowaniem ze względów środowiskowych i w celu obniżenia kosztów produkcji. W artykule przedstawiono badania nad wydzielaniem rozpuszczalników organicznych takich jak acetonitryl, metanol, aceton i toluen z wieloskładnikowej mieszaniny ciekłych odpadów organicznych. Jest to element gospodarki o obiegu zamkniętym i zapobiega emisji lotnych związków organicznych do środowiska. W celu rozdzielenia mieszaniny i odzyskania rozpuszczalników zastosowano destylację frakcyjną i destylację próżniową wraz z wstępną obróbką odpadów metodą sorpcji na żelu krzemionkowym i tlenku wapnia. Analizę składu odpadów oraz frakcji po rozdziale mieszaniny przeprowadzono metodą chromatografii gazowej sprzężonej ze spektrometrem mas (GC-MS). W wyniku przeprowadzonych prób stężenie acetonitrylu po destylacji frakcyjnej wzrosło do 90,7%.